Expression pattern of the novel freeze-responsive genes *li16*, *fr10* and *fr47* in the wood frog, *Rana sylvatica*

by

Katrina Johanna Sullivan

B. Sc. Honours – University of Victoria, 2008

A thesis submitted to the Faculty of Graduate and Postdoctoral Affairs in partial fulfillment of the requirements for the degree of

Master of Science

Department of Biology

Carleton University

Ottawa, Ontario, Canada

Your file Votre référence
ISBN: 978-0-494-83135-9
Our file Notre référence
ISBN: 978-0-494-83135-9

Abstract

The ability of the wood frog (*Rana sylvatica*) to freeze up to 65% of its total body water allows it to endure subzero temperatures encountered during winter. To survive the stresses associated with freezing, frogs have evolved multiple molecular adaptations including expression of three novel genes: *li16*, *fr10* and *fr47*. All three genes were found to be freeze responsive in a tissue-dependent manner. They also all respond to anoxia and dehydration stresses, suggesting that the transcription of these genes is triggered by the low oxygen conditions common to all three stresses. Protein levels were elevated after freezing for Li16; however FR10 and FR47 generally showed no change or a decrease in protein after freezing. Transcripts of all three genes were also detected during tadpole development, indicating a possible additional role for metamorphosis. Finally, bioinformatic analysis of their sequences provided insight into functional motifs and potential regulatory sites on the proteins.

Acknowledgements

I would like to thank my supervisor Dr. Ken Storey for trusting me with such an amazing project and for welcoming me into his lab with open arms. Thank you for all your support and advice and for trying your hardest to break me of my celebrity gossip habit! I am also eternally thankful to Janet Storey for her countless hours editing my work. You can never know how much I appreciate your ability to keep my writing on point, while providing guidance and suggestions that were sorely needed.

I'd also like to acknowledge my fellow lab mates for all they have done for me the last two years. Your willingness to talk through any problem and the ability to draw on your own experiences to provide me with solutions was vital to my success. I feel so fortunate that I was able to work alongside you each and every day. Allan, Anastasia, Alyx, Ben, Bryan, Jing, Kyle, Marcus, Mike, Neal, Ryan, Shannon, and Yulia; you made my time at Carleton a joy.

Finally I'd like to thank my family for their unwavering encouragement and support. Mom, Dad, Meghan, Lindsay and James, I couldn't have done it without you!

Table of Contents

List of Abbreviations

aa	Amino acid
AFP	Antifreeze protein
ANOVA	Analysis of Variance
APS	Ammonium persulfate
BLAST	Basic Local Alignment Search Tool
bp	Base pair
BSA	Bovine serum albumin
cDNA	Complimentary deoxyribonucleic acid
cGMP	Cyclic 3',5'-guanosine monophosphate
dd-H_2O	Double distilled H_2O
DEPC	Diethylpyrocarbonate
DNA	Deoxynucleic acid
dNTP	Deoxynucleotide triphosphate
DTT	Dithiothreitol
ECL	Enzymatic chemiluminescence
EDTA	Ethylenediamine tetraacetic acid
EGTA	Ethylene glycol tetraacetic acid
EtBr	Ethidium bromide
GTP	Guanosine triphosphate
HIV	Human immunodeficiency virus
hnRNP A1	Heterogeneous nuclear ribonucleoprotein A1
HRP	Horseradish peroxidise
IP_3	Inositol 1,4,5-triphosphate
kb	Kilobase
kDa	Kilodalton
mRNA	Messenger ribonucleic acid
MW	Molecular weight
NES	Nuclear export signal
NO	Nitric oxide
Oligo-dT	Oligodeoxythymidylic acid

ORF	Open reading frame
PAGE	Polyacrylamide gel electrophoresis
PCR	Polymerase chain reaction
PKC	Phospholipid dependent protein kinase C
PKI	Protein kinase A inhibitor protein
PKG	cGMP dependent protein kinase
PMA	Phorbol 12-myristate 13-acetate
PVA	Polyvinyl acetate
PVDF	Polyvinylidene difluoride
RACE	Rapid amplification of cDNA ends
RNA	Ribonucleic acid
RT-PCR	Reverse transcriptase polymerase chain reaction
RT	Room temperature
SDS	Sodium dodecyl sulfate (lauryl sulfate)
SEM	Standard error of mean
SG	Stress granule
sGC	Soluble guanylyl cyclase
TBST	Tris-buffered saline with Tween-20
TEMED	Tetramethylethylenediamine
TIA	T cell internal antigen
T_M	Melting Temperature
Tris	Tris(hydroxymethyl)aminomethane
tRNA	Transfer RNA
UV	Ultraviolet

List of Tables

List of Figures

Chapter 1

General Introduction

1.1 Adaptations to extreme environments

Any animal that must endure subzero environmental temperatures during the winter is required to have mechanisms in place that prevent the freezing of their bodily fluids. For warm blooded animals this is accomplished by remaining active, migrating to warmer regions or hibernating for the cold winter months. Cold blooded organisms are more limited in that migration and activity are not viable options, and therefore they must choose between hibernation, freeze avoidance or freeze tolerance. Freeze avoidance is most commonly practiced by intertidal and inshore marine invertebrates and fish, as well as terrestrial arthropods and other invertebrates, and it consists mainly of the accumulation of antifreeze metabolites and proteins in their bodily fluids. This allows the organism to suppress their freezing and/or supercooling points to below the ambient environmental temperature (Storey and Storey, 2008). Freeze tolerance, on the other hand, embraces freezing by allowing ice crystals to form in extracellular spaces while maintaining a liquid state within individual cells. It is the chosen winter strategy of many insects, some intertidal marine molluscs, and several terrestrially hibernating amphibians and reptiles (Storey and Storey, 2004a). Of all the winter hardiness strategies, freeze tolerance is one of the least popular choices as it comes with a large number of undesirable ramifications. These potential stresses include (i) physical damage to delicate tissues caused by ice crystal formation, (ii) dehydration caused by water outflow from the cells into extracellular ice masses, (iii) ischemia due to the freezing of blood plasma which halts oxygen and nutrient delivery, waste removal and the transmission of blood-borne signals, (iv) anoxia caused by the freezing of the lungs, heart and blood plasma, and (v) the halting of vital processes such as neuronal signalling. Problems also

arise upon thawing where mechanisms are needed to deal with (vi) reactive oxygen species (ROS) that form due to the sudden reperfusion of oxygenated blood, and (vii) the reuptake of extracellular water so as to not lyse the cells. Organisms that employ freeze tolerance have multiple adaptations that counteract the negative effects of freezing to preserve their cells and allow for recovery of normal cell function upon thawing.

1.2 Freeze tolerant model organism

Freeze tolerance is the method of survival for several species of woodland frogs that hibernate under layers of loose leaf litter during the winter months. Of the five species of North American frogs that are known to tolerate whole body freezing during the winter, wood frogs (*Rana sylvatica*) are the primary vertebrate model studied (Storey and Storey, 1986 and 1992). The distribution of the wood frog ranges from north-eastern USA, across the boreal forests of Canada and up to the tree line in Alaska and the Yukon (Storey, 2008) (Figure 1.1). Although the air temperature of these regions may fall below -20 °C, insulating layers of organic litter and snow on top of the soil (and therefore the wood frog) ensures a buffered temperature that rarely falls below -5 °C (Storey and Storey, 2004a). This is essential since the lowest temperature the wood frog can survive is approximately -9 °C (Cai and Storey, 1997a). Upon the drop into subzero temperatures and coming in contact with ice crystals, the wood frog begins to freeze within 30 seconds. The ability of the wood frog to endure repeated freezing of as much as 65% of its total body water facilitates its winter survival. This strategy gives wood frogs a reproductive advantage by allowing them to breed very early in the spring in ephemeral meltwater ponds, while aquatic frogs may be still locked in ice-covered ponds.

1.3 Wood frog metamorphosis; from embryo to fully developed frog

The life cycle of the wood frog begins with its embryonic stages, where the female lays a gelatinous egg mass containing thousands of eggs in the water. The number and size of the jelly envelopes, as well as the size and rate of development of the embryo are individually and specifically variable (Gosner, 1960). However, all embryos will undergo the same sequence of metamorphosis from fertilization, through cleavage, blastula and gastrula. These changes, representing Gosner stages 1 - 13 are not conspicuous and are difficult to discern without a trained eye and proper equipment. Upon stage 14, the neural fold begins to form, which is characterized by elongation of the embryo and the elevation of two lateral ridges separated by the neural groove. Neural fold development continues until stage 16, when the neural folds close to make the neural tube (Gosner, 1960). The next visible, physical change occurs at Gosner stage 21, where the embryos hatch into tadpoles. Stages 21 – 25 concern the transition to a feeding and free swimming tadpole. Also during this time period, there is initial formation of pigment patterns (stages 23 – 25). The larval stages are defined as Gosner stages 26 – 40, where identification of the stage of life is determined by examining the hind limbs. Specifically, at stage 26 the back limb buds appear, at stage 31 the "foot" becomes paddle shaped, and stages 36 – 40 are differentiated by the appearance and growth of individual toes (Gosner, 1960). Forelimbs become apparent at stage 42, and the tail is almost fully absorbed by stage 44 (it is called a tail stub at this point). At stage 46, metamorphosis is essentially complete (Gosner, 1960) (Figure 1.2).

1.4 Physiology and biochemistry of the wood frog

In an attempt to minimize damage caused by freezing, the wood frog has developed adaptations and strategies that counteract the negative effects of freezing. One mechanism of paramount importance is the ability to control the formation of ice. As a result, the wood frog has several methods to trigger ice nucleation and control ice propagation. The major mode of nucleation appears to be physical contact with environmental ice, as proven by Costanzo *et al.* (1999). They showed that 98% of frogs held at -2 °C would freeze when in contact with humic soil or damp leaf mould, while only 20% would freeze in dry containers. Another method is the utilization of ice-nucleating bacteria of the *Pseudomonas* and *Enterobacter* genera that have been found in the gut and skin of the wood frog. They are able to promote crystallization even without direct contact with external ice (Lee *et al.*, 1995). Finally wood frog plasma contains ice nucleating proteins that appear to aid in the propagation of ice through the fluid spaces of the body. While the wood frog is able to supercool when on a dry substrate, it is more advantageous for the frog to begin freezing just under the equilibrium freezing point of their body fluids (approximately -0.5 °C). This is because an initial surge of ice formation and the rate of ice accumulation are minimized at the upper range of freezing temperatures, which allows maximal time to implement adaptations that aid in freezing survival (Storey and Storey, 2004a). As such, it is interesting to note that when wood frogs are nucleated at -2 °C the exothermic reaction of ice crystallization causes the body temperature of the wood frog to increase to just under the freezing point (-0.5 °C). This temperature is maintained for several hours as a consequence of exothermic ice formation, resulting in ice forming slowly at a mean rate that is typically less than 5% of

total body water per hour. Following this, the body temperature gradually drops to match the ambient temperature (Layne and Lee, 1987).

The freezing of the wood frogs body water has the potential to result in dramatic cell dehydration. This is because the formation of extracellular ice from pure water raises the osmolality of remaining extracellular fluids and places a hyperosmotic stress on the unfrozen cells. This draws water out of cells, resulting in a sharp decrease in cell volume and an increase in cytoplasmic osmolality and ionic strength. At a behavioural level, the wood frog attempts to prevent this by wintering in the moist microhabitat under forest leaf litter. Biochemically, most freeze-tolerant organisms (*R. sylvatica* included) produce cryoprotectants that stabilize membrane structure and act in a colligative manner to limit cell volume reduction. The best known cryoprotective mechanism used by wood frogs is the rapid production of high amounts of glucose by the liver, which is triggered within 2 to 5 min of the skin starting to freeze (Cai and Storey, 1997a). Blood glucose levels typically rise to 150 – 300 mM in animals exposed to freezing conditions, compared with 1 – 5 mM seen in unfrozen controls (Storey and Storey, 1984, 1986). Glucose is then delivered to all other organs via circulation to aid in colligative resistance to excessive cell volume reduction (Storey and Storey, 2001).

The wood frog must also have mechanisms in place to deal with decreased energy reserves that are a consequence of the anoxia and ischemia faced by the frog during freezing. In an effort to save energy, *Rana sylvatica* undergo metabolic rate depression and enter a state of hypometabolism. During this time, priorities for energy expenditure are re-arranged to allow for the continuation of critical functions at the cost of others (Hochachka *et al.*, 1996). One such process that is sensitive to the availability of energy

is protein synthesis, which requires about five ATP equivalents per peptide bond formed (Hochachka *et al.*, 1996). This energy expensive process is strongly reduced during hypometabolism, thus saving ATP for more essential processes. Enzyme functioning also decreases during freezing as shown by Cowan and Storey (2001) who found a freeze induced reduction in the activities of 75% of the enzymes investigated. Energy savings are also accomplished through physiological changes, as hypometabolism is typically associated with no eating (to save the energetic costs of digestion, absorption and peristalsis), lack of voluntary muscle movement, a decrease in heart beat and respiration, and reduced kidney filtration (Storey and Storey, 2004b).

Despite the tendency to decrease energy consumption, certain genes are differentially up-regulated during freezing (Storey *et al.*, 1997; Storey and Storey 2004a). Freeze-induced changes in gene expression have been identified from cDNA libraries, by heterologous screening of DNA arrays, or by use of differential display technology (Cai and Storey, 1997b; Cai *et al.*, 1997; Storey, 2004; Wu and Storey, 2005; Wu et al., 2008, 2009). Of particular interest, screening of cDNA libraries made from liver of frozen wood frogs revealed freeze-induced up-regulation of several unique clones. Two of these genes were identified as the α and γ subunits of fibrinogen, which are believed to be upregulated to increase plasma clotting capacity to deal with any ice damage to organ microvasculature (Cai and Storey, 1997a). Another was the ADP/ATP translocase which is essential for mitochondrial energy regulation during freezing (Cai and Storey, 1997c). The remaining clones showed no homology to any identified gene/protein in sequence banks and were subsequently named *fr10*, *li16* and *fr47* (Cai and Storey, 1997a, McNally *et al.*, 2002, 2003). The role that these genes and their encoded proteins play in the

response to freezing is examined in this thesis.

1.5 The history of *li16*, *fr10* and *fr47*

My thesis is built upon preliminary work done by Cai and Storey (1997a), and McNally *et al.* (2002, 2003) on *fr10*, *li16* and *fr47*, respectively. The initial discovery of these genes began with the construction of a cDNA library from the liver of 24 h frozen frogs, screened against cDNA probes from liver mRNA of control versus frozen frogs. Comparison between the binding of both probes revealed three novel freeze responsive clones, subsequently named *li16*, *fr10* and *fr47*. Isolation of the insert from the clone allowed Northern blots to be performed which confirmed increases in transcript levels over a time course of freezing. Novel inserts were sequenced, which showed *fr47* and *li16* to be missing their 5' ends. The technique of 5' RACE (Rapid Amplification of cDNA Ends) was performed to obtain the full mRNA sequence. Using the software DNAMAN, the nucleotide sequence was analysed for open reading frames, and Western blots were performed to confirm the size of the translated protein (Cai and Storey, 1997a, McNally *et al.*, 2002, 2003).

1.6 *li16*, *fr10* and *fr47* in this thesis

The present thesis characterizes the novel genes *li16*, *fr10* and *fr47* and what their role might be in the survival of the wood frog during freezing. To accomplish this, relative transcript levels were determined over the course of freezing as well as in response to two component stresses of freezing; anoxia and dehydration. It was hypothesized that all three genes would be upregulated during freezing (as they were discovered) and that they would similarly respond to at least one of the component stresses tested , as the majority of freeze tolerant adaptations are "borrowed" from

responses to other environmental stresses (Storey and Storey, 2005). Western blotting was used to analyze protein levels over the time course of freezing and thawing. It was predicted that protein levels would mirror changes in mRNA levels. Finally, expression levels were also determined over the course of development and metamorphosis of the wood frog from embryo to tadpole to almost fully formed adult. It was hypothesized that the presence of these genes during development might indicate an alternative, second role for the protein, in addition to environmental stress tolerance.

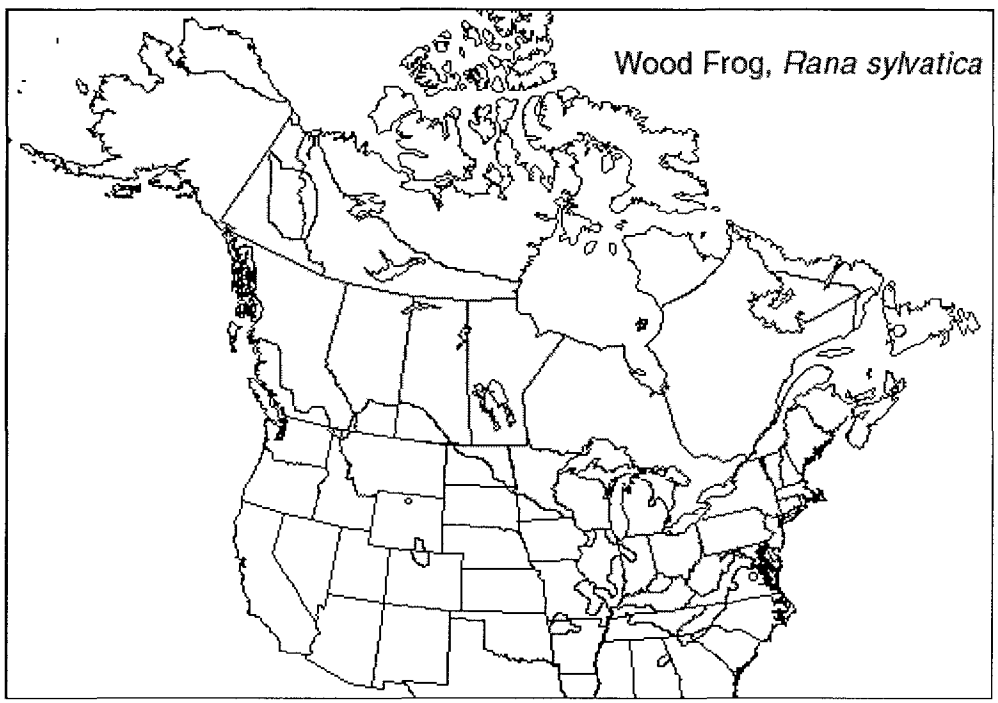

Figure 1.1: Species distribution of the wood frog, *R. sylvatica*, ranges from north-eastern USA, across the boreal forests of Canada, and up to the tree line in Alaska and the Yukon. From Wikipedia, "Wood Frog": http://en.wikipedia.org/wiki/File:Rana-sylvatica_Range.gif.

Stages 14–20: Neural fold development[1]

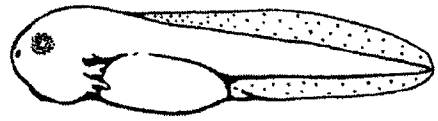

Stages 21–25: Tadpole is hatched[2]

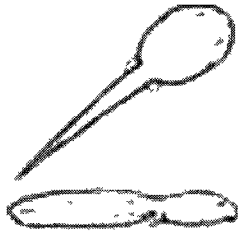

Stages 26–30: Back limb bud emerges[1]

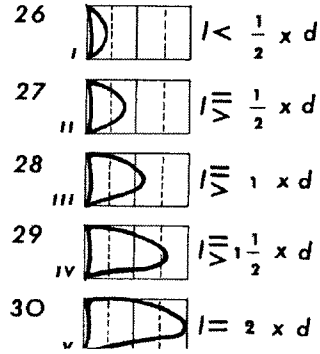

Stages 31–35: "Paddle feet" develop[2]

Stages 36–41: Back limp develops toes[2]

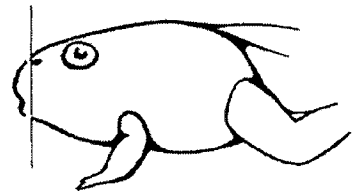

Stages 42–43: Front limb buds appear[2]

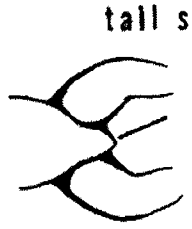

Stages 44 – 45: Tail absorbed into a "stub"[2]

Stage 46: Development complete[1]

Figure 1.2: Gosner stages of development in the metamorphosis of the wood frog, *Rana sylvatica*, from embryo to fully developed adult. [1]From "Gosner Stages": http://froglet.us/Development/gosner_stages.html. [2] From Gosner, 1960.

Chapter 2

General Materials and Methods

2.1 Animal treatment and tissue preparation

Adult male wood frogs and wood frog eggs were collected from breeding ponds near Bishop's Mills, Ontario in early spring. Frogs were washed in a tetracycline bath and held in plastic boxes with damp sphagnum moss at 5 °C for 1-2 weeks before use. Control frogs were sampled from this condition. For freezing exposure, frogs were placed in plastic boxes lined with damp paper towel and transferred to an incubator set at -4 °C. At this temperature, frogs cool and begin to freeze within 45 to 60 min (Storey and Storey, 1985). After 60 min, the temperature was raised to -2.5 °C and freeze duration was timed from this point. Frogs were sampled after 4 or 24 hours of freezing. In addition, some wood frogs were frozen for 24 h and were then returned to control conditions at 5 °C, where they were sampled after 8 h of thawing.

For anoxia experiments, 5 °C acclimated frogs were placed in plastic jars held on ice (700 ml jars, 5-6 frogs per jar) that had been previously flushed with nitrogen gas for 15 min via a syringe port in the lid (another port vented gas). A piece of damp paper towelling on the bottom maintained humidity (the towel was wetted with distilled water that was previously bubbled with 100% nitrogen gas). The jars containing frogs were then flushed with nitrogen gas for a further 20 min and then the syringe ports were capped and the tops of the jars were sealed with parafilm. Jars were then placed in a 5 °C incubator for 24 h. After this time, the nitrogen gas line was reconnected and frogs were rapidly sampled.

Frogs destined for dehydration experiments began as 5 °C acclimated frogs. These were individually weighed and ranked from heaviest to lightest and were placed in large plastic buckets, until each bucket held 10 frogs of varying masses. The buckets

were placed in an incubator set at 5 °C where frogs were allowed to lose water by evaporation. At varying intervals the frogs were quickly reweighed and ranked, and the amount of body water lost was calculated using the equation (Mi-Md) / (Mi x $\%H_2O$) where Mi is the initial mass of the animal, Md is the mass at each weighing and $\%H_2O$ is the percentage of total body mass that is water (for control wood frogs, $\%H_2O$ is 80.8 ± 1.2%) (Churchill and Storey, 1994). Initial trials using individually marked frogs showed that the frogs retained their ranking at each weighing, proving this method to be an effective way to monitor water loss. The mean rate of water loss during the experiment was about 0.5% of total body water lost per hour, and animals were sampled after they had lost 40% of their total body water.

All frogs were euthanized by pithing and tissues were rapidly excised, immediately frozen in liquid nitrogen and then stored at -80 °C until use. Protocols for the care, experimentation and euthanasia of the animals were approved by the Carleton University Animal Care Committee in accordance with the guidelines of the Canadian Council on Animals Care.

For wood frog development studies, eggs were housed in a 10 gallon aquarium that contained a mixture of pond water and dechlorinated tap water (~20 °C), bubbled with an air stone. Tadpoles were fed shredded lettuce softened by boiling, as well as goldfish flakes daily. Every 2-3 days, all but 1 L of the aquarium water was removed and this was replaced by fresh dechlorinated tap water. The 1 L of aquarium water was retained to supply any microbes needed in the tapdole environment. As the tadpoles developed, they were sampled at various stages and frozen in liquid nitrogen. Sampling occurred at stages defined by Gosner (1960): (a) stages 14 – 20, where the unhatched

embryo has developed a neural fold, (b) stages 21 – 25 where they are hatched tadpoles, (c) stages 26 – 30 where back limb buds have emerged, (d) stages 31 – 35 where back limb buds have developed into "paddle" feet (ie. no toes), (e) stages 36 – 41 where back limbs have developed individual toes, (f) stages 42 – 43 where a front limb has developed, and (g) stages 44 – 45 where the tail is almost completely absorbed and appears as a stub.

2.2 RNA preparation and cDNA synthesis

All plasticware, buffers and solutions used for RNA extraction were treated with 0.1% (v/v) diethylpyrocarbonate (DEPC) and autoclaved, except for ethanol solutions. Frozen tissues were weighed (100 mg for heart, skin and hind leg skeletal muscle and 50 mg for all others) and ground to a powder under liquid nitrogen using a mortar and pestle. To each sample, 1 mL of Trizol™ reagent (Invitrogen) was added, followed by homogenization using a Polytron PT-10 homogenizer. To this, 200 µL of chloroform was added and the contents were mixed thoroughly. Samples were centrifuged at 10 000 *x g* for 15 min at 4 °C. The aqueous supernatant containing the RNA was removed to a 1.5 mL tube, precipitated with 500 µL isopropanol, incubated for 20 min at room temperature, and centrifuged at 12 000 *x g* for 15 min at 4 °C. The resulting pellet was washed with 1 mL of 70% ethanol (in DEPC treated dd-H_2O) and centrifuged again at 7 500 *x g* for 5 min at 4 °C. The pellet was allowed to air dry for 10 min and was then resuspended in 25 µL of DEPC treated dd-H_2O. RNA quality was judged based on the ratio of absorbances at 260 and 280 nm and quantity was determined using a UV spectrophotometer at 260 nm. Once the RNA concentrations and purities were assessed, normalization of RNA concentrations was done by diluting samples to a final

concentration, typically ranging from 1 to 3 μg/μL. Total RNA was separately extracted from wood frogs exposed to six different conditions: control (n=6-8 for twelve tissues), 4 h freezing (n=5 for two tissues), 24 h freezing (n=6 for twelve tissues), 24 h anoxia (n=6 for seven tissues), dehydration of 40% of total body water content (n=6 for seven tissues) and tadpole maturation of the wood frog (n=6 for each of the seven stages of development).

To make cDNA, an aliquot containing 3 μg of RNA was diluted with DEPC water to a final volume of 10 μL. To this, 1 μL of 200 ng/μL *oligo dT* primer (5'-TTTTTTTTTTTTTTTTTTTTTTV-3'; where V = A, G, or C) was added which forms a hybrid with the poly(A) tail of mRNA. This was incubated for 5 min at 65 °C followed by rapid cooling on ice for 1 min. Subsequently, 4 μL 5X first strand buffer, 2 μL 100 mM DTT, 1 μL dNTP mixture (10 mM each) and 1 μL reverse transcriptase (RT) M-MLV (all reagents from Invitrogen) were added, followed by incubation for 1 h at 42 °C and chilling on ice. The resulting cDNA samples were serially diluted (10^{-1} to 10^{-3}) and all samples were kept at -40 °C until used for PCR amplifications.

2.3 Reverse Transcriptase (RT)-PCR amplification

For RT-PCR, a mixture of 15 μL sterile DEPC water, 5 μL diluted cDNA, 1.25 μL primer mixture (0.5 μM forward and 0.5 μM reverse primers), 0.75 μL 10X PCR buffer (Invitrogen), 1.5 μL 50 mM $MgCl_2$, 0.5 μL dNTP mixture (10 mM each) and 1 μL of *Taq* polymerase was combined for a total volume of 25 μL. The PCR protocol started with an initial step of 95 °C for 7 min, followed by 28 cycles of 94 °C for 1 min, 62.5 °C for 1 min, and 72 °C for 1.5 min, and finally was finished with 72 °C for 10 min. PCR products were separated on 1% agarose gels, stained with 0.01% v/v ethidium bromide

(EtBr) and visualized using the ChemiGenius imaging system (Syngene, Frederick, MD, USA) under UV light. To ensure saturation did not occur, the number of PCR cycles was optimized based on the cycle test results, and the most dilute cDNA samples that produced visible bands were used for quantification by the GeneTools program. The ratio of the desired gene band intensity against the *α-tubulin* band was used as a measure of relative mRNA levels.

2.4 Western Blotting

Soluble protein extracts were prepared by homogenizing 500 mg of frozen tissue in 1 mL of homogenization buffer (20 mM Tris-base, 150 mM NaCl, 1 mM EDTA, 1 mM EGTA, 1 mM NaF, 10 mM β-glycerophosphate, 1% v/v Triton X-100 and 1 mM phenylmethylsulfonyl fluoride) and homogenizing using a Polytron PT-10. Samples were centrifuged at 10 000 x g for 15 min at 4 °C and the supernatant containing the protein was moved into a 1.5 mL tube held on ice. Soluble protein concentration was determined using the Coomassie blue dye-binding method with BioRad prepared reagent, using bovine serum albumin (BSA) as a standard (BioRad, Hercules, CA). The reagent was diluted 5-fold and usually protein extracts were diluted 40-fold in distilled deionized water before the assay. Typically the assay consisted of 10 µL of diluted protein and 190 µL of diluted Bio-Rad reagent in each microplate well, with each sample done in triplicates. Colour development occurred over 10 min and samples were read at 595 nm using a microplate reader. Protein concentrations were then calculated based on the BSA standard curve. Samples were normalized to 10 µg/mL by addition of small amounts of homogenizing buffer and were mixed 1:1 (v/v) with SDS-PAGE loading buffer (100 mM Tris–HCl, pH 6.8, 4% w:v SDS, 20% v:v glycerol, 0.2 w:v bromophenol blue, 10% v:v

2-mercaptoethanol) to a final concentration of 5 μg/mL. Samples were boiled for 5 min and stored at -40 °C until use. Normalizing of samples was done to minimize the variance in sample loading.

Based on the size of the protein to be resolved, Western blot gels were either SDS-polyacrylamide or tris-tricine gels. For each gel, an equal amount of soluble protein (ranging from 15 – 100 μg depending on the protein to be detected and the tissue used) was loaded into each well and the proteins were separated electrophoretically. Again, the conditions of electrophoresis and the buffers used depended on the gel that was used for protein separation. To estimate the size of the proteins, an aliquot of Kaleidoscope prestained molecular mass ladder (Fermentas) was loaded into one well. Resolved proteins were electroblotted onto polyvinylidene difluoride membranes (Millipore) (pore size was determined by desired protein size) by wet transfer. The amperage and time of the transfer depended on the type of resolving gel used. Blots were blocked with polyvinyl acetate (PVA), with the concentration and size of PVA and time of blocking depending on the protein and tissue observed. All membranes were thoroughly washed in Tris buffered saline containing 1% v/v Tween-20 (TBST) before being incubated with primary antibody at 4 °C overnight. Following this incubation, blots were washed in 0.05% TBST and incubated with HRP linked anti-rabbit secondary antibody in TBST. A final wash in 1% TBST was performed before the signal was detected using enzymatic chemiluminescence (ECL). The chemiluminescence was detected using the Chemi-Genius Bioimaging system (Syngene, MD, USA), and band densities were analyzed using the associated Gene Tools software. To correct for any minor variations in sample loading, the blots were stained and normalized against Coomassie blue stained bands in

the same lane. For the specific conditions used for each protein and antibody, please see as detailed in the corresponding chapters.

2.5 Normalization and Statistical Analysis

Quantification of band intensity for both Western blots and RT-PCR products was performed using the Chemi-Genius Bio Imaging System and its associated Gene Tools software (SynGene, MD, USA). For RT-PCR, band intensities were quantified for the desired gene and were then normalized against the corresponding *α-tubulin* band intensity, amplified as a standard from the same cDNA sample. For Western blots, the intensity of the desired band revealed through chemiluminesce was quantified and normalized against Coomassie brilliant blue stained bands in the same lane. This served as both a loading and experimental control and was able to correct for any minor variations in sample loading as the Coomassie stained bands represented proteins whose quantity did not change in response to the given stress.

All values were reported as mean ± S.E.M. Independent sample sizes were 4 – 8 for RT-PCR experiments and 4 for protein Western blots. For each data set, the control group was normalized to a value of 1. The means were analyzed by unpaired Student's t-test, one-way ANOVA, and with Student-Newman-Keuls post hoc testing. Values of $p<0.05$ were deemed as significant which was indicated on graphs through lettering. Specifically, a, b and c represent significant differences between control and the indicated stress and d, e and f indicate significant differences between the indicated stress and the time point previous to it; a and d indicate $p<0.05$, b and e indicate $p<0.01$ and c and f indicate $p<0.005$.

Chapter 3

Li16

3.1 Introduction

The freeze-responsive *li16* transcript isolated from *R. sylvatica* was 446 base pairs (bp), with the predicted open reading frame extending from nucleotide 3 to 347 (McNally *et al.*, 2002). This encodes a protein with 115 amino acids (aa). Sixteen of the amino acids in Li16 are strongly basic and eleven are strongly acidic, resulting in an estimated isoelectric point of pH 8.29. Computer modelling indicated strong hydrophobicity near the N terminus and suggested a possible transmembrane region from amino acid 1 to 21. The calculated molecular mass of the Li16 protein is 12.8 kDa, although Western blotting indicates the protein band appears to be closer to 15 kDa. Neither transcript nor protein sequence show significant similarity to any known gene or protein (McNally *et al.*, 2002). The present study analyzes changes in *li16* transcripts and Li16 protein levels in wood frog organs comparing responses to multiple conditions: 4 and 24 h frozen, 8 h thawed, 24 h anoxia exposure, and dehydration of 40% total body water. Changes in *li16* expression over the course of wood frog metamorphosis, from embryo to adult, were also examined. The data provides new insights into the possible role of the *li16* gene product in natural freezing survival by wood frogs.

3.2 Materials and Methods

Animal treatment and tissue preparation

Male wood frogs were treated, sacrificed and tissues were collected as previously described in Chapter 2.

RNA preparation and cDNA synthesis

RNA was isolated and used to synthesize cDNA as previously described in Chapter 2.

Reverse-Transcriptase (RT)-PCR amplification

Primers used were designed using the Primer Design Program v.3 (Scientific and Educational Software) based on the sequence for *li16* (GenBank ID: AF175980). Primers were tested and the PCR products were sent for sequencing to confirm that the target genes were amplified. The PCR primers for each gene, the optimal melting temperature (T_M), and the cDNA fragment size amplified are shown below in Table 3.1.

Table 3.1 Optimal conditions for RT-PCR of *li16* related genes

Gene	Primer Sequence	T_M	Size
li16	Forward 5'-TAGAATGTCGCAGTGGTCAG-3' Reverse 5'-TTGTCGCCTCCTGGTGATGG-3'	68 77	223 bp
α-tubulin	Forward 5'-GCCTCATTGTCCACCATGAA-3' Reverse 5'-GTGTCGGTACTGGATCTGGC-3'	73 71	179 bp

Western blotting

Total protein was isolated and treated as previously described in Chapter 2. A Tris-Tricine discontinuous gel system was used to resolve proteins, using 5% stacking (1.57 mL water, 750 µL 3M Tris-HCl/SDS pH 8.45, 506 µL 30% acrylamide, 30 µL 10% APS and 3 µL TEMED) and 15% separating gels (631 µL water, 3.75 mL 3M Tris-HCl/SDS pH 8.45, 5.75 mL 30% acrylamide, 1.125 mL glycerol, 225 µL 10% APS and 7 µL TEMED). Lanes were loaded with 40 µg total soluble protein for liver, 50 µg for heart and kidney, 60 µg for muscle, 70 µg for brain and 18 µg for dorsal skin. Gels were run in a Mini-Protean III apparatus (BioRad) in anode (24.2 g Tris base in 1 L dH_2O, made to pH 8.8 using concentrated HCl) and cathode (12.11 g Tris base, 117.92 g

Tricine, and 1.0 g SDS in 1 L dH_2O, made to pH 8.3 using concentrated HCl) running buffer at 30 V for 1 h, followed by 150 V for 2.5 h at room temperature (RT). Resolved proteins were electroblotted onto 0.2 μm pore size polyvinylidene difluoride (PVDF) membranes (Millipore) by wet transfer (transfer buffer consisted of 25 mM Tris (pH 8.5), 192 mM glycine and 10% v/v methanol) at 30 mA for 15 min, followed by 160 mA for 45 min at RT. All six membrane blots (corresponding to the six tissues Li16 protein levels were examined in) were blocked using 3 mg/mL of polyvinyl acetate (30 – 70 kDa) dissolved in 0.05% TBST on a rocking platform for 30 s. After thorough washing, the membranes were incubated overnight in 1:1000 v/v primary antibody (diluted in 0.05% TBST) at 4 °C. Primary rabbit antibodies for Li16 were produced against a synthetic peptide (DCCQGPLCNA) corresponding to the C-terminal end of the Li16 protein by Sigma Genosys (Woodlands, Texas). Again membranes were washed and were incubated with 1:4000 v/v HRP-linked anti-rabbit secondary in 0.05% TBST for 45 min. Protein signal was developed and measured as described in Chapter 2.

3.3 Results

cDNA cloning of li16

The PCR product that was amplified by *li16* primers (Table 3.1) was confirmed as encoding portions of the *li16* sequences using BLASTN. The obtained *li16* product was 223 base pairs which represents about 52% of the full 429 bp mRNA sequence.

Li16 protein detection

Antiserum raised against the Li16 C-terminal peptide cross reacted with one major protein band of approximately 15 kDa which is close to the molecular weight of

the predicted protein for Li16 at 12.8 kDa. Previous work by McNally *et al.* (2002) approximated the MW and location of the Li16 protein on immunoblots to be 14 kDa.

The effect of freezing on li16 transcription

Initial studies analyzed *li16* transcript levels in liver and skeletal muscle of wood frogs after 4 or 24 h of freezing exposure. Relative transcript levels increased significantly in liver after 4 h of freezing by 2.12 ± 0.23 fold and remained high after 24 h of freezing at 1.69 ± 0.22 fold control values (Figure 3.1). Skeletal muscle showed a significant increase in *li16* transcript levels only after 24 h of freezing with an mRNA value 1.95 ± 0.17 fold that of control. After 4 h freezing, the modest increase in muscle tissue to 1.13 ± 0.02 control levels was not statistically significant. Because significant increases in transcript levels occurred in both tissues only after 24 h of freezing, *li16* expression in other tissues was analyzed only in 24 h frozen frogs.

Analysis of ten additional tissues comparing control versus 24 h frozen values showed widespread enhancement of *li16* expression in response to freezing. Figure 3.2 shows that after a 24 h freeze, *li16* mRNA levels were over two times higher in heart (2.37 ± 0.29), ventral skin (2.37 ± 0.17), testes (2.86 ± 0.54) and lung (2.12 ± 0.19) tissue than in control tissues, and were 1.6 ± 0.2 higher in 24 h frozen brain tissue compared to control. Five tissues, however, showed no change in *li16* gene expression between 24 h frozen and control time points. The "gut" tissues; stomach (1.32 ± 0.16), small intestines (1.16 ± 0.11), and large intestines (0.96 ± 0.09) showed no change, as did kidney (0.85 ± 0.08) and dorsal skin (0.93 ± 0.05).

Analysis of Li16 protein levels during freezing and thawing

Changes in *li16* transcript levels were often mirrored by changes in Li16 protein levels for the same tissues. As seen in Figure 3.3, 24 h freezing triggered a 4.5 ± 0.77 fold increase in Li16 protein levels in skeletal muscle as compared to controls. Protein levels also increased after 24 h freezing in heart and brain, by 2.07 ± 0.31 and 2.75 ± 0.21 fold, respectively, compared to control values. In kidney, however, a 2.18 ± 0.29 fold increase in Li16 was seen after 24 h of freezing although no change in *li16* transcript levels was seen. Dorsal skin was similar in that Li16 protein levels dropped to 0.23 ± 0.04 of control values while there had been no change in *li16* transcripts at that same time point. Finally liver did not show a significant change in Li16 protein after either 24 h freezing or 8 h thawing, despite the strong increase in *li16* transcripts seen after 4 and 24 h freezing. It is also interesting to note that Li16 protein levels, although elevated after 24 h freezing in brain, kidney, and muscle, had returned to control levels after 8 h of thawing. The exceptions to this were heart, where Li16 remained high after thawing (2.7 ± 0.45 fold higher than control) and dorsal skin where protein levels had risen after 8 h thawing (3.21 ± 0.04 fold higher than in 24 h frozen) but were still lower than control dorsal skin (0.72 ± 0.04 as compared with controls).

The effect of anoxia and 40% total body water dehydration on li16 transcription

Two of the components of freezing, anoxia and dehydration, were tested separately to investigate the effects of each stress on *li16* gene expression. Figure 3.4 shows that all tissues, except one, responded to 24 h anoxia by either maintaining transcript levels seen in controls or by increasing transcription significantly. Heart, kidney and brain belonged to the latter group with increases of 1.99 ± 0.14, 1.83 ± 0.21,

and 1.5 ± 0.08, respectively, compared to control values. No significant change in *li16* transcript level was detected in muscle (0.84 ± 0.05), testes (0.79 ± 0.11), and lung (0.92 ± 0.12), while liver acted uniquely after 24 h of anoxia by showing reduced transcript levels of *li16* (0.68 ± 0.02 of control levels). Interestingly, *li16* expression in several tissues responded to 40% total body water dehydration similarly to how they responded to anoxia (Figure 3.5). Again brain (1.4 ± 0.13), heart (1.8 ± 0.18), and kidney (1.64 ± 0.21) from 40% dehydrated frogs showed significant increases in *li16* transcription compared to control values. In addition, *li16* transcripts in testes increased by 1.81 ± 0.3 fold in dehydrated frogs. Liver showed reduced expression of *li16* in dehydrated frogs to 0.67 ± 0.07 of the control values, the same effect as seen under anoxia. Lung also showed a significant decrease in *li16* mRNA levels to 0.62 ± 0.04 of control whereas *li16* in muscle was not significantly affected by dehydration (0.73 ± 0.13).

Analysis of li16 transcript levels throughout wood frog metamorphosis

Figure 3.6 shows the expression of *li16* transcripts over seven stages of development of *R. sylvatica*. Overall expression levels generally remained constant throughout development except at Gosner stages 31 – 35, at which point the tadpoles develop digits on its back leg, and at Gosner stages 44 – 45, where tadpoles catabolize their long tail creating a "stub" tail. At both of these stages significantly increased *li16* expression was seen compared to the first sampling time (Gosner stages 14 – 20, where tadpoles are still embryonic). Here *li16* transcript levels were elevated by 1.62 ± 0.09 fold at Gosner stages 31 – 35 and by 1.38 ± 0.05 fold at Gosner stages 44 – 45.

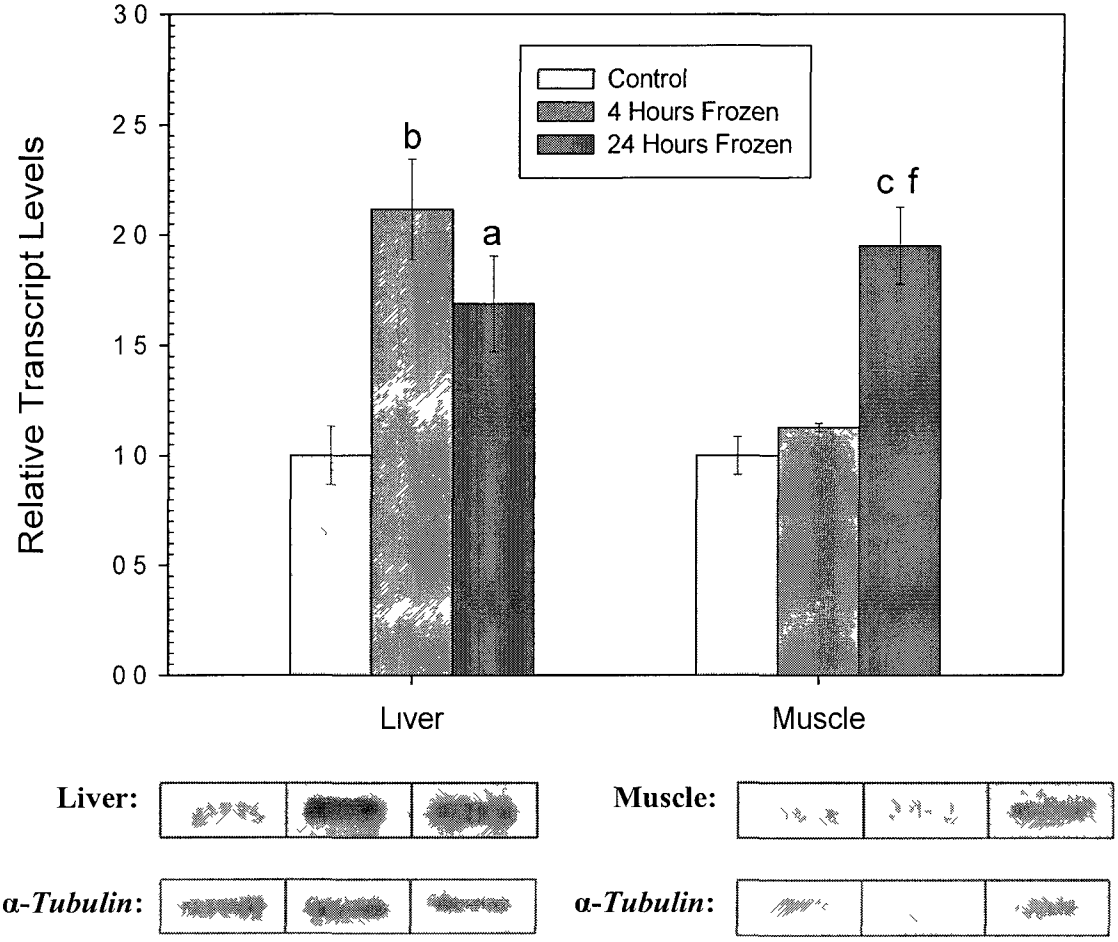

Figure 3.1: RT-PCR analysis showing the effect of 4 h or 24 h freezing on *li16* mRNA transcript levels in liver and hind leg skeletal muscle of the wood frog. Representative PCR product bands on agarose gels are shown along with a histogram showing mean normalized band intensities (± SEM, n=5 independent samples). Band intensities for *li16* were normalized against *α-tubulin* bands amplified from the same sample Data were analyzed using analysis of variance with a post hoc Student-Newman-Keuls test where the letters a, b and c represent significant differences between indicated stress and control, and d, e and f represent significant differences between the indicated stress and the time point previous to it; a and d indicate $p<0.05$, b and e indicate $p<0.01$ and c and f indicate $p<0.005$

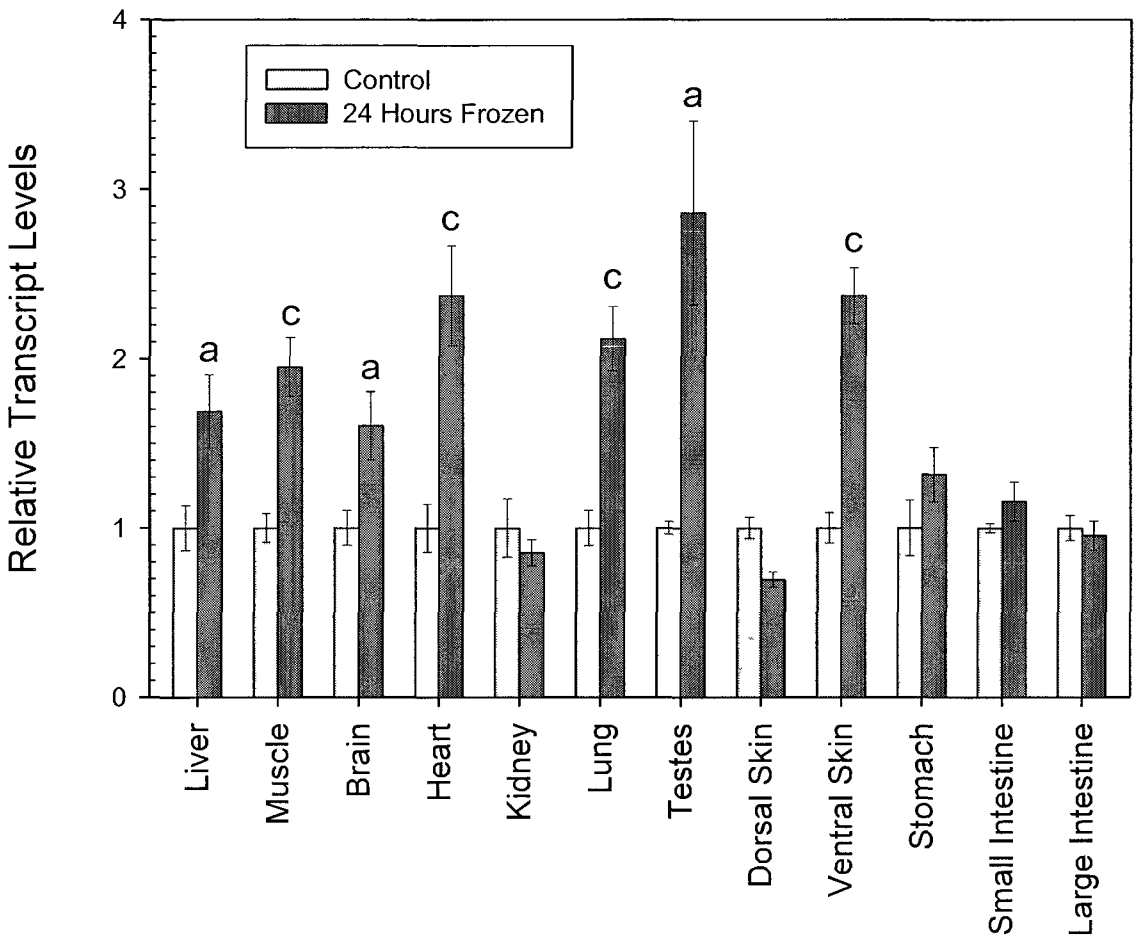

Figure 3.2: RT-PCR analysis showing the effects of 24 h freezing on *li16* mRNA transcript levels in twelve wood frog tissues. Representative PCR product bands on gels are shown along with a histogram with mean normalized values (± SEM, n=4-6 independent samples). Representative *li16* and α-*tubulin* bands are located on the next page. Other information as in Figure 3.1.

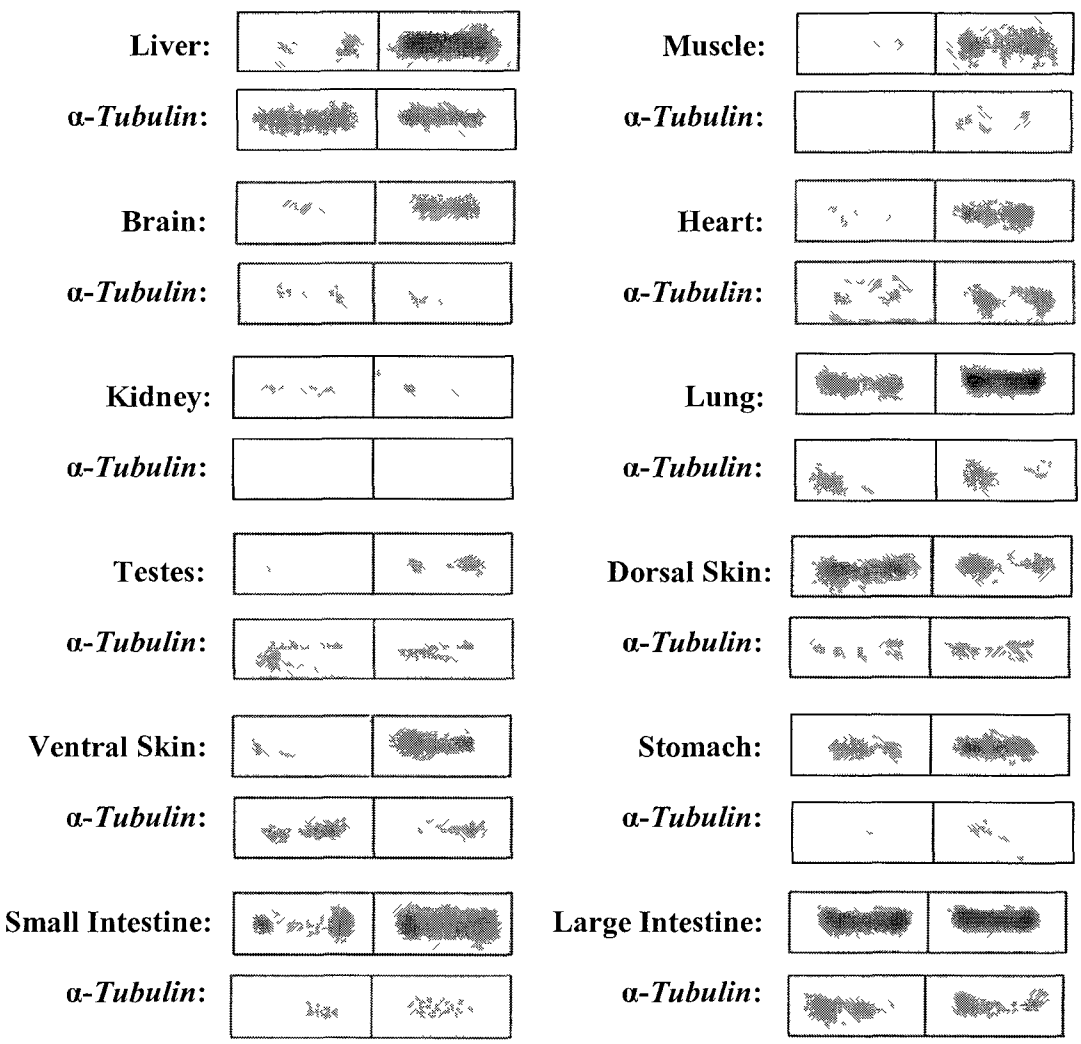

Figure 3.2: Continued (see legend on previous page)

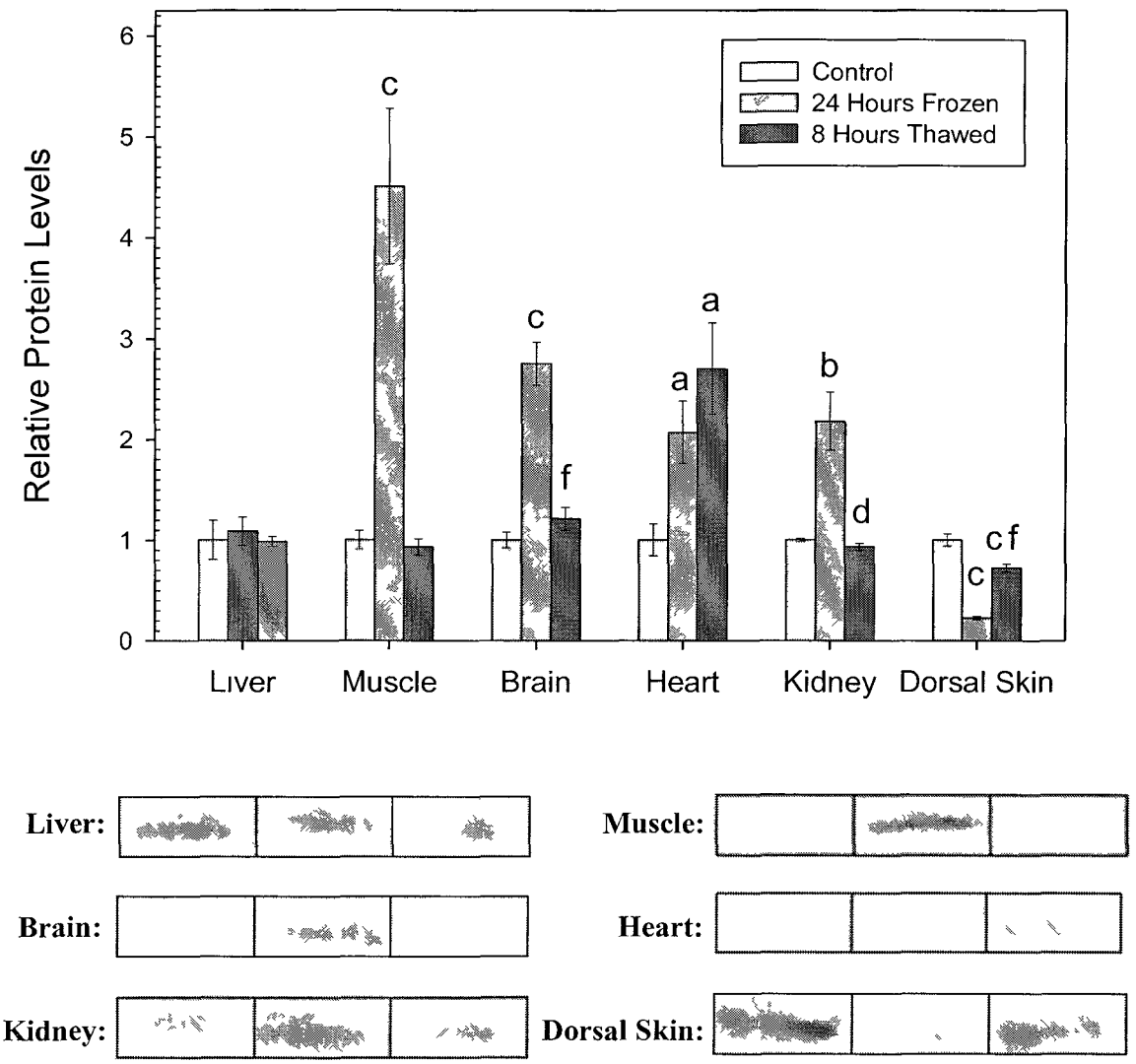

Figure 3.3: Western blot analysis showing the effects of 24 h freezing, followed by 8 h of thawing on Li16 protein levels in six tissues of wood frogs Representative Western blots and histogram show mean normalized values (± SEM, n=4 independent samples) for Li16. Information on statistical testing as in Figure 3 1.

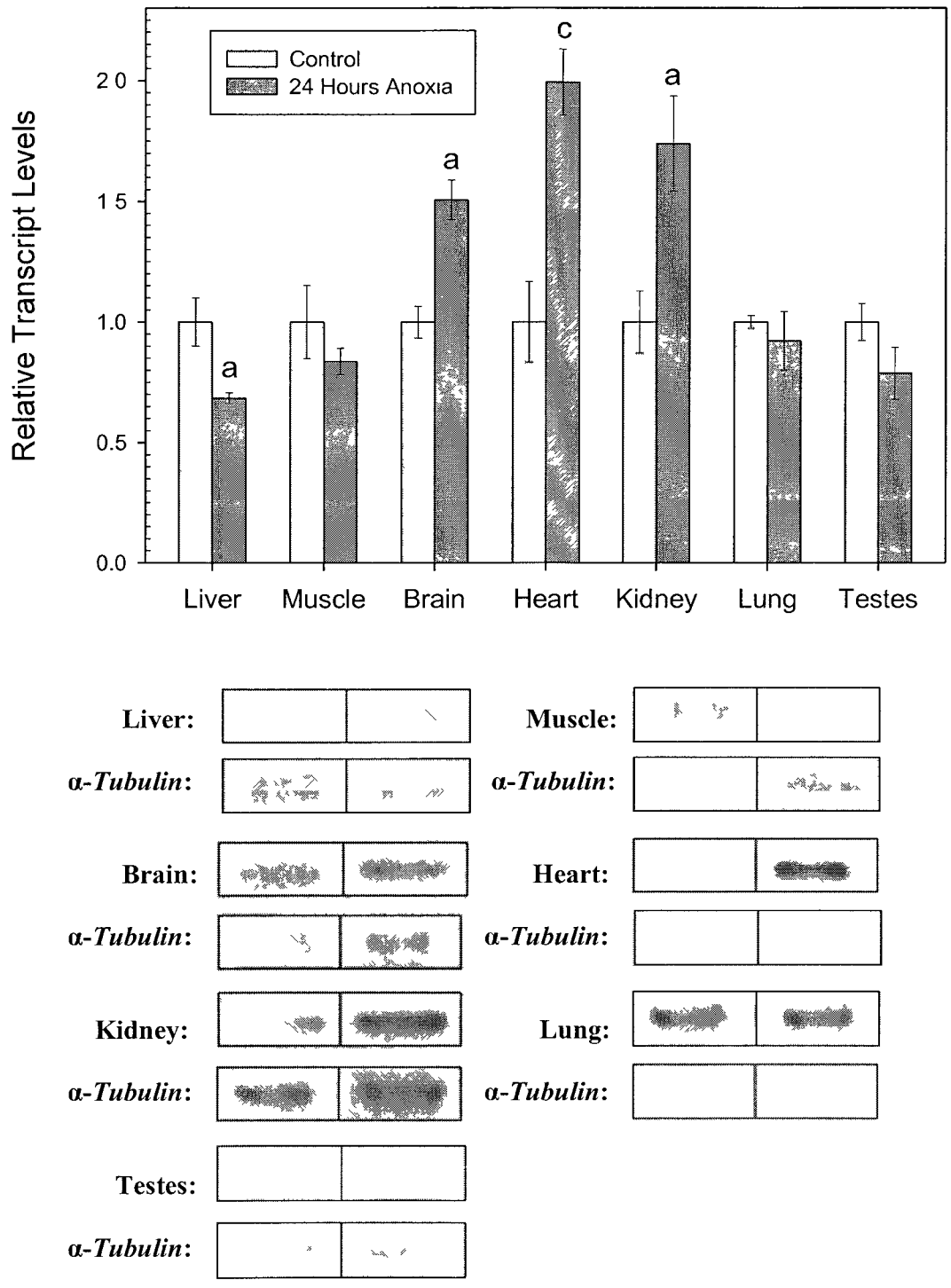

Figure 3.4: RT-PCR analysis showing the effects of 24 h of anoxia exposure at 5 °C on *h16* transcript levels in seven tissues of the wood frog. Representative PCR product bands on gels are shown along with a histogram showing mean normalized transcript levels (± SEM, n=5-8 independent determinations). Other information as in Figure 3.1.

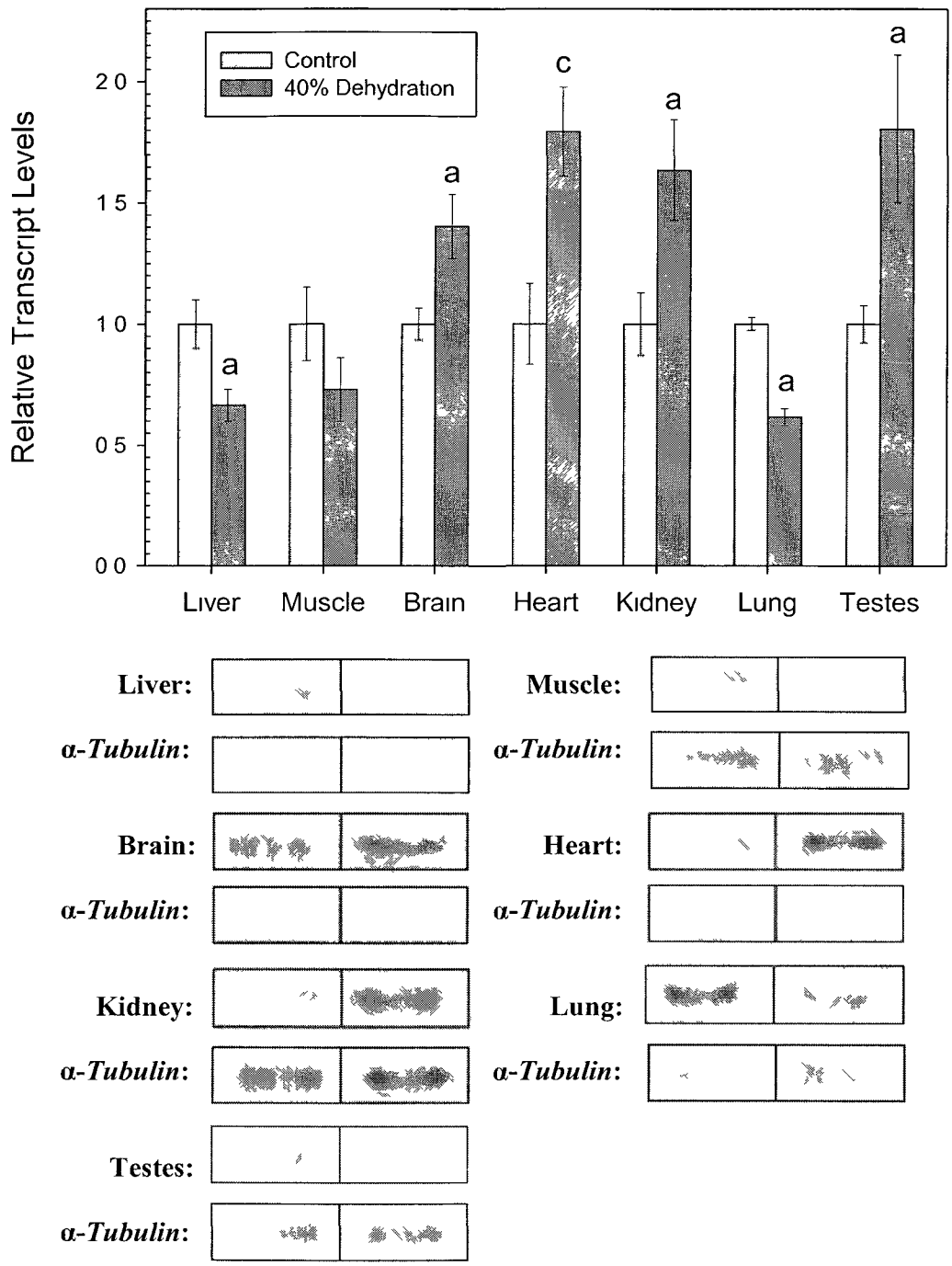

Figure 3.5: RT-PCR analysis showing the effects of 40% dehydration at 5 °C on *li16* transcript levels in seven tissues of the wood frog Representative PCR product bands on gels are shown and histogram shows mean normalized values (± SEM, n=5-8 independent determinations) Other information as in Figure 3 1

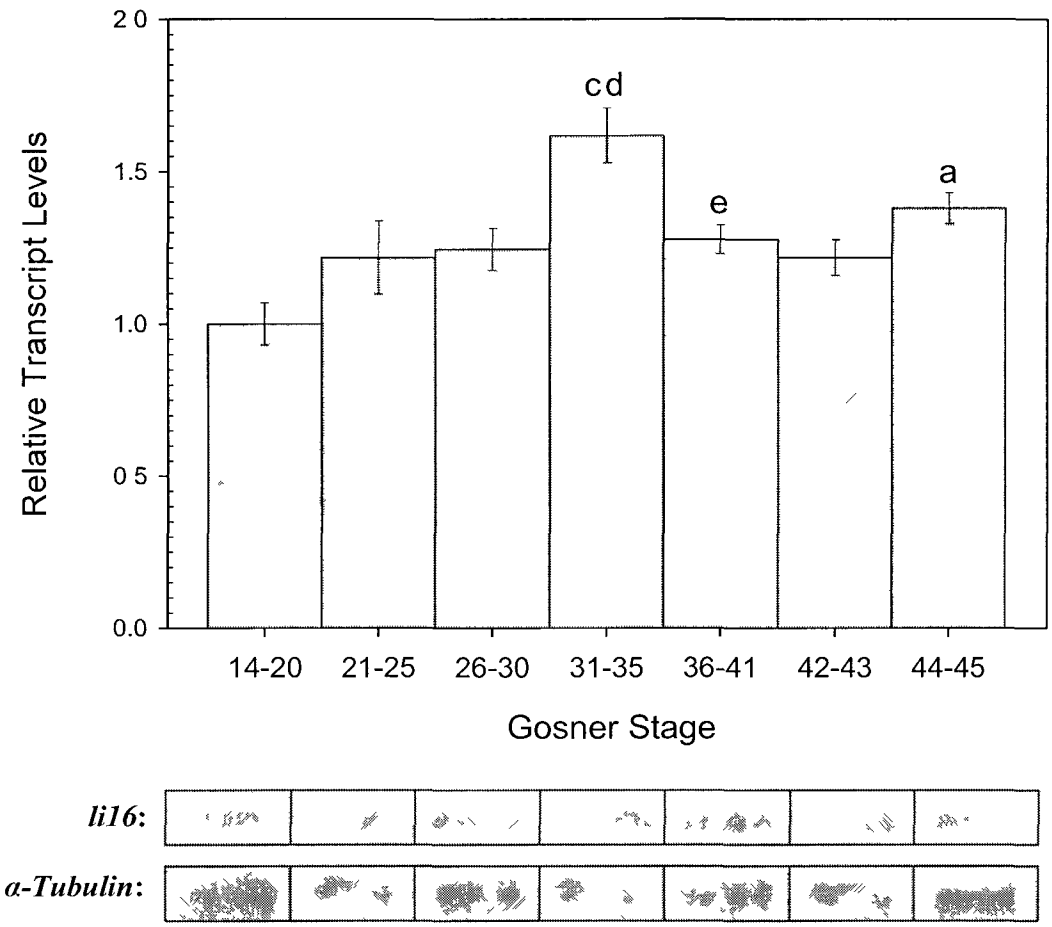

Figure 3.6: Changes in *li16* mRNA transcript levels over the course of tadpole development in wood frogs. Representative PCR product bands on gels are shown and the histogram shows mean normalized values (± SEM, n=5-6 independent determinations). The letters a, b and c represent significant differences between Gosner stages 14 – 20 and the indicated stage, whereas d, e and f indicate significant differences between the indicated stage and the stage immediately preceding it; a and d indicate $p<0.05$, b and e indicate $p<0.01$, and c and f indicate $p<0.005$.

3.4 Discussion

The effect of freezing on li16 transcription

Transcripts of *li16* were found in all twelve tissues tested, and more importantly transcript levels increased significantly during freezing in seven of these tissues (Figures 3.1 and 3.2). The increase in *li16* transcript levels varied from a 1.6-fold in brain to 2.86-fold in testes. These results show that the *li16* gene is regulated in an organ-specific manner and supports the hypothesis that *li16* has a cryoprotective role in most organs. These results are interesting, since previous work done by McNally *et al.* (2002) on transcript levels using Northern blots found *li16* expression only in liver, heart and gut, with no transcripts detected in brain, lung, kidney, or muscle. This could be a consequence of a lower sensitivity of the Northern blot method. Nevertheless, the two tissues for which *li16* levels were examined in both studies (heart and liver) agreed in showing significant increases in transcription upon freezing. Hence, there is strong cumulative evidence that suggests *li16* contributes to freezing survival of the wood frog during winter hibernation.

It was originally hypothesized that the extent of *li16* transcription during freezing might be inversely proportional to the inward movement of the freezing front through the frog's body. As documented by Rubinsky *et al.* (1994) using ^{1}H magnetic resonance imaging, freezing begins at peripheral sites and moves inwards towards the core organs. This delayed onset of freezing in the core organs, especially in brain, liver and heart, should theoretically allow for a higher accumulation of *li16* mRNA (and thus Li16 protein) in these organs (Storey, 1987). However, essentially the opposite response occurred. When looking at *li16* transcript levels, some of the tissues that are first to

freeze showed high increases as compared to unfrozen controls (Figure 3.1 and 3.2). For example, *li16* transcript levels after 24 h of freezing increased by two fold or greater in ventral skin, hind leg skeletal muscle and testes. This level of increase was also experienced by the heart, which is arguably the most important organ to the rapidly freezing frog. Mid-range increases of approximately 1.5 fold were seen in liver and brain, while other abdominal tissues and dorsal skin showed no change in transcript levels between control and freezing. The very strong expression of *li16* in ventral skin may indicate that Li16 protein is important at the onset of freezing, possibly even as part of the "early response". Because ventral skin is in contact with the ground surface, it is typically the first tissue to begin to freeze. As such it may be fully frozen before the more centrally-regulated cryoprotective responses (e.g. glucose output from liver) can contribute significantly to freezing protection in skin. Hence, endogenous synthesis of Li16 protein in both ventral skin and, by the same logic, the underlying skeletal muscle could make important contributions to cryoprotection in these organs. As the first organ to freeze, the skin is also critically placed to have a detecting and signalling function to alert interior organs of the onset of freezing (Wu *et al.*, 2008). For example, cryoprotectant output in the liver is initiated within 2 to 5 min after freezing has started, even though body ice content is negligible and core organs will be untouched by ice for a long time yet (Cai and Storey, 1997a). Perhaps in addition to being a cryoprotectant, Li16 acts in the signalling pathway that warns core organs of the upcoming freeze. An analysis of Li16 structure as predicted by the NetNES 1.1 server showed that the protein has a nuclear export signal running from amino acid residues 5 to 14 that is rich in the amino acid leucine (La Cour *et al.*, 2004). Further bioinformatic investigation on the

Target P 1.1 server also predicted that Li16 contains a signal peptide and is part of a secretory pathway (Emanuelsson, 2000).

Analysis of Li16 protein levels during freezing and thawing

The hypothesis that Li16 is important during freezing is also supported by Western blot data (Figure 3.3). Four out of six tissues tested showed significant increases in Li16 protein levels during freezing and, except for heart, protein levels had returned to control levels after 8 h of thawing. This corresponds with the work of McNally *et al.* (2002), who also showed two of three tissues increasing their Li16 protein levels after 24 h of freezing. Overall, this implies that Li16 has an integral role in the freezing survival of these organs, and that the protein is no longer needed once thawing is well underway.

The effect of anoxia and 40% total body water dehydration on li16 transcription

To further uncover the role of genes and proteins that are upregulated during freezing, the expression patterns in response to some of the component stresses of freezing may be examined. One such component is dehydration, since the formation of extracellular ice causes water to leave the cells, thus sharply decreasing their volume. Another is anoxia as the cessation of blood flow, heart beat and breathing halts the delivery of oxygen to tissues throughout the duration of the freeze. It is interesting to note that various adaptations that deal with freezing are also used by anurans to respond to other environmental stresses. In fact, almost all genes that respond to freezing have also been shown to respond to anoxia or dehydration signals (Storey, 2004). The present results showed that *li16* transcription follows this trend as the gene is up-regulated by 24 h anoxia as well as 40% dehydration exposures of wood frogs, although in an organ dependent manner. As seen in Figure 3.4, heart, kidney and brain tissues showed

significant increases in *li16* mRNA levels in response to anoxia. Similar results were seen in response to dehydration stress as frogs that had lost 40% of their total body water showed increases in *li16* transcript levels in heart, kidney, brain and testes (Figure 3.5). The three tissues for which *li16* transcription increased under both anoxia and dehydration stresses are arguably those organs most crucial for the survival and recovery of the wood frog. Under dehydration stress the heart is essential for the continued circulation of increasingly viscous blood which contains glucose which is required for colligative retention of water, the kidney is responsible for ion balance and the brain coordinates the dehydration response (Churchill and Storey, 1994). Under anoxia, the heart must adjust to sustained periods of no oxygen by reducing heart rate by as much as 5 fold at 5 °C, kidney must maintain acid-base balance in blood that is becoming progressively acidic due to a accumulating lactate, and again the brain must coordinate all body responses to anoxia (Herbert and Jackson, 1985, Jackson and Ultsch, 1982, Ultsch and Jackson, 1982). These results correspond to the *li16* study done by McNally *et al.* (2002) who showed a strong upregulation of *li16* transcription in response to both anoxia and dehydration (although this was seen in liver tissue, which actually decreased in the current study).

Further support for the up-regulation of *li16* in response to either anoxia or dehydration can be found in the work of McNally *et al.* (2002) who showed that isolated wood frog hepatocytes can be induced to transcribe *li16* by incubation with the second messenger cyclic 3',5' guanosine monophosphate (cGMP). cGMP production is most commonly triggered by endogenous nitric oxide (NO), which binds to the heme moiety of soluble guanylyl cyclase (sGC). This in turn activates the enzyme which synthesizes

cGMP from GTP, increasing its catalytic activity and elevating cGMP levels (Fiscus, 2002). cGMP goes on to activate cGMP dependent protein kinase (PKG), which is a serine/threonine kinase (Lincoln *et al.*, 2001). Although the actions of cGMP are complex and diverse, a well known role of cGMP signalling pathway is as a mediator of the relaxation of vascular smooth muscle. This is a consequence of a reduction of intracellular Ca^{2+} concentration, brought about by the PKG pathway (Rastaldo *et al.*, 2007). This implies a role for cGMP in regulating changes in blood flow, such as occur under ischemic conditions. Several studies have shown an increase in cGMP levels under ischemia and/or anoxia conditions. For example, Depré and Hue (1994) found that 10 min of no flow ischemia and anoxia caused a marked increase (approx. 30 – 50%) in myocardial cGMP content in isolated working rat hearts. Further proof of a connection between cGMP and anoxia is seen in molluscs where gene expression as a result of anoxia appears to be stimulated by a cGMP-mediated signalling cascade. Indeed, every *L. littorea* anoxia-responsive gene tested by Larade and Storey (2002) was upregulated by cGMP while showing little or no response to other second messengers. As for dehydration, it has been shown that rapid cell shrinkage in *Dictyostelium discoideum* induced elevation of both cellular and extracellular cGMP, with a 2.5 min lag. Total cGMP levels continued to rise until a peak was reached between 10 and 15 min, at which point total cGMP gradually declined (Oyama, 1996). Therefore, an elevation in cGMP as a result of anoxia or dehydration stress is proven in the literature, as is the connection between increased *li16* transcription and cGMP incubation. This indirectly supports the results seen in Figures 3.1, 3.4 and 3.5 where *li16 mRNA* levels increased as a result of freezing, anoxic and dehydration exposures.

Analysis of li16 transcript levels throughout wood frog metamorphosis

The role of *li16* in the wood frog also extends beyond freezing tolerance and its constituent stresses, as seen in Figure 3.6 which shows transcription of *li16* during tadpole development. The presence of *li16* is surprising since wood frog eggs were collected in early April and were allowed to develop completely at RT, never experiencing subzero temperatures in either nature or the lab. This indicates that *li16* has a role in the development of the wood frog, in addition to aiding in freeze tolerance. Overall, the level of transcription remained fairly constant throughout development, except for increases at Gosner stages 31-35 (identified by a "paddle foot" hind limb) and stages 44 – 45 (where the tail is almost completely metabolized) (Gosner, 1960). These results suggest that *li16* is necessary throughout development, and perhaps even into the adult stages of life given that *li16* transcripts were found in control unfrozen wood frogs in all 12 tissues analyzed.

Conclusions

The increased transcript and protein level in response to 24 h freezing confirms the role of this gene/protein in freeze tolerance of the wood frog. Elevated *li16* mRNA levels in response to anoxia or dehydration also indicate that the protein plays a significant role in the component stresses of freezing. One possible link between the three stresses is that all limit oxygen delivery to organs: freezing by halting blood circulation, dehydration by increasing blood viscosity and decreasing blood volume so that effective circulation can be compromised, and anoxia by depleting oxygen availability. Finally, *li16* appears to be important throughout development of wood frog tadpoles, indicating another role for *li16* in addition to freeze tolerance.

Chapter 4

FR10

4.1 Introduction

The gene *fr10* was isolated from a clone that was found to be 457 bp upon sequencing (Cai and Storey, 1997a). Northern blot analysis estimated the full mRNA sequence to be about 550 bp. Analysis of the sequence with the computer software DNAMAN predicted an open reading frame from nucleotide 42 to 314 (based on the sequenced 457 bp transcript), which would code for a 90 aa, 10 kDa polypeptide. The polypeptide chain consists of 9 strongly basic amino acids and 11 strongly acid amino acids resulting in an overall estimated isoelectric point of 5.25. The N-terminal region covering the first 21 residues is highly hydrophobic, while the remaining peptide is strongly hydrophilic. Computer programming predicted that the secondary structure of the hydrophilic region is α helix, whereas the hydrophobic region is mainly coiling structures and β sheets. The hydrophobic region also contains a 13 amino acid sequence rich in leucine residues that resembles a nuclear exporting signal (NES). The initial search for similarities using BLAST, performed in 1997, found that this sequence shared no significant homology to any known genes or proteins (Cai and Storey, 1997a). By looking at the pattern of expression of the *fr10* gene and FR10 protein under freezing, anoxia and dehydration stresses, as well as during wood frog development, the present chapter adds key information about the role of FR10 in natural freeze tolerance.

4.2 Materials and Methods

Animal treatment and tissue preparation

Male wood frogs were treated, sacrificed and tissues were collected as previously described in Chapter 2.

cDNA synthesis and Reverse-Transcriptase (RT)-PCR amplification

RNA was isolated and used to synthesize cDNA as previously described in Chapter 2. Primers used were designed using the Primer Design Program v.3 (Scientific and Educational Software) based on the sequence for *fr10* (GenBank ID: U44831). Primers were tested and the PCR products were sent for sequencing to confirm that the target genes were amplified. The PCR primers for each gene, the optimal melting temperature (T_M), and the cDNA fragment size amplified are shown below in Table 4.1.

Table 4.1 Optimal conditions for RT-PCR of *fr10* related genes

Gene	Primer Sequence	T_M	Size
fr10	Forward 5'-AGATTGGCAGAGAACCTCAG-3' Reverse 5'- AGTGCCACGGATCGCAGGAA -3'	68 79	323 bp
α-tubulin	Forward 5'-GCCTCATTGTCCACCATGAA-3' Reverse 5'-GTGTCGGTACTGGATCTGGC-3'	73 71	179 bp

Western blotting

Total protein was isolated and treated as previously described in Chapter 2. A 5% stacking and 15% separating Tris-Tricine discontinuous gel system was used to resolve proteins, as described in Chapter 3.2. Lanes were loaded with 50 μg total soluble protein for liver, 50 μg for heart, 60 μg for muscle, 50 μg for kidney, 100 μg for brain and 18 μg for dorsal skin. Running of the gels, transfer onto PVDF membrane, and blocking of the membranes was as in Chapter 3.2. After thorough washing, the membranes were incubated overnight in 1:1000 v/v primary antibody (diluted in 0.05% TBST) at 4 °C. The antiserum to FR10 was created through immunization of Japanese albino rabbits at the University of Calgary using purified recombinant FR10 protein run out and excised from an SDS-PAGE gel. Membranes were washed and were incubated with 1:4000 v/v HRP-linked anti-rabbit secondary in 0.05% TBST for 45 min. Protein signal was

developed and measured as described in Chapter 2.

4.3 Results

cDNA cloning of fr10

The PCR product that was amplified by the primers designed for *fr10* (Table 4.1) were confirmed as encoding the *fr10* sequence using BLASTN. The obtained *fr10* product was 323 base pairs (bp) which represents about 70% of the full 457 bp mRNA sequence.

FR10 protein detection

The primary antibody designed against FR10 crossreacted with a single major band on the immunoblots at approximately 16 kDa. This is higher than the 10 kDa which was predicted to be the MW of the protein.

The effect of freezing on fr10 transcription

Screening of a cDNA library made from wood frog liver identified *fr10* as a gene whose transcription increased upon freezing exposure (Cai and Storey, 1997a). To validate this, *fr10* transcript levels were analyzed using RT-PCR in liver and hind leg skeletal muscle of frogs held at control conditions, and those frozen for 4 or 24 h (Figure 4.1). In liver, *fr10* transcript levels increased by 2.1 ± 0.34 fold within 4 h of freezing exposure and remained high after 24 h freezing (2.12 ± 0.34 fold increase over controls). Muscle showed a similar response with slightly higher expression levels, a 2.57 ± 0.4 fold increase over control values after 4 h frozen and 2.9 ± 0.3 fold at 24 h frozen. Because both freezing time points displayed virtually identical increases in *fr10* transcription, analysis of *fr10* mRNA levels in other tissues were analyzed only in control

and 24 h frozen frogs.

Transcript levels in other wood frog tissues also confirmed the upregulation of *fr10* upon freezing as they were elevated in 7 out of 10 additional tissues after 24 h of freezing, as compared to controls (Figure 4.2). Freeze-responsive upregulation was highest in testes and heart where *fr10* mRNA levels rose by 3.72 ± 0.55 and 3.67 ± 0.32 fold, respectively. Freezing also triggered 2.92 ± 0.6 fold increase in *fr10* in ventral skin. Furthermore, Figure 4.2 shows that after 24 h of freezing, *fr10* transcript levels were elevated significantly in brain (1.76 ± 0.24), lung (1.79 ± 0.17), large intestine (1.44 ± 0.03), and small intestine (1.58 ± 0.17), as compared with their respective controls. Only one tissue, dorsal skin, showed no change in *fr10* transcript levels (0.93 ± 0.17), whereas both kidney and stomach showed reduced transcription of *fr10* upon freezing to 55 ± 5% and 22 ± 4% of control values.

Analysis of FR10 protein levels during freezing and thawing

Western blotting was used to examine FR10 protein levels in wood frog tissues, comparing unfrozen controls, 24 h frozen and 8 h thawed frogs (Figure 4.3). The data shows that only two of the six tissues examined displayed a significant increase in FR10 protein level in response to 24 h freezing. More specifically, freezing exposure resulted in a 1.6 ± 0.12 fold increase in FR10 protein in brain as compared with controls, and kidney showed a 1.41 ± 0.05 fold increase. The remaining tissues experienced no change in their FR10 protein level between control and 24 h frozen with values of 1.19 ± 0.09 for heart, 1.12 ± 0.16 for liver, 1.11 ± 0.04 for muscle and 0.98 ± 0.05 for dorsal skin. When 24 h frozen frogs were allowed to thaw for 8 h, liver, heart and dorsal skin again showed no significant change in FR10 levels at 1.07 ± 0.03, 0.94 ± 0.1, and 0.74 ± 0.08 fold that

of control, respectively, whereas FR10 levels in kidney dropped back to control levels (0.95 ± 0.05). Finally, skeletal muscle showed a significant decrease in FR10 after 8 h of thawing, dropping to a value that was 83 ± 4% of the control value.

The effect of anoxia and 40% total body water dehydration on fr10 transcription

To obtain more information about the nature of *fr10* transcription in the face of environmental stress, *fr10* mRNA transcript levels were also analyzed in frogs given 24 h anoxia exposure or dehydration of 40% of their total body water. Both anoxia and dehydration are components of whole body freezing and, more importantly, it has been shown that virtually every freeze responsive gene also responds to anoxia versus dehydration signals (Storey, 2004). Figure 4.4 shows the changes in *fr10* transcripts after 24 h anoxia exposure in seven tissues of wood frogs. Transcript levels increased significantly compared to control in three tissues, with increases of 1.82 ± 0.08 fold for heart, 1.68 ± 0.09 fold for lung, and 1.71 ± 0.24 fold for kidney. The remaining tissues did not display statistically significant changes in *fr10* mRNA levels; liver transcription was 0.71 ± 0.1 that of control, muscle was 1.0 ± 0.11, testes was 0.9 ± 0.13, and brain was 0.93 ± 0.16. The responses to 40% dehydration varied widely depending on the tissue, as shown in Figure 4.5. Two tissues showed significant increases in *fr10* expression in dehydrated frogs; transcript levels in heart and brain increased by 1.57 ± 0.15 and 1.54 ± 0.08 fold respectively, compared with control values. Kidney also showed a trend towards elevated *fr10* (1.35 ± 0.23 fold over controls) however the change was not found to be significant, while liver and testes showed no change with dehydration (0.7 ± 0.14 and 0.96 ± 0.15, respectively). Interestingly, transcript levels were reduced significantly in lung and muscle in response to dehydration, decreasing to

65 ± 4% and 50 ± 7% of control values, respectively.

Analysis of fr10 transcript levels throughout wood frog metamorphosis

Transcription of *fr10* was examined during the stages of development of the wood frog, from embryo to tadpole to almost fully formed adult (Figure 4.6). While *fr10* was transcribed at all stages of development, there did not seem to be a discernable consistent trend in expression. Four of the seven stages sampled showed *fr10* expression at a level that is approximately 1.4 fold higher than embryonic Gosner stages 14 – 20 (used as a standardized starting point). However, at Gosner stages 31 – 35 and 42 – 43 transcript levels were significantly reduced to 72 ± 7% and 61 ± 6% the value at stages 14 – 20. Stages 31 – 35 are characterized by the development of a "paddle" foot (i.e. yet to develop individual toes), while stages 42 – 43 are distinguished by the appearance of front limb buds.

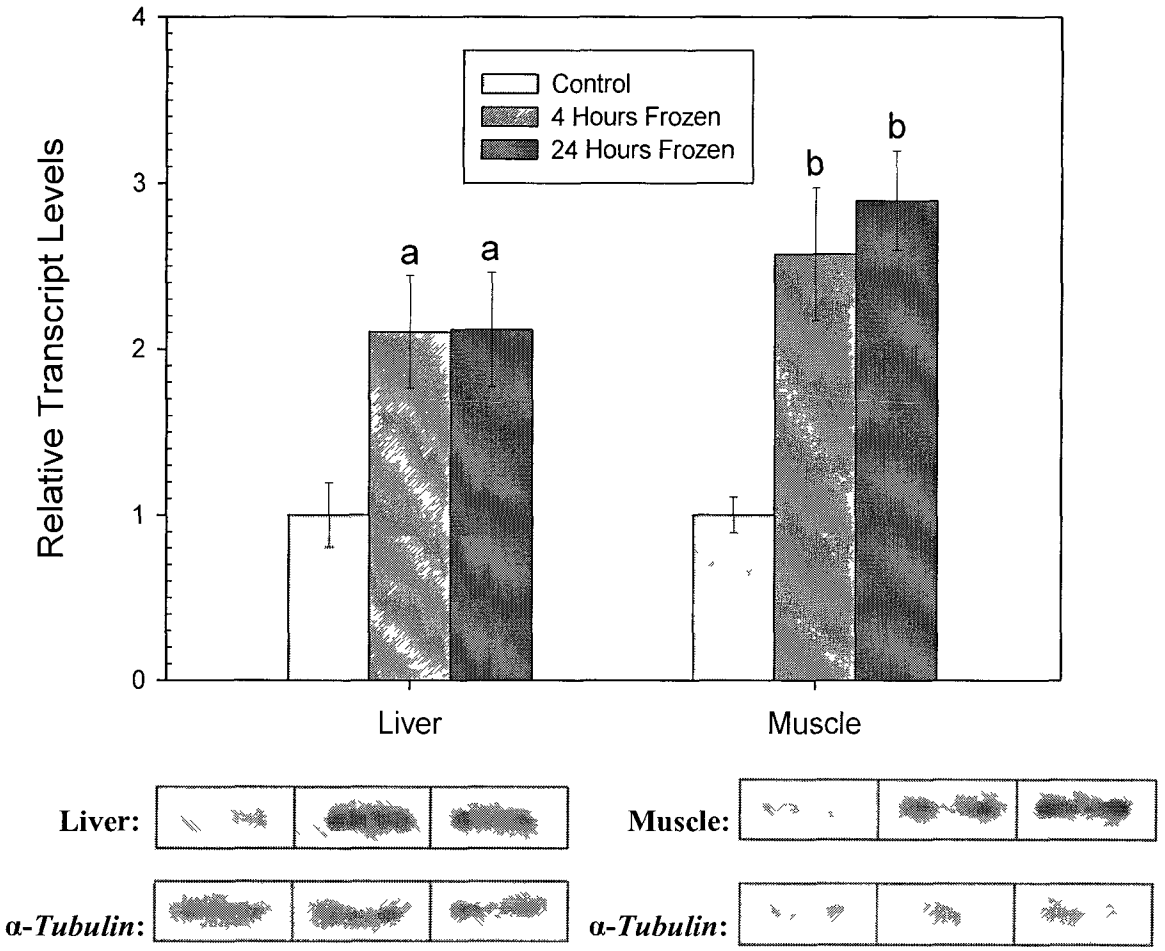

Figure 4.1: RT-PCR analysis showing effects of 4 h and 24 h freezing on *fr10* mRNA transcript levels in liver and hind leg skeletal muscle of wood frogs. Representative PCR product bands on agarose gels are shown along with a histogram showing mean normalized band intensities (± SEM, n=5 ındependent samples). Band intensıties for *fr10* were normalized against *α-tubulın* bands amplified from the same sample. Data were analyzed using analysis of variance with a post hoc Student-Newman-Keuls test where the letters a, b and c represent significant dıfferences between indicated stress and control and d, e and f represent significant differences between the indicated stress and the time point previous to it; a and d indicate $p<0$ 05, b and e are $p<0.01$ and c and f are $p<0.005$.

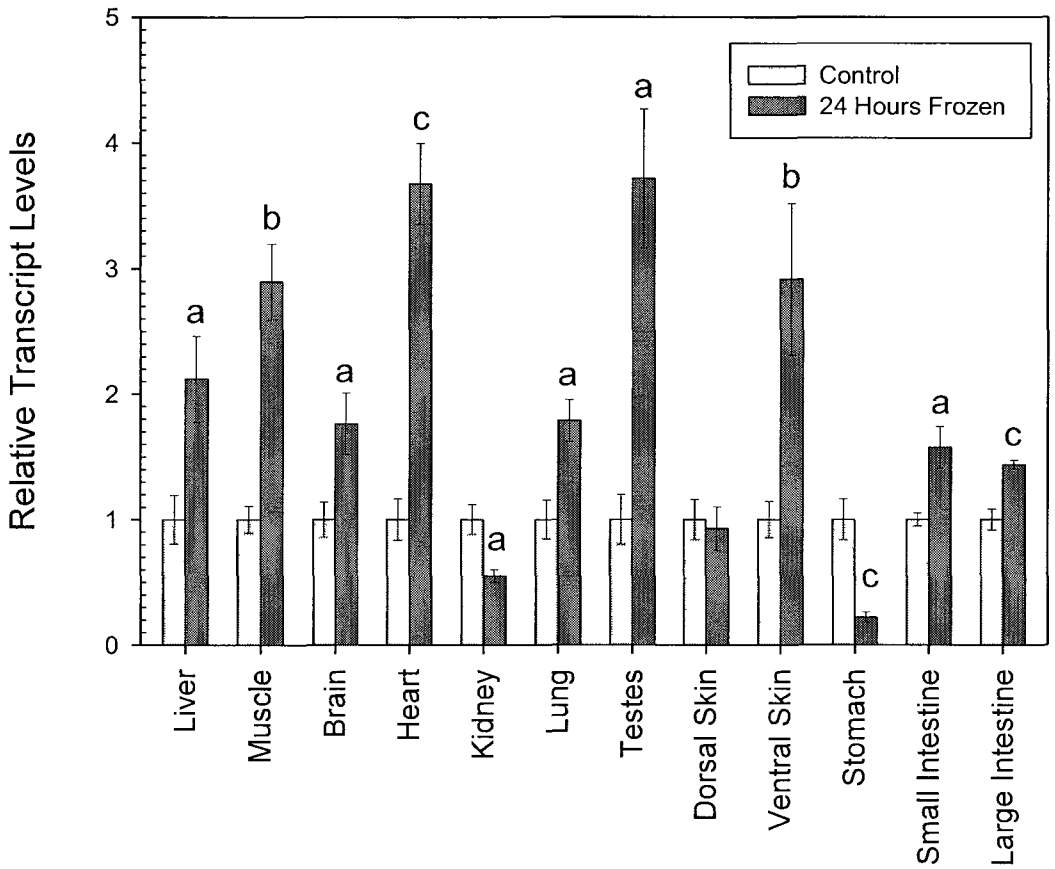

Figure 4.2: RT-PCR analysis showing the effects of 24 h freezing on *fr10* mRNA transcript levels in twelve wood frog tissues. Representative PCR product bands on gels are shown along with a histogram with mean normalized values (± SEM, n=4-6 independent samples). Representative *fr10* and α-*tubulin* bands are shown on the next page. Other information as in Figure 4.1.

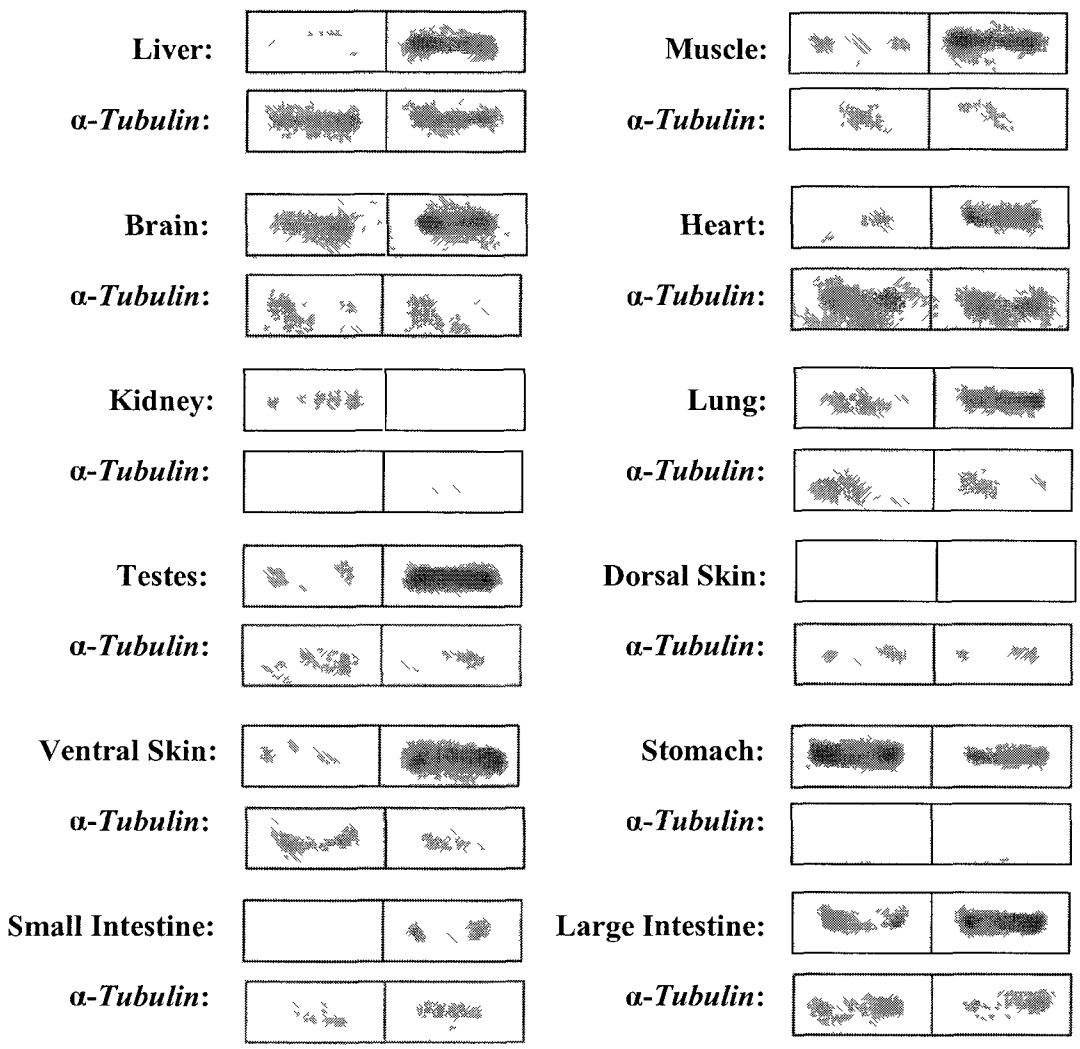

Figure 4.2: Continued (see legend on previous page)

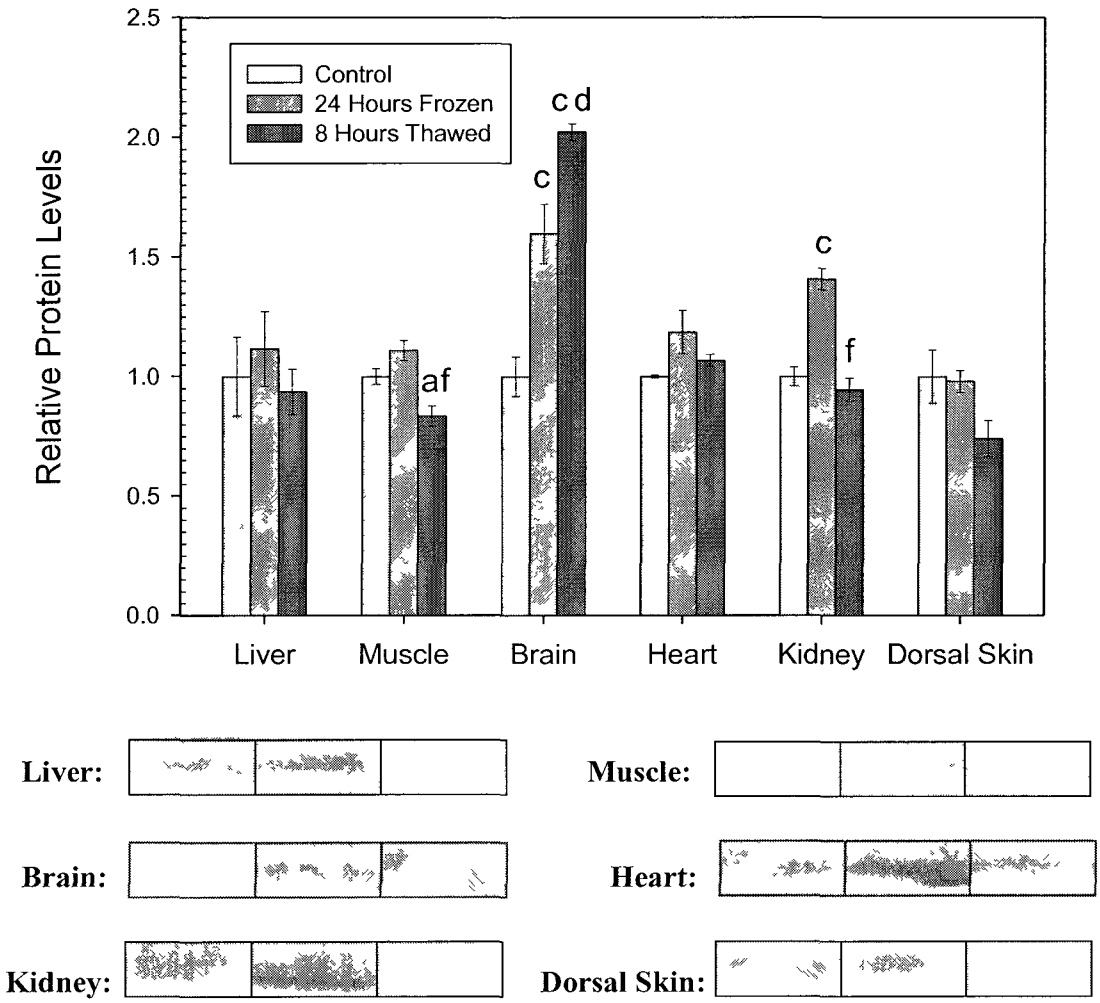

Figure 4.3: Western blot analysis showing the effects of 24 h freezing, followed by 8 h of thawing on FR10 protein levels in six tissues of the wood frog. Representative Western blots and histogram show mean normalized values (± SEM, n=4 independent samples) for FR10. Information on statistical testing as in Figure 4.1.

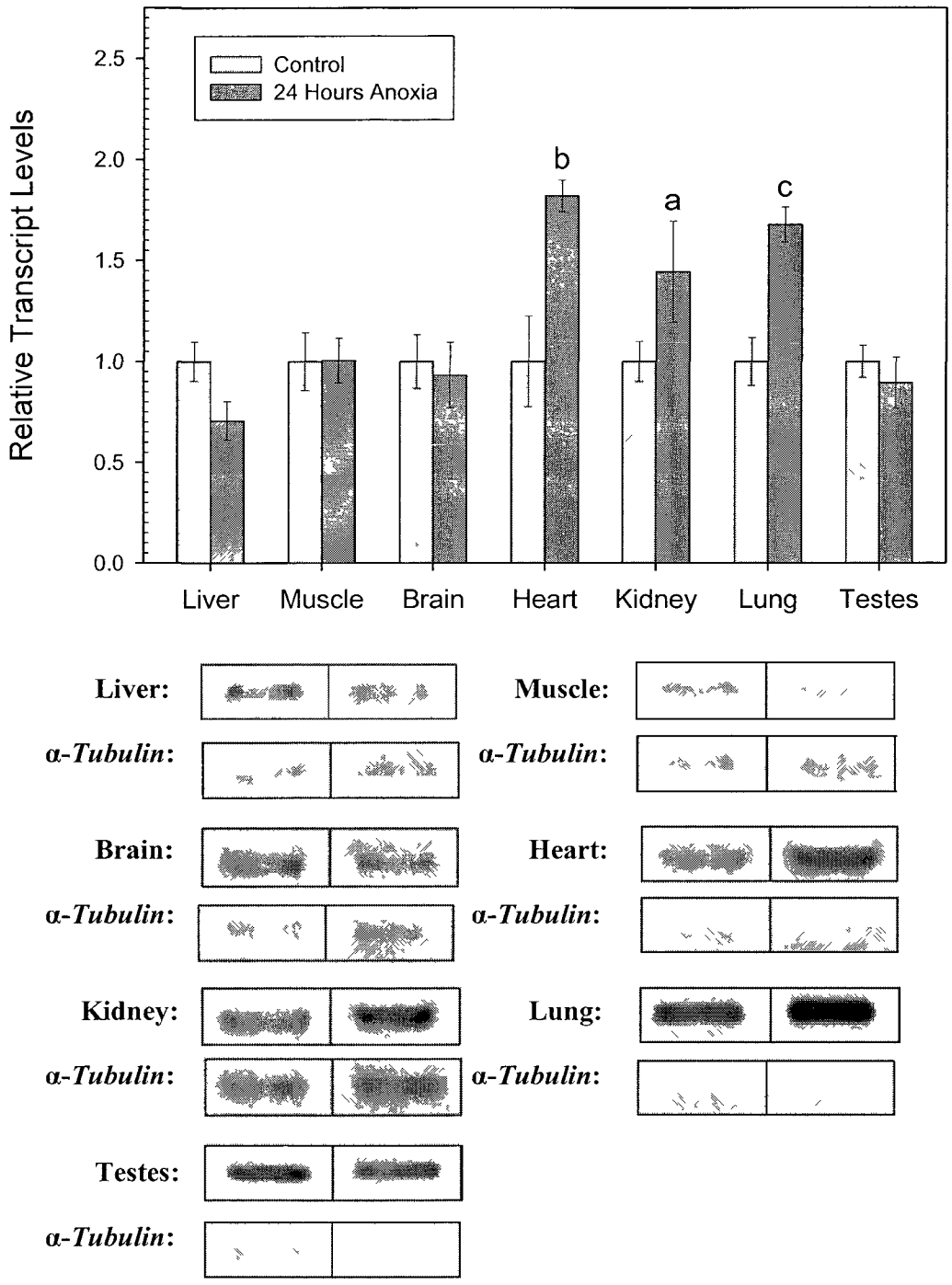

Figure 4.4: RT-PCR analysis showing the effects of 24 h of anoxia exposure at 5 °C on *fr10* transcript levels in seven tissues of the wood frog. Representative transcript bands on gels are shown along with a histogram showing mean normalized transcript levels (± SEM, n=5-8 independent determinations). Other information as in Figure 4.1.

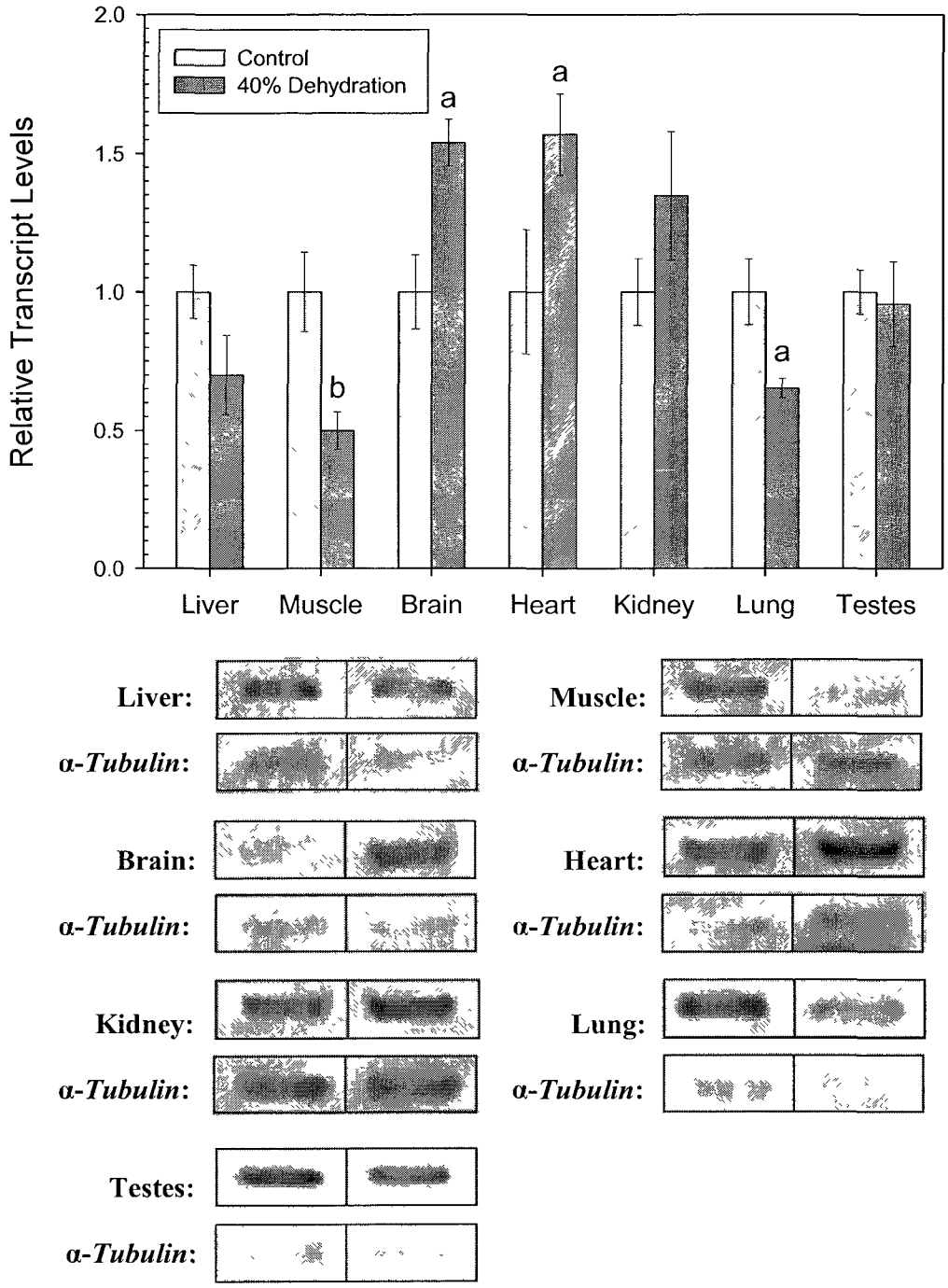

Figure 4.5: RT-PCR analysis showing the effects of 40% dehydration at 5 °C on *fr10* transcript levels in seven tissues of the wood frog. Representative PCR product bands on gels are shown and histogram shows mean normalized values (± SEM, n=5-8 independent determinations). Other information as in Figure 4.1.

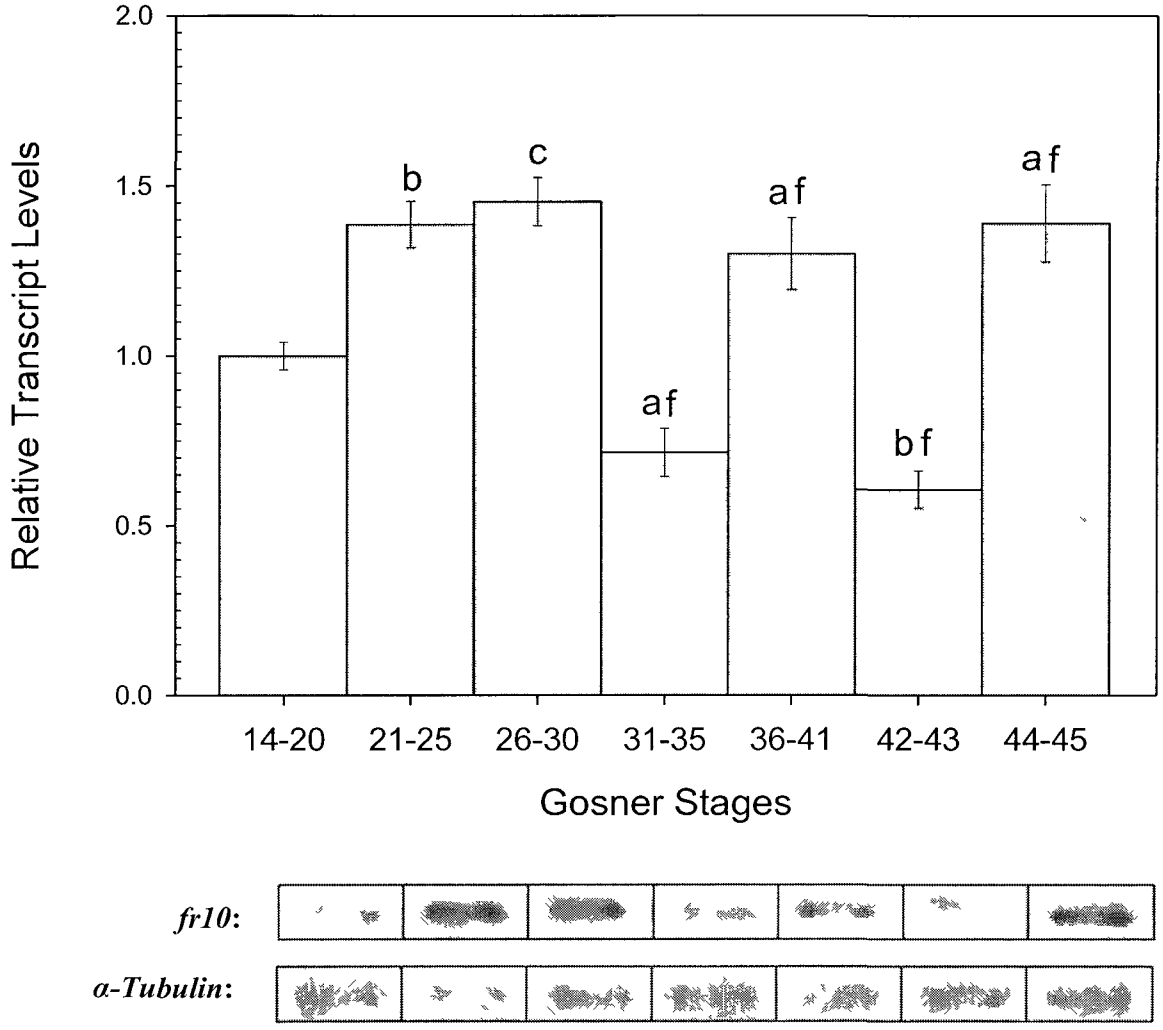

Figure 4.6: Changes in *fr10* mRNA transcript levels over the course of tadpole development in wood frogs. Representative PCR product bands on gels are shown and the histogram shows mean normalized values (± SEM, n=5-6 independent determinations). The letters a, b and c represent significant differences between Gosner stages 14 – 20 and the indicated stage whereas d, e and f indicate significant differences between the indicated stage and the stage immediately preceding it; a and d indicate $p<0.05$, b and e indicates $p<0.01$, and c and f indicate $p<0.005$

4.4 Discussion

The effect of freezing on fr10 transcription

It has been determined that *fr10* is expressed universally in all tissues tested, and that most often the gene is upregulated in response to freezing. Figure 4.2 shows that of the 12 tissues examined, 9 showed increases in transcription with only kidney, stomach and dorsal skin failing to increase their transcription after 24 h of freezing. In an earlier study, Northern blot analysis applied to several tissues showed identical results for the effects of freezing on *fr10* transcript levels in brain, heart, lung, liver, and kidney; with the only difference occurring in skeletal muscle which showed no change in the earlier study (Cai and Storey, 1997a). The upregulation of *fr10* occurred as an early event and is maintained throughout freezing, as seen in Figure 4.1 where mRNA levels were maximal by 4 h of freezing exposure in both liver and muscle and remained high after 24 h. This is consistent with the work of Cai and Storey (1997a) who also reported an early upregulation in liver, with a 2-fold increase in *fr10* transcript levels within 1 h of freezing exposure.

The combination of the widespread distribution of *fr10* and its presence throughout freezing argues for a key function of *fr10* in the cyroprotection of organs. A hint as to what this role might be is revealed by the predicted protein sequence which shows a nuclear export signal (NES) in the N-terminal region. This 13 amino acid sequence, LALVVLVIAISGL, is similar to the NES that occurs in the human immunodeficiency virus type 1 – Rev (HIV-1 Rev); LPPLERLTL (Sorokin *et al.*, 2007), and that of the protein kinase A inhibitor protein (PKI); LALKLAGLDI (Wen *et al.*, 1995) (Figure 4.7). In total, at least 75 proteins have been identified as containing a

hydrophobic NES (La Cour *et al.*, 2003) including transcription factors and cell cycle regulators. These NES sequences are recognized by the exportin Crm1, which binds to the nuclear export signal of their cargo either directly or through an adapter and ensures that it is transported into the cytoplasm (Sorokin *et al.*, 2007). The three best characterized NES containing proteins; HIV-1 Rev, PKI and hnRNP A1, have all been shown to shuttle between the nucleus and the cytoplasm to mediate the export of associated molecules. However, they differ in what the associated molecule may be. The proteins HIV-1 Rev (Fischer *et al.*, 1995) and heterogeneous nuclear ribonucleoprotein A1 (hnRNP A1) (Michael *et al.*, 1995) are involved in the export of RNA from the nucleus, whereas PKI exports the catalytic subunit of protein kinase A out of the nucleus (Fantozzi *et al.*, 1994). While none of the NES sequences are identical, they do share a similar amino acid alignment (Figure 4.7). More specifically, they share the location of a high number of leucine and isoleucine residues. According to the work done by Wen *et al.* (1995) on the nuclear trafficking pathway of PKI, it is the hydrophobic residues leucine and isoleucine that are critical to the nuclear exporting function. Therefore, based on the high degree of similarity of the NES in FR10 and that of PKI and HIV-1 Rev, it can be hypothesized that FR10 has a nuclear exporting function, possibly transporting RNA into the cytoplasm with the help of the exportin Crm1. The significant upregulation of *fr10* during freezing indicates that perhaps the putative RNA whose movement it facilitates is involved cryoprotection. Further work using yeast-two-hybrid screens or mass spectrometry could confirm these results.

Analysis of FR10 protein levels during freezing and thawing

Although freezing invoked a significant increase in *fr10* transcription, it appears

that this mRNA was not immediately translated into a protein product. As seen in Figure 4.3, four of the six organs examined showed no change in their FR10 protein level between control and 24 h frozen frogs. In fact, the only consistency between mRNA and protein levels was for dorsal skin and brain tissue which showed no change or an increase, respectively, as compared to controls after 24 h of freezing. This discordance between protein and mRNA indicates that, at least in part, control of FR10 expression occurs posttranscriptionally. When cells are under stress situations, a common response is to rapidly shut down energy-expensive processes, protein synthesis being a major one. However, rather than destroy large numbers of mRNA transcripts that are awaiting translation (transcripts that are both energy-expensive to make and to degrade), transcripts can instead be stored in stress granules where they are preserved. Stress granules (SG) are cytoplasmic domains into which specific mRNA transcripts are sequestered for the duration of the stress. They are formed in response to certain types of environmental stresses, which activate the expression of a family of eukaryotic translation initiation factor 2 alpha (eIF-2α) kinases. These kinases phosphorylate eIF-2α on serine 51 causing protein translation to halt (Kimball, 1999). This is because eIF-2α, along with the two other subunits β and γ, compose eIF-2 which is part of the ternary complex eIF2-GTP-$tRNA_{Met}$. This complex is needed to transfer $tRNA_{Met}$ onto the small ribosomal subunit in order to initiate protein translation. Phosphorylation of eIF-2α prevents its dissociation from eIF-2β, thus preventing the GDP-GTP exchange needed to charge the eIF2-GTP-$tRNA_{Met}$ ternary complex (Kedersha and Anderson, 2002). The reduced level of eIF2-GTP-$tRNA_{Met}$ allows for the RNA-binding proteins T-cell internal antigen-1 (TIA-1) and TIA-1 related protein (TIAR) to bind to the small ribosomal

subunit, promoting polysome disassembly. This then organizes into discrete domains called stress granules caused by the auto-aggregation of the prion-like C-termini of TIA-1 proteins (Kendersha and Anderson, 2002). Other RNA-binding proteins that promote mRNA stability such as Hu protein R (HuR), and those that destabilize mRNA, such as tristetraprolin (TTP), are also recruited to SGs by unknown mechanisms (Kendersha and Anderson, 2002). Stress granules were first described in heat shocked tomato cells where small heat shock proteins (HSPs) (Nover *et al.*, 1983) were stored, in addition to RNA (Nover *et al.*, 1989). Here it was discovered that the contents of the stress granules were selective, since they contained mRNAs encoding housekeeping genes but excluded newly synthesized heat shock mRNAs (Nover *et al.*, 1989). By sequestering most of the cytoplasmic mRNA from the translational machinery, stress granules may promote selective translation of those transcripts needed under stress conditions. While HSPs are found in stress granules induced by heat shock, they are not components of stress granules formed in response to other stresses. These stresses have been shown to include ultraviolet irradiation, viral infection, oxidative stress, endoplasmic reticulum stress, amino acid starvation, and changes in available heme during erythrocyte differentiation (Williams, 2001; Harding *et al.*, 2000; Kimball, 2001; Han *et al.*, 2001; Lu *et al.*, 2001). While the mRNA is transcriptionally inactive in stress granules, it may be translated after the cell has recovered from the stress. Therefore it is possible in the case of FR10 that while transcription is increased in response to freezing, these mRNA transcripts are sequestered in stress granules until the frogs recover during thawing.

However, as seen in Figure 4.3, after 8 h of thawing 4 of the 6 wood frog tissues examined still showed no change in FR10 protein levels compared to control values.

Only FR10 in brain increased significantly after thawing compared to control and 24 h of freezing, whereas muscle actually experienced a significant reduction in FR10 protein level. It is possible that FR10 protein has a role that is essential in the early stages of thawing, while the frog is still heavily frozen. For example, after 2 h of thawing at 5 °C frogs are only about half thawed and have yet to resume a heartbeat. By about 4 h heart beat is typically restored and ice is generally gone but skeletal muscles are unresponsive and frogs cannot yet hold a normal posture. After 8 h of thawing, heart beat and breathing have fully reinstated, most show good posture and movement and internal organs appear to have rehydrated to normal size (most noticeable for liver). Therefore, the best conclusion that can be drawn from the current analysis of *fr10* mRNA versus FR10 protein levels is that translation of mRNA transcripts must be controlled post-transcriptionally (i.e. transcription of the gene versus translation of the mRNA are disconnected). One may also conclude that FR10 protein must no longer be needed once recovery is well advanced, as evident by the lack of FR10 upregulation in 8 h thawed frogs.

Additional work done by E. Kotani and K.B. Storey (unpublished) does support a role for the FR10 protein in freezing survival. They found that Bm-N4 insect cells transfected with FR10 showed approximately 84-92% viability after 1 h of freezing at -6 °C, when assessed 24 h post thaw. However, cells transfected with the vector but not FR10 (a sham control) had only about 55% of cells survive the same conditions. Therefore, although the exact role and timing of translation of FR10 in wood frog cells is currently not known, it is possible to conclude that FR10 plays an essential role in freeze tolerance of the wood frog.

The effect of anoxia and 40% total body water dehydration on fr10 transcription

To obtain additional information about the basis of *fr10* transcription, mRNA levels were also analyzed in wood frogs that had been under anoxic or dehydration stresses, two components of the natural freezing experience. When *fr10* mRNA levels were measured in tissues of wood frogs that had undergone 24 h of anoxia, it was found that organs showed either no change or a significant increase in their *fr10* transcript levels when compared to controls (Figure 4.4). Interestingly, the three organs that showed a significant increase; kidney, lung and heart, are arguably those organs that would be significantly affected by anoxic conditions. The initial onset of nitrogen anoxia (which was used to induce anoxic stress in the wood frogs used in this experiment) results in an increase in ventilation frequency, heart rate, pulmonary blood flow and systemic blow flow in red-eared slider turtles (Hicks and Wang, 1998). Like wood frogs, the red-eared sliders can tolerate anoxia and acidosis for months at temperatures less than 10 °C, and therefore their responses provide a good model for the physiological changes that could be expected to occur in the wood frog as well. These initial responses are intended to increase the uptake and delivery of any remaining oxygen to tissues in an attempt to sustain normal levels of tissue oxygen consumption. These responses last up to 1 h until there is little or no oxygen remaining in tissues (Hicks and Wang, 1998). After this point the turtle switches to long term solutions for dealing with anoxia by decreasing its metabolic rate overall including decreasing heart rate by 50% (bradycardia) and developing a large right to left shunt in the heart (thereby bypassing the lungs), which accounts for approximately 80% of the cardiac output. These changes last for the duration of the anoxic exposure and upon return to normoxic conditions they are rapidly

reversed (Hicks and Wang, 1998). Stecyk and Farrell (2007) indicate that the decrease in the turtle's heart rate after 24 h of anoxia could be as much as 80%, from 5 min^{-1} to less than 1 min^{-1}. Additionally, during prolonged anoxia, the blood of the turtle will progressively become anoxic, hyperkalemic and acidic as blood lactate levels are greatly elevated during anoxia (Ultsch and Jackson, 1982; Jackson and Ultsch, 1982; Herbert and Jackson, 1985). The combination of acidosis, hyperkalemia and oxygen deprivation negatively affect the inotropic ability of the heart (Yee and Jackson, 1984; Farrell et al., 1994; Kalinin and Gesser, 2002; Overgaard et al., 2005). The kidney is affected by these changes in the blood as well, as it is responsible for the maintenance of acid base balance. Specifically the lung and kidney work in unison to maintain acid base homeostasis, with the lungs regulating bicarbonate (HCO_3^-) concentration and the kidneys reabsorbing bicarbonate from the urine and excreting hydrogen ions into urine. In addition, the kidney regulates the changing blood pressure seen during anoxia by maintaining salt and water balance, and it produces hormones such as erythropoietin which is released in response to hypoxia in the red-eared slider turtle (Milton *et al.*, 2006). Therefore, it is possible that *fr10* is involved in the protection of those organs most affected by anoxic conditions.

Figure 4.5 shows that dehydration of 40% of total body water results in an organ specific response concerning *fr10* expression in wood frogs. Specifically, brain and heart significantly increased expression compared to controls; kidney, liver and testes showing no change; and muscle and lung actually decreased their *fr10* transcript levels. This pattern of expression allows for several interpretations of what the role of *fr10* might be in dehydration. For example, dehydration tolerant *Rana sylvatica* and *Rana pipiens* have

been shown to defend water content of the core organs during dehydration of the whole organism. In *R. pipiens* significant decreases in water content are first observed in peripheral organs, namely skeletal muscles (Churchill and Storey, 1994). Following this, significant changes were seen for gut, kidney and heart upon 25.8% dehydration, for liver at 36.6% and brain only at 50% dehydration (Churchill and Storey, 1995). In *R. sylvatica* no significant difference in water content was observed for liver, kidney and heart at 50% dehydration, while muscle, gut and brain all showed a significant decrease at the same stage of dehydration (Churchill and Storey, 1993). Given that at 40% dehydration brain and heart showed significant increases in *fr10* mRNA whereas transcript levels in kidney and liver were unchanged compared to controls, it is possible that the protein coded by *fr10* participates in helping to defend the water content of these organs. In organs where water loss may be less critical, such as skeletal muscle, a decrease in *fr10* levels (and presumably FR10 protein) could be tolerated Meanwhile those organs whose function is critical, such as heart and brain, experience an increase in *fr10* which helps to strongly defend against water loss. Another possible explanation has to do with glucose content in the organs. In response to dehydration the wood frog stimulates liver glycogenolysis and exports high concentrations of glucose to the blood and other organs (Churchill and Storey, 1993). High glucose acts in the colligative retention of cell water during dehydration (Churchill and Storey, 1995). Churchill and Storey (1993) found that in frogs dehydrated to 50% of total body water showed a significant increase in glucose levels in the liver, kidney, brain and heart, but not in muscle and gut tissue. Moreover, the largest relative increase in glucose between control and 50% dehydrated frogs occurred in the brain, whose increase was 7.4 fold. This was followed by heart which

experienced a 3.1 fold increase and liver and kidney which both showed a 2.6 fold increase over control levels. Perhaps *fr10* is upregulated in response to relative glucose levels and its role is to prevent the detrimental effects normally associated with hyperglycemia. Other possibilities include that FR10 protein is involved in blocking the catabolism of glucose when it is taken up by cells, thus ensuring glucose pools remain throughout a freeze or dehydration episode. Another is that FR10 could counteract the normal homeostatic mechanisms that all vertebrates have that prevent glucose from rising to high levels. For example, normally as soon as glucose reaches a threshold level, glycogen phosphorylase is shut down and glycogen synthase is activated. However, this is not the case in frogs responding to freezing or dehydration. Here glycogen phosphorylase remains high during freezing/dehydration and glycogen synthase only rises again during thawing. Finally, *fr10* levels seem to reflect the work load on that organ for the duration of the dehydration stress. For example, both muscle and lung have decreased *fr10* mRNA in 40% dehydrated frogs and both experienced a decreased work load during dehydration. The muscles of the frog are largely inactive as the frog assumes a stance that reduces exposed surface area and therefore evaporative loss (Heatwole *et al.*, 1969), while oxygen consumption decreases by about 25% as animals dehydrate over time at a low temperature (Wu *et al.*, 2008). Meanwhile the heart, brain, kidney and liver all experience an increased work load as the heart must pump harder against viscous blood, the brain must coordinate dehydration behaviour, the kidney must maintain ion balance and the liver must produce glucose. Correspondingly, *fr10* levels in these tissues either maintained control conditions (liver and kidney) or significantly increased (brain and heart). What can be said regarding *fr10* and dehydration is that it is involved in the

protection of those organs most important to the wood frog, namely the heart and brain.

Analysis of fr10 transcript levels throughout wood frog metamorphosis

To further explore the potential role of *fr10*, expression levels were monitored over the course of metamorphosis of the wood frog, from Gosner stages 14 – 20 to stages 44 – 45 (Gosner, 1960). As seen in Figure 4.6, *fr10* expression appeared to be Gosner stage specific but with no clear overall trend emerging. Most developmental stages sampled expressed *fr10* at a transcription level of approximately 1.4 (compared with *fr10* expression at Gosner stages 14 – 20 that was assigned a transcription level of 1), except for a significant decrease at Gosner stages 31 – 35 and 42 – 43. The expression of *fr10* during tadpole development is surprising, since both in nature and in the lab environment the tadpoles never experienced cold or freezing temperatures. Therefore, *fr10* must play an additional role to that of freeze protection. It is possible that the protein has multiple functions at different life stages or physiological conditions, and that they will reveal themselves as having underlying similarities once the actual function of FR10 is discovered.

Conclusions

The overall role of *fr10* and the FR10 protein within the wood frog still remains unknown, however by examining its pattern of expression, several characteristics become evident. Expression of *fr10* is universal in the wood frog and the majority of organs tested experienced early and sustained transcription over the course of freezing. While this indicates a role for *fr10* in cryoprotection, Western blot data revealed a general lack of response by FR10 protein levels after freezing and thawing. It is possible that stress granules are acting to intercept and hold untranslated *fr10* mRNA while frogs are frozen,

until more favourable conditions for FR10 translation return. Further investigation revealed that *fr10* is also transcribed under anoxic and dehydration conditions, both of which are component stresses of freezing. This implicates *fr10* in a role that is common to all three physiological stresses. Finally, *fr10* appears to be important throughout development of the wood frog from embryo to fully developed frog, and therefore it may have another novel role in addition to cryoprotection.

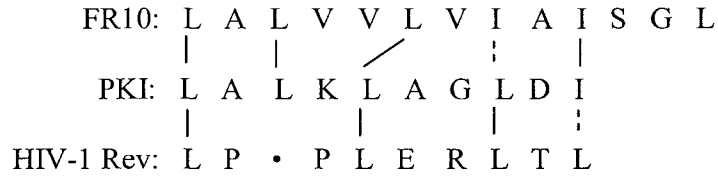

Figure 4.7: Amino acid alignment for the nuclear export signal (NES) sequences of FR10, human immunodeficiency virus type-1 Rev (HIV-1 Rev) and protein kinase A inhibitor protein (PKI). The hydrophobic residues leucine and isoleucine are critical to the nuclear exporting function. A solid line represents identical amino acids (either leucine or isoleucine) between two or more of the sequences, while a dashed line indicates similar amino acids. The black dot indicates an introduced space to allow for better alignment.

Chapter 5

FR47

5.1 Introduction

The *fr47* sequence obtained from the clone and extended by 5' RACE was found to be 3678 bp (McNally *et al.,* 2003). When the full nucleotide sequence was analyzed for an open reading frame, two possible start sites were found at 2004 and 2163 bp, and one stop codon at 3176 bp. Theoretically this would produce polypeptides of 390 and 337 aa in length, with molecular weights of 45.7 and 39.8 kDa, respectively. As the name of the gene implies, McNally *et al.* (2003) determined the protein product to be approximately 47 kDa, therefore corresponding to the first start codon at 2004 bp. A Kyte-Doolittle hydrophobicity plot of the putative FR47 protein indicated a highly hydrophobic region near the C terminus of the protein from amino acid positions 350 to 370 (McNally *et al.*, 2003). Such a hydrophobic region is common amongst proteins and likely represents a transmembrane segment to the protein. A BLAST search of both the nucleotide and polypeptide sequence showed no significant similarity to any known gene or protein (McNally *et al.*, 2003). The present study presents an in-depth analysis of the expression of *fr47* gene transcripts and FR47 protein in multiple organs of wood frogs in response to freezing, thawing, anoxia and dehydration stresses, as well as metamorphosis. The data provide greater insight into the potential role of the FR47 protein in vertebrate freeze tolerance.

5.2 Materials and Methods

Animal treatment and tissue preparation

Male wood frogs were treated, sacrificed and tissues were collected as previously described in Chapter 2.

cDNA synthesis and Reverse-Transcriptase (RT)-PCR amplification

RNA was isolated and used to synthesize cDNA as previously described in Chapter 2. Primers used were designed using the Primer Design Program v.3 (Scientific and Educational Software) based on the sequence for *fr47* (GenBank ID: AY100690). Primers were tested and the PCR products were sent for sequencing to confirm the target genes were amplified. The PCR primers for each gene, the optimal melting temperature (T_M), and the cDNA fragment size amplified is shown below in Table 5.1.

Table 5.1 Optimal conditions for RT-PCR of *fr47* related genes

Gene	Primer Sequence	T_M	Size
fr47	Forward 5'-GTTGACATCGTCCTCCTCTC-3' Reverse 5'- CGT GTC GGC ACC GAG CTT AA -3'	62.3 67.6	479 bp
fr47	Forward 5'-TCCACCAGCTTCTCTGTACC-3' Reverse 5'- GAGTCAGGATCTGGAATGGA -3'	64 61.5	784 bp
α-tubulin	Forward 5'-GCCTCATTGTCCACCATGAA-3' Reverse 5'-GTGTCGGTACTGGATCTGGC-3'	73 71	179 bp

The first set of primers, producing a 479 bp PCR product, were used in for the amplification of *fr47* mRNA in 4 h and 24 h frozen liver and muscle, and 24 h frozen brain, kidney, ventral skin, dorsal skin, testes and heart tissues. Because of problems with consistency, the second set of primers was used for 24 h frozen lung, stomach, small intestine, large intestine, as well as all development, anoxia and dehydration studies.

Western blotting

Total protein was isolated and treated as previously described in Chapter 2. SDS-polyacrylamide gels were prepared with a 10% stacking (10% acrylamide, 400 mM Tris pH 8.8, 0.1% w/v SDS, 0.1% w/v APS, 0.04% v/v TEMED) and a 10% upper separating gel (10% acrylamide, 130 nM Tris pH 6.8, 0.1% w/v SDS, 0.1% w/v APS, 0.1% v/v TEMED). This was loaded with 25 μg total soluble protein for brain, 30 μg for heart, 25

μg for kidney, 15 μg for liver, 30 μg for muscle and 18 μg for dorsal skin. The gel ran in a Mini-Protean III apparatus (BioRad) at 180 V for 45 min at RT in SDS-PAGE running buffer. This running buffer was diluted 10-fold from the stock solution (25.5 g Tris-base, 460 g glycine, 25 g SDS, adjusted to 2.5 L with water) before use. Resolved proteins were electroblotted onto 0.45 μm pore size polyvinylidene difluoride membranes (Millipore) at RT for 90 min at 160 mA by wet transfer (transfer buffer: 25 mM Tris (pH 8.5), 192 mM glycine and 10% v/v methanol). The blots were blocked differently depending on the tissue, as summarized in Table 5.2. After being extensively washed, membranes were incubated overnight in 1:1000 v/v primary antibody in TBST at 4 °C, save for dorsal skin which was incubated in 1:2000 v/v primary in TBST. These primary rabbit antibodies were produced against a synthetic peptide (KRLKRRFSTEW) corresponding to the C-terminal end of the FR47 protein by Sigma Genosys (The Woodlands, Texas). Following incubation, blots were washed and incubated with HRP linked anti-rabbit secondary in TBST (1:4000 v/v dilution) for 45 min. Protein signal was developed and measured as described in Chapter 2.

Table 5.2 Summary of blocking conditions used in FR47 Western blots

Tissue	Blocking Agent	Concentration	Time
Brain	70 – 100 kDa PVA	1 mg/mL	30 s
Heart	70 – 100 kDa PVA	1 mg/mL	30 s
Liver	70 – 100 kDa PVA	1 mg/mL	2 min
Dorsal Skin	70 – 100 kDa PVA	1 mg/mL	2 min
Kidney	30 – 70 kDa PVA	1 mg/mL	30 s
Muscle	30 – 70 kDa PVA	3 mg/mL	2 min

5.3 Results

cDNA cloning of fr47

The PCR products that were amplified by primers designed for *fr47* (Table 5.1) were confirmed as encoding portions of the *fr47* sequence using BLASTN. The obtained *fr47* product using the first set of primers was 479, which represents about 13% of the full 3678 bp mRNA sequence. The second set of *fr47* primers produced a 784 base pair (bp) PCR product, which represents about 21% of the mRNA sequence.

FR47 protein detection

The antiserum for FR47 created against the C-terminal end of the protein was found to cross react with a major band at approximately 47 kDa. This corresponds to the 47 kDa MW observed by McNally *et al.* (2003) for the protein, as well as the predicted molecular weight of 47 kDa.

The effect of freezing on fr47 transcription

An initial analysis of the *fr47* transcriptional response to freezing was conducted on wood frog liver and skeletal muscle, assessing the effects of 4 h and 24 h of freezing. Both tissues showed a strong significant increase in *fr47* transcripts as compared to control values after 4 h of freezing (Figure 5.1); transcript levels of *fr47* increased by 2.08 ± 0.19 fold in liver and by 2.47 ± 0.14 fold in muscle. Transcript levels remained elevated after 24 h frozen at 1.48 ± 0.08 and 1.75 ± 0.1 fold controls for liver and muscle, respectively. However, in both cases this represented a statistically significant decrease in *fr47* transcript levels between 4 and 24 h frozen.

A subsequent multi-tissue analysis of *fr47* mRNA levels supported an overall pattern of increased transcription upon freezing of wood frogs. Figure 5.2 shows that 24

h of freezing increased *fr47* transcript levels in heart by 4.66 ± 0.41 fold as compared with controls. Elevated transcript levels were also observed in kidney, lung and testes after 24 h frozen, where levels were 1.99 ± 0.07, 2.86 ± 0.55, and 1.48 ± 0.14 fold higher than respective control values. Three tissues each showed no change or a significant decrease in *fr47* mRNA levels between control and 24 h frozen frogs. More specifically, frozen brain had *fr47* transcript levels 1.17 ± 0.06 fold that of control, frozen ventral skin was 0.92 ± 0.13 of control, and frozen small intestine was 0.91 ± 0.09 of control, all of which are not statistically significant differences. Relative transcript levels in dorsal skin, stomach and large intestine of 24 h frozen frogs showed significant decreases to 59 ± 6%, 24 ± 4% and 64 ± 4% of control levels, respectively.

Analysis of FR47 protein levels during freezing and thawing

Based on the general increase in transcript levels in response to freezing, it was expected that protein levels would follow correspondingly. However, this was not the case (Figure 5.3). Brain, heart, dorsal skin and kidney all showed no change in their FR47 protein level between control and 24 h frozen frogs with values of 1.24 ± 0.15, 0.81 ± 0.08, 0.95 ± 0.11, and 0.88 ± 0.2, respectively, as compared with controls. Liver and muscle were unique in that they experienced a significant decrease upon freezing to 0.29 ± 0.03 and 0.76 ± 0.05 of control levels. Even more surprising, most protein levels stayed consistent with control levels after thawing for 8 h. Figure 5.3 shows that after thawing, FR47 levels were 0.93 ± 0.11 that of control in brain, 0.99 ± 0.11 in muscle, 0.98 ± 0.14 in heart, and 0.89 ± 0.1 in dorsal skin. Kidney showed a decrease after 8 h of thaw to 0.75 ± 0.04 of control levels. Liver continued to be unique in that FR47 protein levels after 8 h thaw were significantly less than those at the control time point (0.57 ±

0.03), but were significantly higher than the 24 h frozen time point (1.99 ± 0.03 fold increase).

The effect of anoxia and 40% total body water dehydration on fr47 transcription

To further explore the factors that could be triggering *fr47* expression during freezing, transcript levels were analyzed in frogs exposed to two of the component stresses of freezing: anoxia and dehydration. Compared to control values, *fr47* mRNA levels increased in all tissues (except for testes) after frogs were held for 24 h under anoxic conditions (Figure 5.4). Liver showed the greatest increase in *fr47* expression at 12.65 ± 2.4 fold higher than control values, followed by skeletal muscle (3.86 ± 0.64 fold), brain (3.07 ± 0.41 fold), lung (2.9 ± 0.61 fold), heart (2.22 ± 0.19 fold) and kidney (1.59 ± 0.1 fold). Only testes showed no change in *fr47* expression after 24 h anoxia. Dehydration of 40% of the total body water also triggered increased expression of *fr47* in three of the seven tissues tested (Figure 5.5). Liver, heart and brain showed increases of 7.98 ± 1.29, 3.93 ± 0.31 and 2.51 ± 0.43 fold compared to control values, respectively. The remaining four tissues showed no change in *fr47* expression in response to dehydration (1.01 ± 0.23 for lung, 1.24 ± 0.19 for muscle, 1.01 ± 0.09 for testes and 1.28 ± 0.09 for kidney).

Analysis of fr47 transcript levels throughout wood frog metamorphosis

The *fr47* transcript was detected throughout the stages of development in the wood frog (Figure 5.6). Expression gradually increased throughout development finally resulting in an 8.28 ± 0.94 total increase in *fr47* mRNA between Gosner stages 14 – 20 (where the embryo has a neural fold – used as a starting point) and Gosner stages 44 – 45 (where the frog is almost fully developed). The increase first became apparent at stages

26 – 30, where the back limp buds first appear, with a 3.02 ± 0.17 fold increase over the starting point. The level of *fr47* transcription remained fairly consistent over the next three stages of development, with final stages 44 – 45 showing a greater than 2 fold increase over the previous stage.

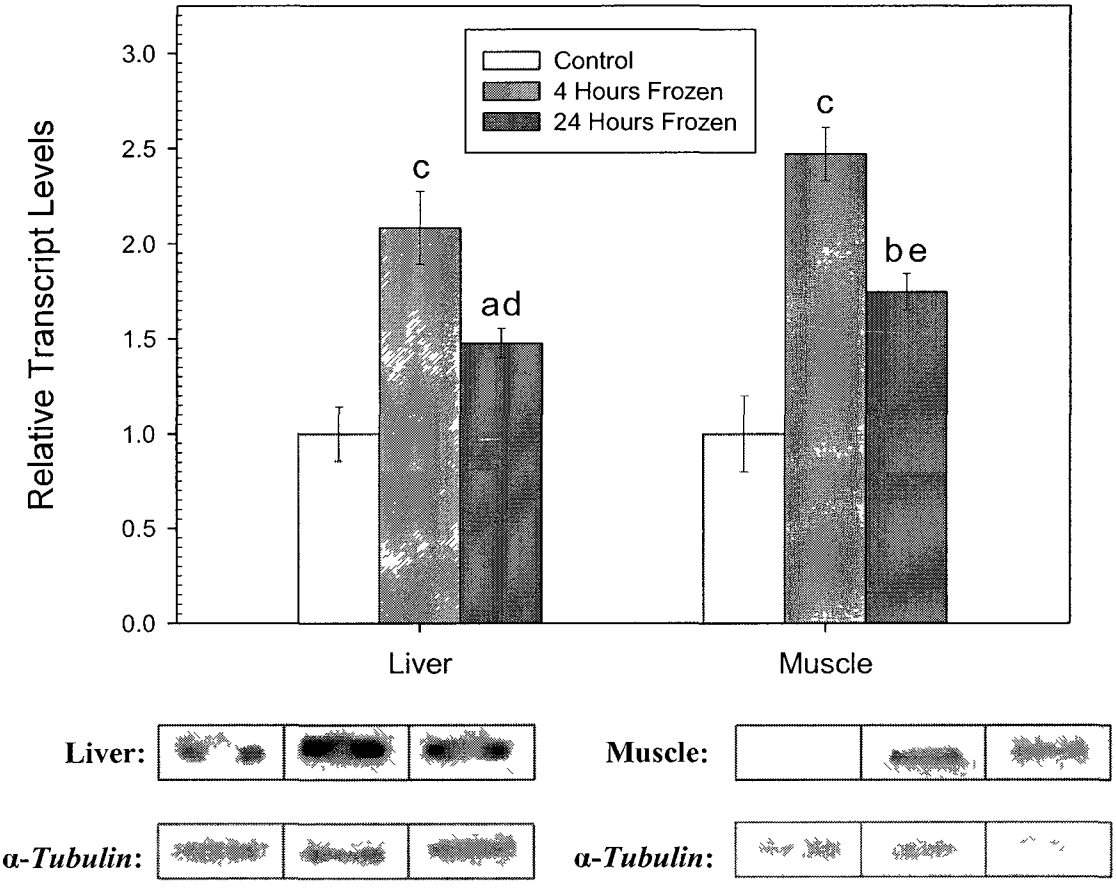

Figure 5.1: RT-PCR analysis showing the effects of 4 h and 24 h freezing on *fr47* mRNA transcript levels in liver and hind leg skeletal muscle of the wood frog. Representative PCR product bands on agarose gels are shown along with a histogram showing mean mean normalized band intensities (± SEM, n=4-5 independent determinations). Band intensities for *fr47* were normalized against α-*tubulin* bands amplified from the same sample. Data were analyzed using analysis of variance with a post hoc Student-Newman-Keuls test where the letters a, b and c represent significant differences between indicated stress and control and d, e and f represent significant differences between the indicated stress and the time point previous to it; a and d indicate $p<0.05$, b and e indicate $p<0.01$ and c and f indicate $p<0.005$.

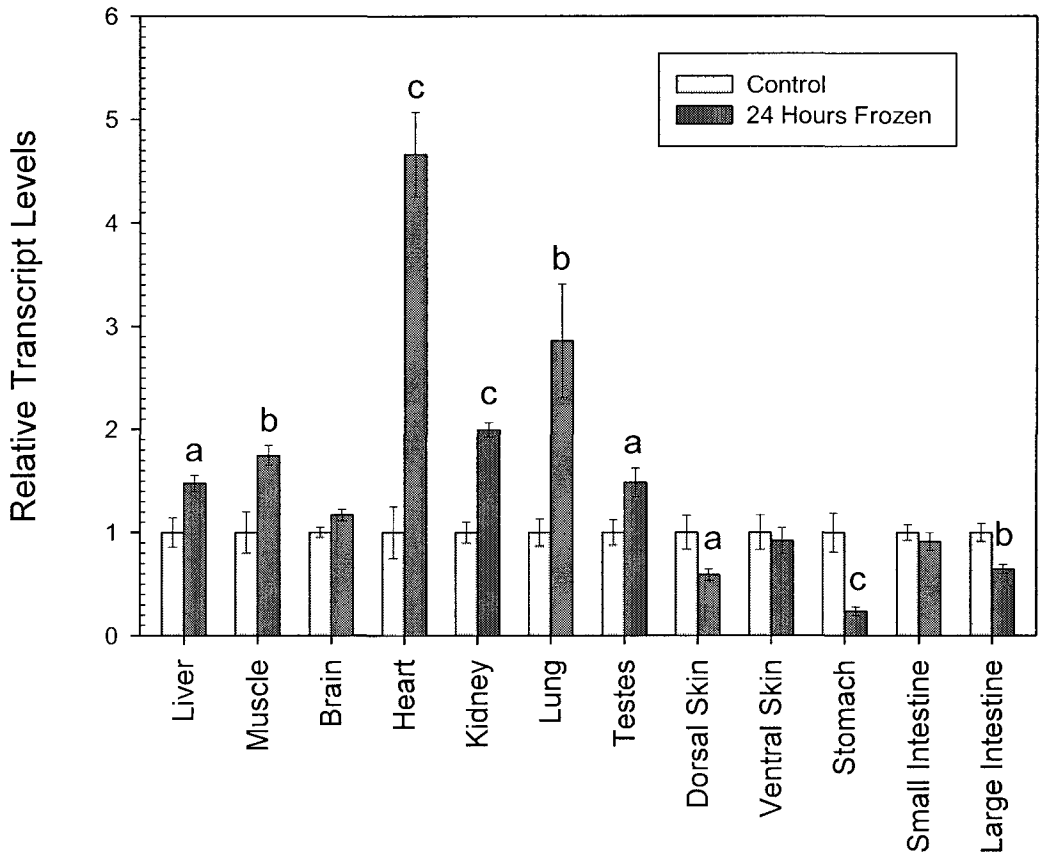

Figure 5.2: RT-PCR analysis showing the effects of 24 h freezing on *fr47* mRNA transcript levels in twelve tissues of the wood frog. Representative PCR product bands on gels are shown along with a histogram with mean normalized values (± SEM, n=4-6 independent samples). Representative *fr47* and α-*tubulin* bands are located on the next page. Other information as in Figure 5.1.

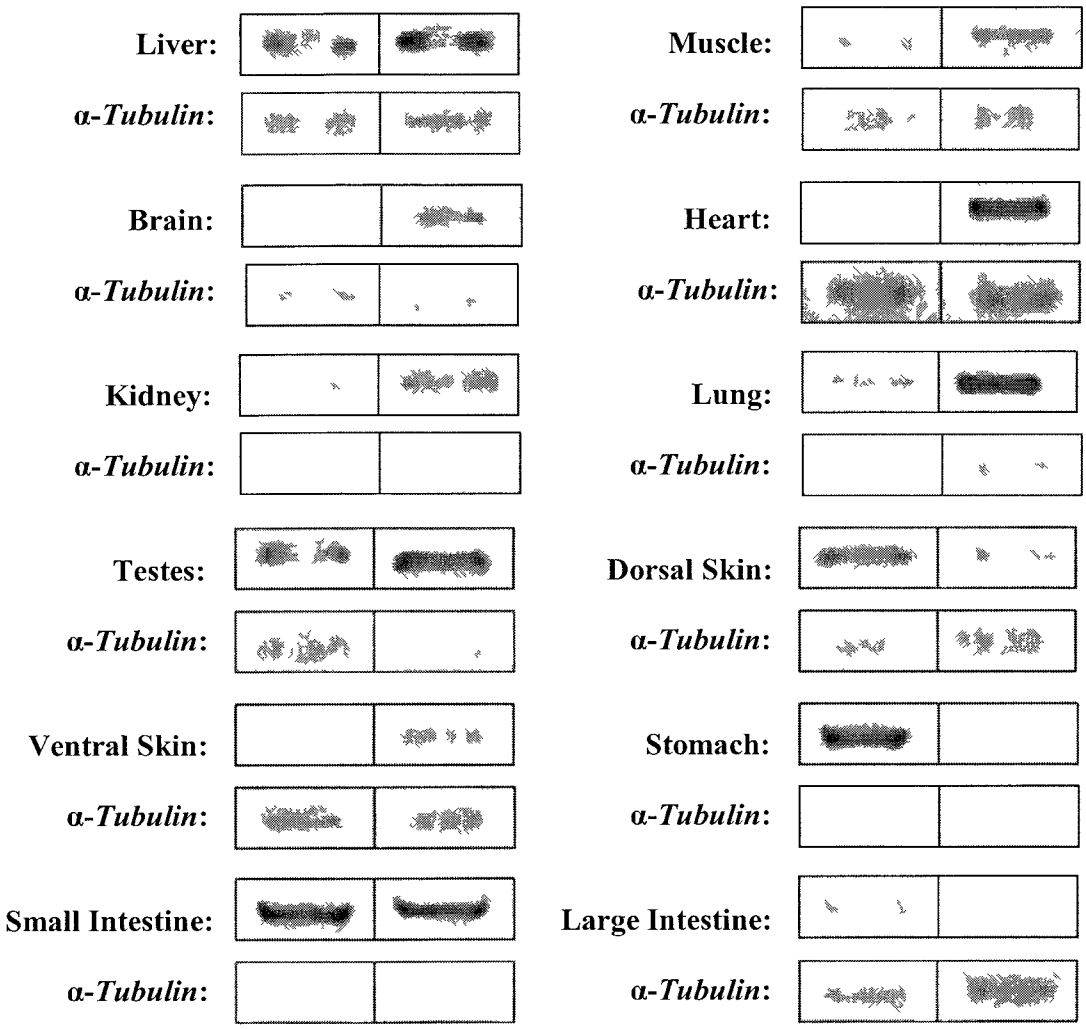

Figure 5.2 Continued (see legend on previous page)

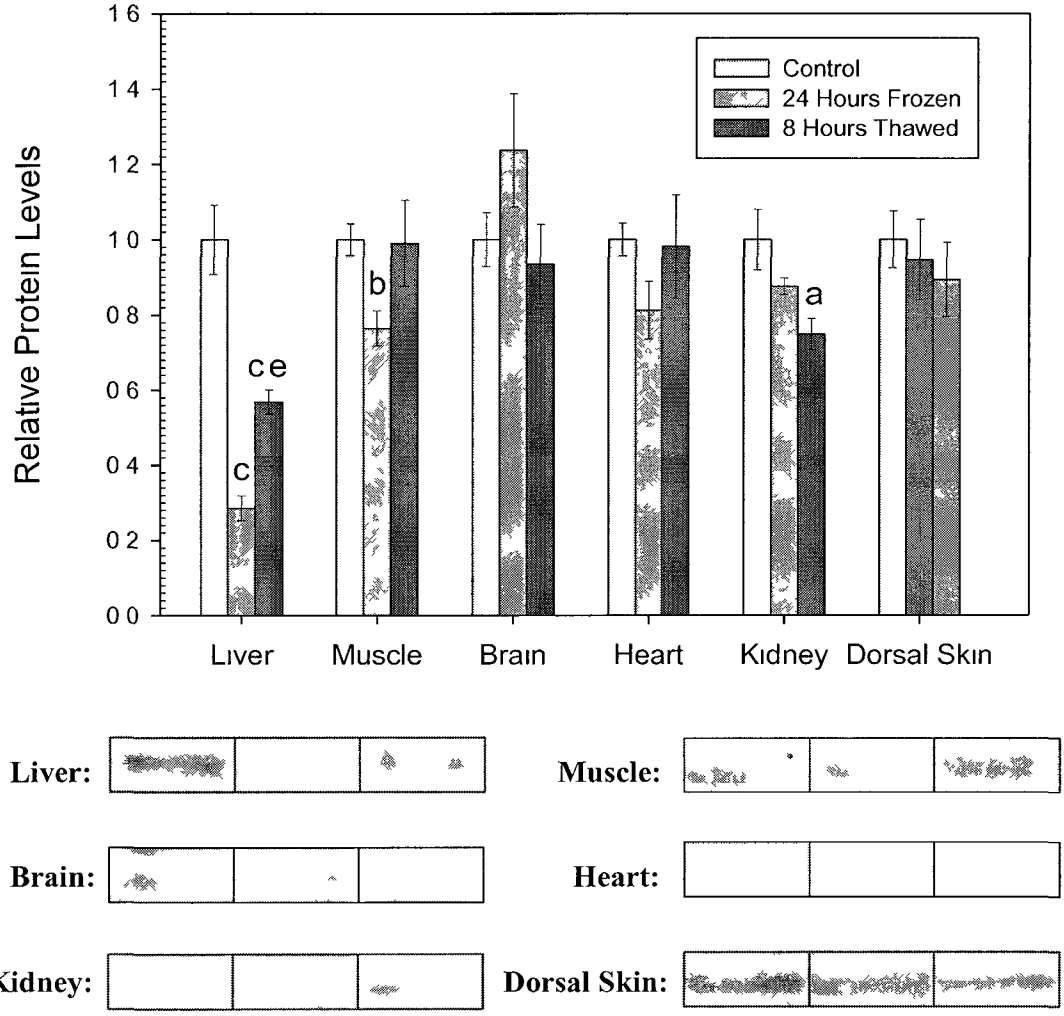

Figure 5.3 Western blot analysis showing the effects of 24 h freezing, followed by 8 h thawing on FR47 protein levels in six tissues of the wood frog Representative Western blots are shown and the histogram shows mean normalized values (± SEM, n=4 independent samples) for FR47 Information on statistical testing is as in Figure 5 1

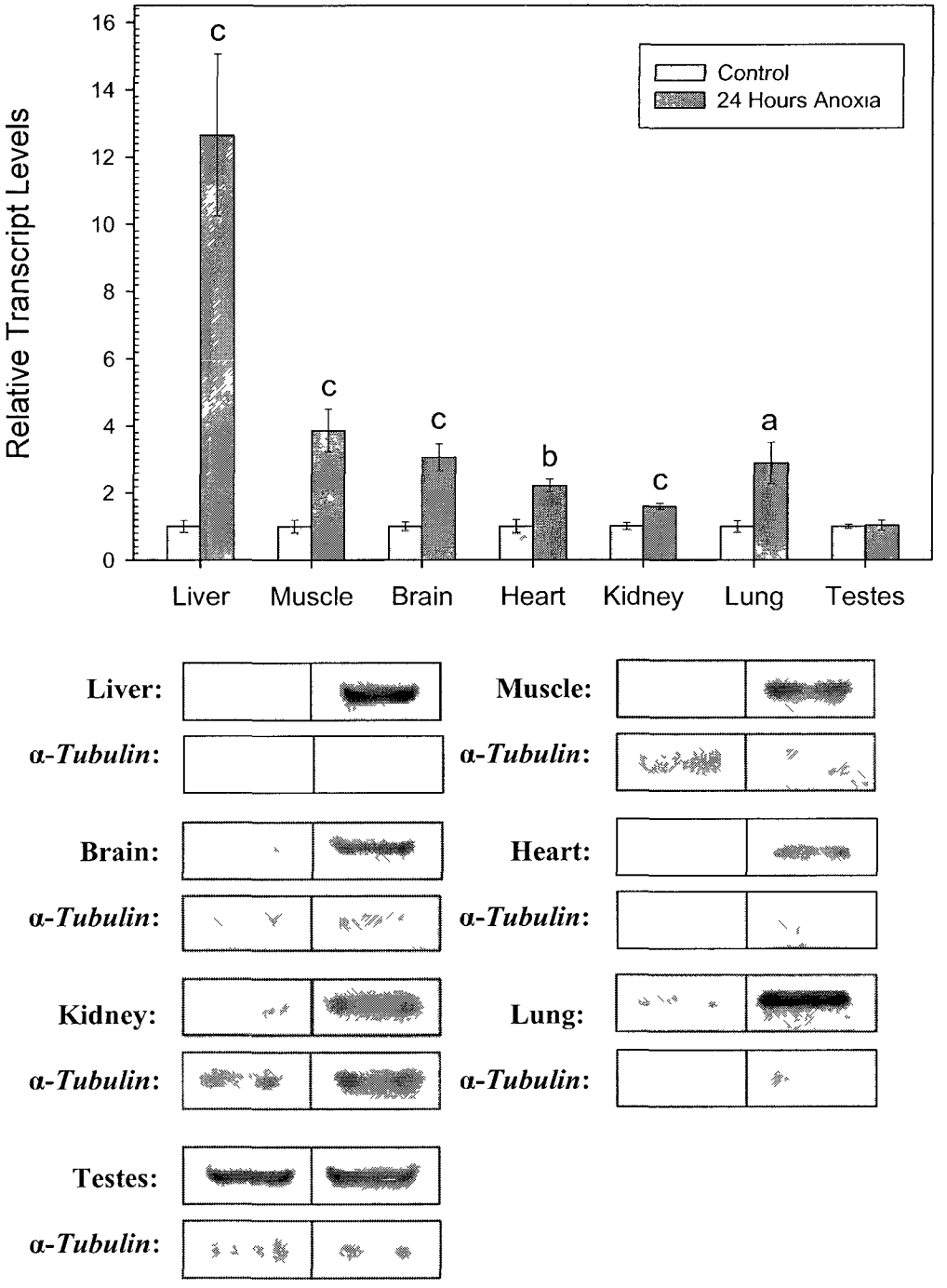

Figure 5.4: RT-PCR analysis showing the effects of 24 h anoxia exposure at 5 °C on *fr47* transcript levels in seven tissues of the wood frog. Representative PCR product bands on gels are shown along with a histogram showing mean normalized transcript levels (± SEM, n=5-8 independent determinations). Other information as in Figure 5.1.

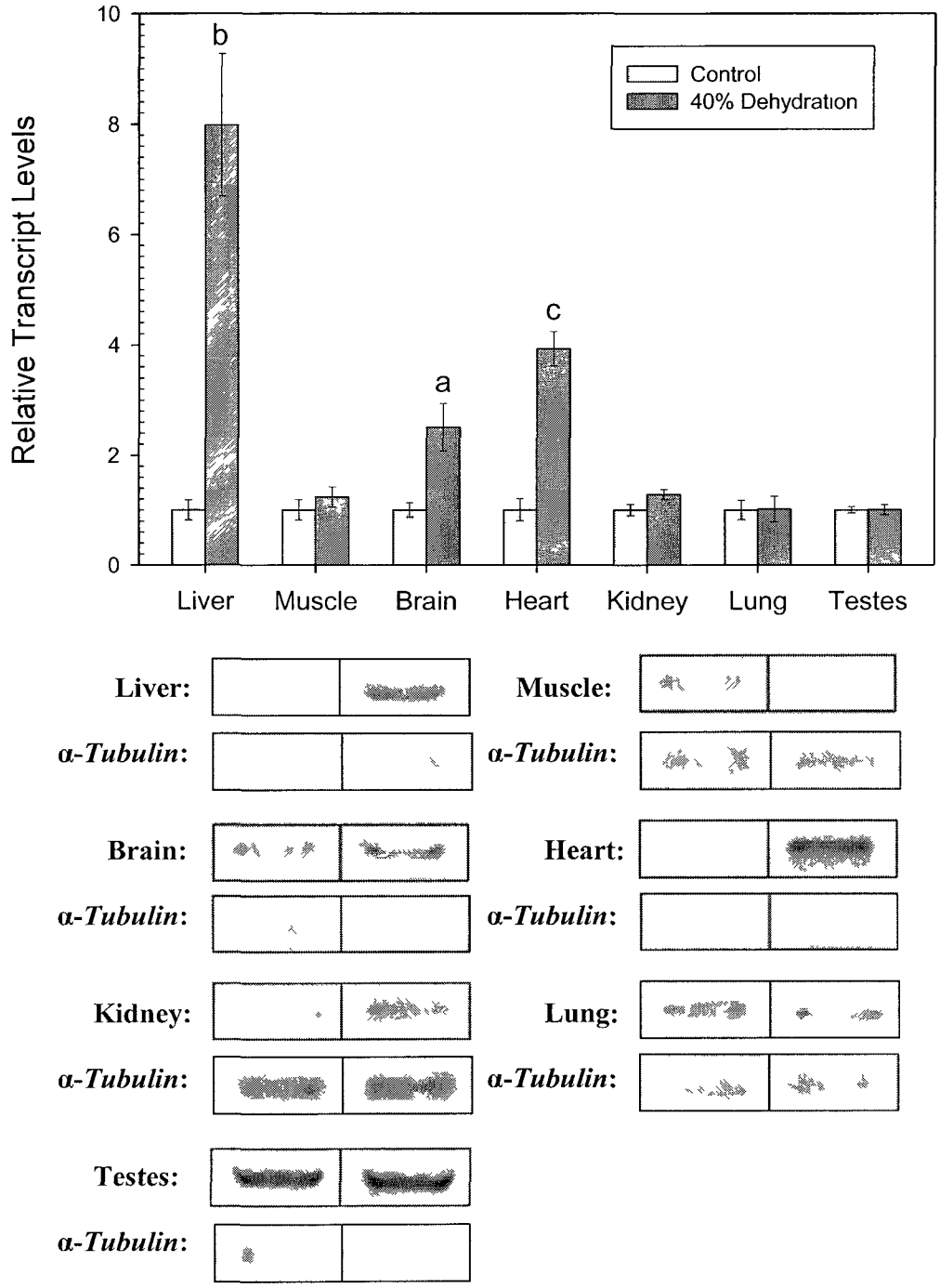

Figure 5.5. RT-PCR analysis showing the effects of 40% dehydration at 5 °C on *fr47* transcript levels in seven tissues of the wood frog. Representative PCR product bands on gels are shown and histogram shows mean normalized values (± SEM, n=5-8 independent determinations). Other information as in Figure 5.1.

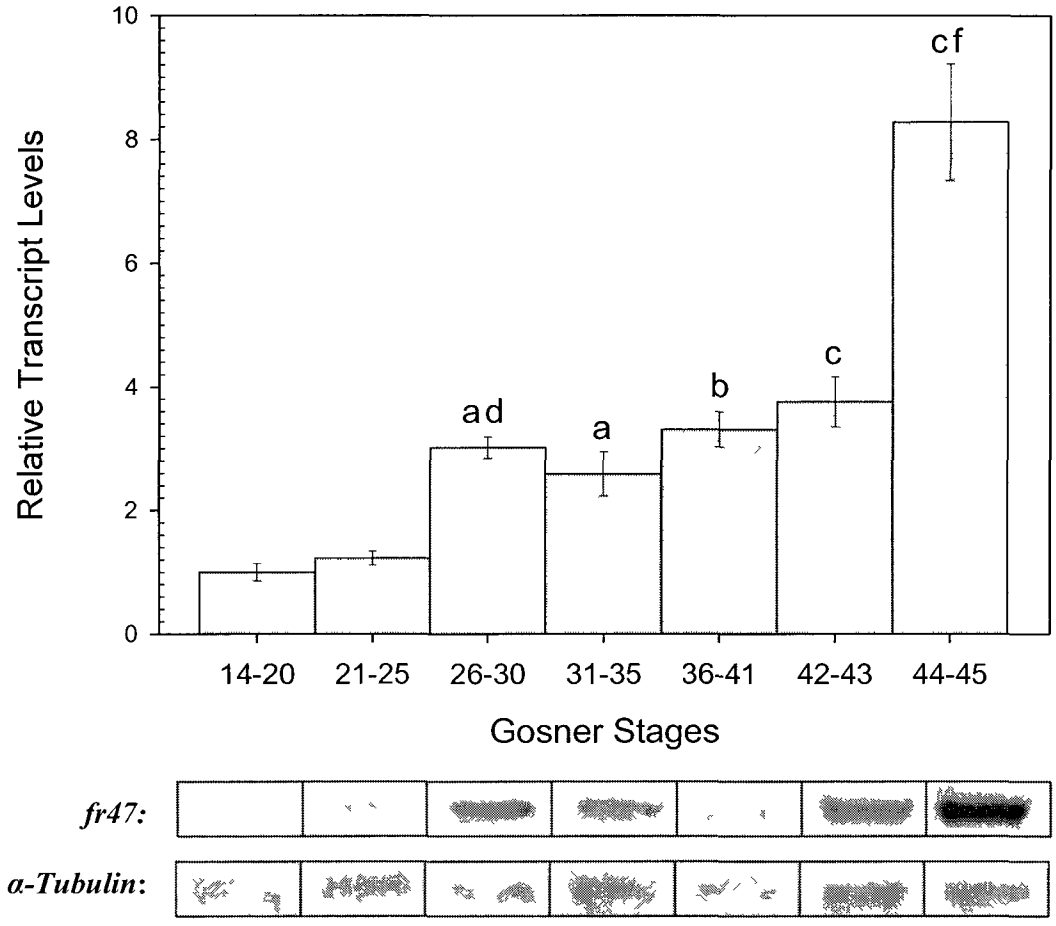

Figure 5.6: Changes in *fr47* mRNA transcript levels over the course of tadpole development in the wood frog. Representative PCR product bands on gels are shown and the histogram shows mean normalized values (± SEM, n=5-6 independent determinations). The letters a, b and c represent significant differences between Gosner stages 14 – 20 and the indicated stage whereas d, e and f indicate significant differences between the indicated stage and the stage immediately preceding it; a and d indicate $p<0.05$, b and e indicate $p<0.01$, and c and f indicate $p<0.005$.

5.4 Discussion

The effect of freezing on fr47 transcription

RT-PCR analysis showed that *fr47* is expressed in all twelve wood frog tissues tested. This differs from previous data based on Northern blotting that detected *fr47* transcripts in liver but not in brain, heart, lung, kidney, muscle or gut tissues (McNally *et al.* 2003). The difference in these findings is likely due to the greater sensitivity of PCR compared with the Northern blotting technique. These new findings suggest that the *fr47* probably has a function that is required in all cells for freezing survival. However, the magnitude of the response of *fr47* transcript levels to 24 h of freezing exposure was dependent on the organ. Freezing increased the expression of *fr47* in six of the twelve tissues tested with transcript levels rising 1.4 to 4.7 fold as compared with control, unfrozen frogs. Of the remaining six tissues, half showed no change in *fr47* levels after 24 h freezing where as dorsal skin, stomach and large intestine actually showed reduced expression after freezing. Taken as a whole, these results indicate that the *fr47* gene is responsive to signals arising from specific tissue freezing. One hypothesis for the mechanism of *fr47* upregulation is taken from the activation of the cryoprotectant glucose. It is well known that within 2 to 5 min after freezing begins on the frog skin surface, glucose production by liver and export into the blood is rapidly increasing (Storey and Storey, 2001). It appears that glucose synthesis arises from an extreme exaggeration of the "fight or flight" response that increases blood glucose levels in all vertebrates during times of stress (Storey and Storey, 1990). This concept is supported by the fact that compounds that block the action of adrenaline (which mediates the fight or flight response) on wood frog liver also effectively block glucose synthesis during

freezing (Storey and Storey 1990, 1996). However, this hypoglycaemic effect has been altered to respond to ice nucleation as the stimulus, and feedback mechanisms that normally limit the magnitude of the glucose response are inhibited or overridden to allow for the massive increase in glucose seen during freezing (Storey and Storey, 1988). A potential parallel with the "fight or flight" pathway (adrenaline stimulated, cAMP mediated) is proposed as a possible control of *fr47* upregulation, as those organs vital to "fight or flight" are also those that show strong upregulation of *fr47* during freezing. For example, physiological responses associated with "fight or flight" include an increase in heart rate, an increase in respiration, increased skeletal muscle activity, a release of sugar from the liver and a suppression of circulation to and activity of the digestive organs (Funkenstein, 1958). Correspondingly, the strongest increases in *fr47* transcription upon freezing occurred in the heart (4.67 fold), lung (2.86 fold), kidney (1.99 fold), liver (1.48 fold) and muscle (1.42 fold) (Figure 5.2) with even higher transcript levels in liver and muscle after 4 h of freezing (Figure 5.1). If "fight or flight" is being activated in the frog in response to ice nucleation, these are the organs that would respond. Indeed, it has previously been shown that the onset of freezing triggers an immediate two-fold increase in the heart beat of wood frogs which gradually slows over time as ice accumulates (Layne *et al.*, 1989). Therefore, *fr47* maybe acting in a cryoprotective manner to ensure these "fight or flight" organs are the last to freeze or first to thaw, which would allow the wood frog to maintain defence during a critical time period. This concept is further supported by the fact that *fr47* transcript levels stay the same or decrease compared to controls in ventral skin, small intestines, dorsal skin, stomach and large intestines. When in "fight or flight" blood is directed away from these organs as processes like digestion

are not as evolutionarily important during a relatively brief period of threat.

Analysis of FR47 protein levels during freezing and thawing

The increase in *fr47* transcription with freezing was not mirrored by an increase in FR47 protein expression over the time frame examined. As seen in Figure 5.3, four of the six tissues examined showed no change in FR47 protein levels after 24 h of freezing, and the two remaining tissues showed reduced FR47 in frozen frogs as compared to controls. This pattern largely remained after 8 h of thawing except for a partial recovery of FR47 in liver and a further reduction in kidney. This might indicate that FR47 is not vital to the wood frog during freezing and thawing, or that *fr47* transcripts are controlled by post-transcriptional mechanisms. This later hypothesis is entirely possible based on the very large predicted 5' and 3' untranslated regions (UTR) of *fr47*. The 5'UTR of *fr47* is predicted to be over 5 kb in length (McNally *et al.*, 2003), whereas the same region of more than 90% of characterized mRNAs is between 20 and 100 nucleotides in length (Kozak, 1987 and Kozak, 1991). A long 5'UTR is usually indicative of messages that are regulated by translation initiation (Pain, 1996). It has also been suggested that for 5' UTRs, a greater length together with a lower potential to form secondary structure near the cap confers a transcriptional advantage (Kozak, 1994). Such mRNAs are translated very efficiently and show strong resistance to inhibition of translation during times of cellular stress that impair overall protein synthesis (Pain, 1996).

The theory that the FR47 protein is not essential during freezing and thawing seems improbable given additional information. For example, a total of five frog species have been examined for the presence of the FR47 protein (McNally *et al.*, 2003). Three were freeze tolerant (*R. sylvatica*, *Pseudacris crucifer*, and *Hyla versicolor*) and two were

freeze intolerant (*R. pipiens* and *Scaphiopus couchii*). Western blotting showed that the FR47 protein was detected only in the freeze tolerant frogs, which suggests the function of this protein is related to freezing survival (McNally *et al.*, 2003). Furthermore, McNally *et al.* (2003) found that protein levels for FR47 increased by 1.6 ± 0.1 fold over controls after 24 h of freezing in *R. sylvatica* liver, and rose even higher in the early stages of thawing (1, 2 and 4 h), only to return to freezing levels after 8 h of thawing. They concluded that FR47 had a function that became increasingly important with long term freezing exposure, or that it is needed during the early hours of thawing. Based on these conclusions, as well as the data obtained in this study, it is hypothesized that although *fr47* mRNA transcripts increase significantly during freezing, the translation of *fr47* is delayed until the frog begins to recover during thawing. This is may be because the freezing of blood plasma leads to an ischemic state which limits ATP-expensive processes such as protein synthesis for the duration of the freeze. The increased transcription of *fr47* during freezing allows for an immediate synthesis of the FR47 protein as soon as thawing begins (McNally *et al.*, 2002 and 2003). Based on this, a possible role for FR47 would be in the recovery of cell function after the stress of freezing. Again, it is possible that FR47 is specifically important in those organs involved in the "fight or flight" response, thus allowing frog to obtain defences and return to functionality as soon as possible. Therefore, it is likely that the lack of change in FR47 protein levels seen in this study may have been due to not enough time points being examined, specifically during thawing. In the future at least the 2 h thawing time point should be examined, as this is where FR47 protein levels reached their peak for liver in the McNally *et al.* (2003) study.

The effect of anoxia and 40% total body water dehydration on fr47 transcription

It has been discovered that nearly every wood frog gene that alters its expression in response to freezing also responds to either anoxia or dehydration signals, both of which are component stresses of freezing (Storey, 2004). The current data (Figure 5.4 and 5.5) show that *fr47* transcript levels are increased after 24 h of anoxia in six of the seven tissues tested, and that three tissues showed an increase in transcript levels in response to 40% dehydration. Previous work by McNally *et al.* (2003) on liver alone concur with the present results, showing a strong increase in *fr47* transcription as a result of 24 h anoxia and a lesser response to 20% dehydration. It is likely that the increases in *fr47* observed at a much higher level of dehydration (40%) in the present study are compounded by the hypoxia that develops at high water loss. This is because at 40% dehydration, the increased viscosity and reduced blood volume makes oxygenation of organs increasingly difficult (Wu *et al.*, 2009). Further support for the role of FR47 in anoxia survival as well as freezing is the response of *fr47* to phorbol 12-myristate 13-acetate (PMA), which is a stimulator of phospholipid dependent protein kinase C (PKC). McNally *et al.* (2003) showed that *fr47* transcription in the liver increased in both a dose dependent and time dependent manner in response to the secondary messenger PMA. This ties back into freezing stress as it has been previously shown that inositol 1,4,5-triphosphate (IP_3) levels, an intracellular secondary messenger of PKC, also rises progressively during freezing in wood frog liver. IP_3 levels are approximately 3-fold greater than controls after 4 h freezing and 11-fold greater at 24 h freezing (Holden *et al.*, 1996). Brain also showed elevated levels of IP_3 upon freezing, however it responded most strongly at intermediate lengths of 4 h and 8 h freezing. Finally skeletal muscle also

showed a 55% increase in IP_3 after 24 h of freezing (Holden *et al.*, 1996). IP_3 levels also rose by 8 fold in the liver of wood frogs exposed to 30 min of anoxia, but were less responsive to 20% dehydration (an ~3 fold increase) (Storey, 2004). Therefore, freezing, anoxia and dehydration stimulated IP_3, most likely as a consequence of increased PMA. Increased PMA directly results in increased transcription of *fr47*, thus indirectly supporting the conclusion of this study that FR47 has a function in freezing and its component stresses anoxia and dehydration.

Analysis of fr47 transcript levels throughout wood frog metamorphosis

The role of *fr47* was further examined during development of the wood frog from embryo to fully developed frog (Figure 5.6). Expression of *fr47* increased steadily throughout development until the final Gosner stages 44 – 45 (Gosner, 1960), where the frog has almost fully catabolized its tail. The rise in *fr47* transcripts first became significant at Gosner stages 26 – 30 (when the back limp buds had appeared) and continued to rise until the last stage of development where *fr47* transcription was over 8 fold greater than in the embryos (Gosner stages 14 – 20). This is significant since wood frog eggs are typically laid in April, when the threat of freezing has largely passed. Moreover, in the present study, development from eggs to adults all occurred at room temperature and therefore the animals never experienced cold. This indicates that *fr47* has a role in wood frog development in addition to freezing. Interestingly, Gosner stages 26 – 30 (where the increase in *fr47* transcripts first became significant) also marks the development and use of the lungs by tadpoles (Gosner, 1960). Perhaps the additional role of *fr47* has to do with the use of their lungs, which would become increasingly important as it develops into a land dwelling adult.

Conclusions

The results for *fr47* expression in the wood frog indicate a multi-function protein whose expression is organ specific. By examining its pattern of expression, it is possible to confirm that *fr47* is involved in freezing survival as well as anoxia and dehydration tolerance. The data also indicate that *fr47* plays an additional role in the developing wood frog. Based on the multi-organ patterns of *fr47* gene expression, we now have strong evidence to indicate an important role for FR47 in wood frog stress tolerance that justifies continuing efforts to characterize the protein and identify its cellular function.

Chapter 6

General Discussion

6.1 Comparison between *li16*, *fr10* and *fr47*

Table 6.1 presents a direct comparison of the properties of the three novel wood frog genes including transcriptional responses to freezing, anoxia, dehydration and tadpole development, and translational responses to freezing and thawing. This table shows that all three genes share some aspects of their expression in response to environmental stresses. All three genes were freeze responsive in a tissue dependent manner, with the majority of tissues tested showing increased expression of *li16*, *fr10* or *fr47*. Furthermore, all three shared significant increases in transcription after 24 h freezing in liver, skeletal muscle, heart, lung and testes. The increases observed in liver, heart and lung makes sense as these organs are of the utmost importance to the freezing frog. Liver creates glucose which provides colligative resistant to volume reduction, heart circulates this glucose and the lungs attempt to maintain oxygenation in the face of increasing hypoxia/anoxia. Enhanced expressional responses in skeletal muscle and testes appear to be more difficult to explain, since these tissues do not have an obvious role in contributing to whole body freeze tolerance. However, protection of testes is arguably a very critical issue since they produce and contain the sperm that are needed for early spring breeding by the frogs (Costanzo *et al.*, 1998). Freezing protection of sperm (and eggs in females) would ensure breeding success. This is especially essential as most wood frogs, male and female, will breed only once in their lives. Very few individuals may breed two or three times (Berven, 1980). Skeletal muscle is one of the first tissues to freeze and has a low capacity for acquiring any centrally-produced (ie. liver) cryoprotectants from the blood. As such, it is likely that muscle must undertake all needed cryoprotective responses by itself, including up-regulation of *li16*, *fr10* and *fr47*.

It was because of their freeze-responsive increase in *li16*, *fr10* and *fr47* expression that these five tissues were further examined to determine their responses to the stresses of anoxia and dehydration (in addition to kidney and brain tissue). In those studies it was found that both heart and kidney showed an increase in the expression of all three genes in response to 24 h anoxia, whereas brain and heart showed increased expression after 40% total body water dehydration. Again, increased transcription in these tissues makes sense as under anoxic conditions the heart must adjust to sustained periods of no oxygen by reducing heart rate b as much as five fold at 5 °C, while the kidney must deal with the increased acidosis of the blood as a result of the lack of oxygen available to the tissues. During dehydration the heart is necessary for the circulation of liver-derived glucose to other organs which allows them to elevate their osmolality and enhance their colligative resistance to water loss, and the brain is essential in the coordination of the responses to dehydration. It is also interesting to note that across all three stresses, only heart experiences increased transcription in all three genes. This probably reflects the critical role of the heart in all three stresses, providing for the inter-tissue transport of oxygen, nutrients, wastes and cryoprotectants for as long as possible to sustain viability of the whole organism.

Interestingly, there was no commonality between tissues concerning protein levels of Li16, FR10 and FR47; no one tissue showed the same protein response across all three proteins. This is probably due to the fact that while Li16 did show some increases in protein levels in response to freezing, both FR10 and FR47 generally did not respond to freezing stress. When just FR10 and FR47 protein levels were compared, it was found that heart and dorsal skin both showed no change in response to 24 h freezing and 8 h

thawing. This is surprising as heart was the only tissue that showed significant increases in transcript levels across all genes and all stresses. This discrepancy might be due to the sequestering of *fr10* and *fr47* mRNA transcripts in stress granules, which allows the cell to conserve energy by decreasing protein synthesis while still retaining the transcripts for later translation. However, the lack of a protein response after 8 h thaw presents a challenge to this concept. Overall, an examination of more frequent time points over the course freezing and thawing would probably provide a better indication of the timeframe of transcription and translation of the three novel genes. For example, it is possible that although the novel genes are up-regulated by the stimulus of freezing, the expression of the proteins might actually be delayed until the early hours of thawing where their critical actions may be to aid in cell or tissue recovery. Beyond commonalities in the pattern of expression, it is difficult to suggest how these genes and their proteins may interact and relate with one another. While it is possible that they all have a similar role in helping the wood frog survive freezing, it is equally possible that they are just three genes, found through a cDNA library that respond to freezing. For example, the cDNA library that identified *li16*, *fr10* and *fr47* also identified α and γ fibrinogen and ADP/ATP translocase as increasing in response to freezing. The only commonality between fibrinogen, which is through to increase clotting capacity during freezing (Cai and Storey, 1997a), and ADP/ATP translocase, which regulates mitochondrial energy during freezing (Cai and Storey, 1997c), is this increased respond to freezing. Such might be the case with *li16*, *fr10* and *fr47*. One approach to determining both relatedness and functionality of the three novel genes is via bioinformatics, which will determine whether the three genes/proteins are related to each other, or if they contain similar domains or functional

groups.

6.2 Homology trees

Homology tree between li16, fr10 and fr47

To uncover the relatedness of the three novel genes *li16*, *fr10* and *fr47*, homology searches were performed. Figure 6.1a shows that when the three genes were aligned using the software DNAMAN, it was found that *fr47* and *li16* share a 46% nucleotide sequence similarity, and that *fr10* is 37% similar to the *fr47*/*li16* grouping. More specifically, the homology matrix (Figure 6.1b) indicated that *fr10* shares a 33.8% sequence similarity with *fr47* and a 39.5% similarity with *li16*. However, when *fr47* and *li16* were compared through BLAST, there was no significant similarity found. This is because BLAST utilizes a "low complexity" filter which masks regions of low compositional complexity in the query sequence by default. These regions represent biologically uninteresting reports from the BLAST output, for example, hits against common acidic-, basic- or proline-rich regions. Short internal repeats and poly A sequences are also considered to be sequences of low complexity. These regions are not allowed to initiate alignments, as most often it is inappropriate to consider matches based on these regions the result of a shared homology. When the filter is turned off, the BLAST search for *fr47* and *li16* alignment results in a max score of 21.1 (where the score is calculated from the sum of rewards for matches and penalties for mismatches, gap open and gap extends) and an E value of 0.66 (representative of the number of alignments expected by chance with that particular score or better). Therefore one could conclude that the majority of the 46% sequence similarity determined through DNAMAN sequence alignment is the result of regions of low complexity. This is supported by the

regions found to be similar between *fr47* and *li16* through BLAST. As seen in Figure 6.2a, there are many very short regions of sequence similarity, rather than larger domains that are conserved between the two. This is also the case between *fr47* and *fr10* (Figure 6.2b), who have a slightly better max score and E value of 22.9 and 0.2, respectively. Finally *li16* and *fr10* show the lowest degree of alignment (according to BLAST) was a max score of 17.5 and an E value of 0.99. Again the alignment of these two genes indicates many short regions of sequence similarity, most likely the result of low complexity regions (Figure 6.2c).

Homology trees for li16

Once it had been determined that the three novel genes discovered by freeze responsive cDNA library screening did not share any significant homology, each of the nucleotide sequences were analyzed in BLAST against the existing database. An initial search was performed to determine the closest relatives for each gene, followed by a search for homology against various model organisms. For *li16*, the BLAST search produced a number of similar sequences. A hypothetical *Xenopus tropicalis* protein predicted from automated computational analysis showed the highest degree of similarity with a max score of 46.4 and an E value of 0.16. In fact, this sequence was the only one to have an E value less than 5 (where 10 is the default cutoff point). A homology tree created from those sequences found to align with *li16* in BLAST shows that *li16* is indeed most closely related to the hypothetical *X. tropicalis* protein, with a 46% sequence similarity (Figure 6.3a). Following this, *li16* shares a 43% similarity in nucleotide sequence with a hypothetical *Caenorhabditis remanei* protein (derived from an annotated genomic sequence). Additionally *li16* is equally similar to the *Monosiga brevicolli*

hypothetic protein and the olfactory receptor from *Rattus norvegicus* at 25% (Figure 6.3b). The percentage of sequence similarity between *li16* and respective BLAST products seems to be misleading, as there appears to be only a few regions within the *li16* gene that are found in other sequences. Figure 6.4 shows the graphical result of the BLAST search which indicates that there are only 4 regions of the *li16* mRNA transcript that are repeated in other sequences. The most commonly repeated region appears from approximately 390 to 430 bp on the *li16* transcript, which most likely corresponds to the polyadenylation signal (predicted to occur between 392 and 397 bp). The second most highly occurring region of repeat on *li16* is located from approximately 15 to 50 bp. This corresponds to a predicted membrane spanning domain which extends from nucleotide 3 to 72. This region also contains a predicted nuclear export signal, which should extend from nucleotide 18 to 45. When only the predicted coding sequence of *li16* is used to create a homology tree, essentially the same tree and homology matrix is obtained (Figure 6.5). Most likely this is due to the continued presence of the membrane spanning domain/potential NES and the polyA signal.

To obtain a more comprehensive idea of what the potential role of *li16* could be, further BLAST searches were performed against sequences from the model organisms *Xenopus tropicalis*, *Homo sapiens*, *Caenorhabditis elegans*, *Danio rerio*, and *Mus musculus*. Again *li16* did not show any significant homology, sharing a maximum sequence similarity of 38% with both *actopaxin* and *alpha parvin* from *D. rerio* (zebrafish) (Figure 6.6). Both of these sequences are in the parvin family which are essential components in cell adhesions, spreading and motility (LaLonde *et al.*, 2005). The remaining sequences show low levels of similarity ranging from 28% to 0.1%.

Homology trees as determined by sequence similarities may be misleading, as the graphical representation of the *li16* BLAST in the zebrafish database shows the same two regions of *li16* repeating in the search results (Figure 6.7). Again these most likely correspond to the hydrophobic transmembrane region at the 5' end, and the polyA signal at the 3' end. As a final attempt to clarify what the role of *li16* might be in the frozen frog, a homology search using the predicted amino acid sequence of the Li16 protein was performed (Figure 6.8). Similar to the initial homology tree created using the nucleotide sequence of *li16*, the strongest similarity was seen between Li16 and a hypothetical *X. tropicalis* protein at 45%. Unfortunately this doesn't provide any additional information about a possible role of Li16 in the wood frog. Following this, Li16 is most closely related to a predicted low affinity cationic amino acid transporter 2-like protein from *Apis mellifera* (honey bee) with a 17.6% sequence similarity. The similarity is so low; however, with never more than 5 successive amino acids sharing their identity, that one cannot really infer a role for Li16 based on this relationship. Therefore, based on nucleotide and protein sequence homology trees, one can only conclude that *li16* is a novel gene that does not share any significant homology with any known gene or protein sequence.

Homology trees for fr10

A nucleotide sequence BLAST for the full *fr10* mRNA sequence resulted in an extensive list of similar nucleotide sequences. Due to the large number of query hits, a homology tree was only created based those sequences whose E values were lower than 7. The deduced homology tree indicated that *fr10* shares the strongest sequence similarity (38%) with a predicted *Drosophila willistoni* protein derived from an annotated

genomic sequence (Figure 6.9a). Nine of the remaining ten sequences had sequence similarities that were in the range of 21 to 26.7%, while *Drosophila grimshaw* showed only a 0.1% similarity (Figure 6.9b). Already these homologies are quite low, and therefore it would be unwise to assume a function for *fr10* based on these results. However, to further this hesitance, it appears as though these sequences are only found to be similar due to two regions of *fr10* that are replicated in the BLAST sequence results (Figure 6.10). The first of these regions is responsible for the majority of the BLAST hits and is located from nucleotides 50 to 90. This region has been identified as coding for a nuclear export signal, which specifically occurs from nucleotide 51 to 89. The second region occurs from about nucleotide 420 to 460, which is actually located in the predicted 3' UTR of this full mRNA sequence. When only the predicted coding region was used, the BLAST results were virtually the same due to the continued presence of the NES.

Further information was gathered about *fr10* by performing additional BLAST searches against the sequences for the model organisms *X. tropicalis*, *H. sapiens*, *C. elegans*, *D. rerio*, and *M. musculus*. Not surprisingly *fr10* was found to be most similar to the three *X. tropicalis* sequences; 43% similar to a predicted glutamine rich protein, 27% similar to an active BCR-related gene and 26.6% similar to a predicted serine/threonine-protein kinase SMG1. The remaining sequences had similarities greater than 20% except for the *C. elegans* sequences which were both extremely low (Figure 6.11). As with the first nucleotide BLAST search, the relationships described by the generated homology tree may be misleading due to the two regions of *fr10* that are commonly repeated. For example, BLAST shows that the glutamine rich protein which shares a 43% sequence similarity with *fr10* is only similar across 18 nucleotides which

occur between 420 and 440 bp on *fr10*. When the NES was removed from the coding sequence and BLAST were performed again, only two sequences were found to be similar. Confirming previous results, one was a predicted protein from *Drosophila willistoni* which now showed a 54% sequence similarity to the predicted coding non-NES containing *fr10*. The other was a hypothetical protein belonging to *Paramecium tetraurelia* (derived from an annotated genomic sequence) which was 44.2% similar in its nucleotide sequence (Figure 6.12). This proves that the initial homology tree and the relationships it displayed were primarily the results of the nuclear export signal located in the *fr10* gene.

Since nucleotide BLAST and homology trees had yet to reveal a closely related ancestor from which the role of *fr10* might be inferred, a final protein based homology search was performed. The predicted amino acid sequence of FR10 was found to be 33.3% similar to the sequence for an unnamed *Xenopus laevis* protein that seems to be translated from a lens specific gene. It is also similar to apolipoprotein A-II from *M. muculus* (house mouse) at 26.7%, and a protein of hypothetical function in *Lactobacillus ultunensis* at 23.3% (Figure 6.13). Of these proteins it is most probable that *fr10* could have evolved from an apolipoprotein. Interestingly, when apolipoprotein A-II from *Mus muculus* was used as the query for a BLAST search not only was *fr10* detected, so was a type IV antifreeze protein (AFP) precursor from *D. rerio*. This would suggest that both *fr10* and fish type IV AFP may be related to apolipoproteins, specifically Apo A-II. This is supported by Gauthier *et al.* (2008) whose research has suggested that fish type IV AFP and apolipoproteins are homologous and even that these AFP may be more accurately described as apolipoproteins than as an AFP. Therefore, there is a possibility

that *fr10* (and fish type IV AFP) evolved from an existing apolipoprotein.

Homology trees for fr47

A BLAST search using the full *fr47* mRNA transcript produced a large number of hits, resulting in the homology tree being generated only from those sequences that have an E value less than 5. The highest degree of sequence similarity (39%) was found between *fr47* and a hypothetical protein belonging to *Paramecium tetraurelia*. The next two sequences to show the greatest sequence similarity; *Taeniopygiaguttata* at 31.8% and *X. tropicalis* at 27.5%, were also only predicted or hypothetical sequences (Figure 6.14). The final sequence, which showed a 27% degree of homology with *fr47*, was a G-protein coupled receptor family protein from *Dictyostelium discoideum*. As with the full sequence nucleotide homology trees generated for *li16* and *fr10*, these relationships may be misleading since the *fr47* transcript has certain regions that are popular repeats in the query hits. For *fr47* these regions primarily spanned nucleotides 750 to 790, and 1060 to 1200 (Figure 6.15). Interestingly, these regions are in the middle of the predicted 5' UTR, since the predicted open reading frame does not begin until nucleotide 2004. However, based on the presence of a G protein coupled receptor query hit for the 750 to 790 bp region, it is possible that this region codes for a membrane spanning domain. This would be in keeping with previous BLAST searches of *li16* and *fr10* which found that transmembrane domains are highly repeated in query hits. What nucleotides 1060 to 1200 might code for is unknown, mainly due to the large number of clones and hypothetical proteins that were found to be similar to this region. To minimize the number of query hits that code for an unknown or hypothetical protein, another homology tree was created based on BLAST searches of the model organisms *X. tropicalis*, *H.*

sapien, *C. elegans*, *D. rerio*, and *M. musculus* (Figure 6.16). Here, *fr47* was found to share a 38% similarity with the sequence for an ATPase of the 26S proteasome of *X. tropicalis*. It also shares a 33.3% sequence similarity with the thioredoxin gene from *H. sapien* and a 32.6% similarity with a LIM domain interacting RING finger protein from *X. tropicalis*. While none of these query sequences are located in the highly repeated regions indicated by the initial BLAST search, they are all still located in the predicted 5' UTR of *fr47*. Therefore, it would be irresponsible to infer a possible role for FR47 based on these results, as it is predicted that these regions do not even contribute to the final FR47 protein. In addition to this, the homology tree does not take into consideration the quality of the sequence similarity, which may give rise to misleading percentages. For example, the region found to be similar between the RING finger protein of *X. tropicalis* and *fr47* is actually a string of AGC CAG repeats, which translates to a serine-glutamine repeat. This is not surprising as protein surface loops often consist of residues such as serine which are highly flexible (Ladurner *et al.*, 1997). However, several natural proteins show regular repeats of certain amino acids such as glutamine or serine/arginine. In fact it is believed that such sequences and non-globular regions are present in about 25% of the protein database (Wootton, 1994), indicating that the relationship between these two sequences may not actually be that significant.

In an attempt to resolve these issues, a BLAST search was performed using the predicted coding sequence of *fr47*. Not surprisingly, *fr47* was most closely related to two predicted hypothetical gene sequences belonging to *X. tropicalis*. These sequences were 98% similar to one another, and 36% similar to *fr47*. Following this, *fr47* was found to be approximately 29% similar to a G patch domain protein for *M. musculus* and 26%

similar to nonfunctional *X. tropicalis* endogenous virus XTERV1 (Figure 6.17). It is clear that *fr47* is not a virus, and no information can be gathered from the predicted hypothetical *X. tropicalis* proteins, so the G patch domain protein was investigated further. Translation of the 35 bp nucleotide sequence that was found to be similar between the query and the subject revealed that this region of *fr47* contained only one glycine residue (Figure 6.18). G patch domains, however, are characterized by six highly conserved glycine residues which are not represented in the *fr47* sequence (Aravind and Koonin, 1999). Therefore, it can be concluded that *fr47* does not function like a G-patch domain protein. Moreover, the region that was similar between the two was actually located in the 5' UTR of the G-patch domain protein and thus would not be translated. Therefore, no inference towards the possible role of *fr47* can be made based on its sequence similarity with this G-patch domain protein.

As a final attempt, a homology tree was created based on the predicted amino acid sequence of FR47 (Figure 6.19). Despite the relatively large size of this protein (compared to Li16 and FR10), only three protein sequences were found to be similar to that of FR47. These were a putative bromodomain-containing protein from *Toxoplasma gondii* (6.8% similarity), a hypothetical protein from *Gallus gallus* (17.1%) and a new virus related to avian sarcoma and leukosis viruses in *Bonasa umbellus* (23.3%). Again, FR47 is not a virus, and no information can be gathered concerning a role from the *G. gallus* protein. Finally, as a consequence of the extremely low sequence similarity between FR47 and the bromodomain-containing protein, no information about FR47 and its potential role can be gathered from this homology tree. Therefore, the only conclusion one can make about *fr47* and its FR47 product is that it does not share any significant

homology with any known nucleotide or protein sequence.

6.3 Protein Modifications

As mentioned previously in the individual chapters, the size of the proteins determined by Western blotting was often larger than the size predicted by the open reading frame. For example, Li16 was found be approximately 15 kDa whereas it was predicted that its size would be 12.8 kDa based on the predicted ORF. FR10 was predicted to be approximately 10 kDa but Western blots indicated the size was closer to 16 kDa. FR47 was predicted to be approximately 47 kDa, and a band was found to be present at this size, however additional bands were also seen at higher molecular weights. These discrepancies in size could be due to the addition of post-translational modifications, which would add to the overall size of the protein. To examine this possibility, an extensive computational search of possible protein modifications was performed for Li16, FR10 and FR47 amino acid sequences (shown in Figure 6.20) and Table 6.1 summarizes the results of this search. The results showed that all three proteins could be modified by phosphorylation, glycation, ubiquitylation and the addition of O-linked N-acetylglucosamine (O-GlcNAc). In addition to this, Li16 could undergo palmitoylation, sumoylation, and O-glycosylation; FR10 could undergo methylation; and FR47 could be modified by sulfination, palmitoylation, sumoylation, N-glycosylation and methylation. However, one must note that simply because a protein motif is detected, it does not necessary mean the protein is modified in this manner. For example, FR10 and FR47 contain individual amino acids that were predicted to be modified both by the addition of phosphate and an O-linked N-acetylglucosamine. Such sites are reversible and dynamically modified by O-GlcNAc or phosphate groups at different times in the

cell. Moreover, if the protein is involved in signalling it is unlikely to contain an O-GlcNAc, as such sequences are unlikely to be intracellular and therefore are unlikely to be exposed to the glycosylation machinery. Because of these restrictions, Li16, FR10 and FR47 were examined for the presence of signal peptides in their amino acid sequence. Li16 was predicted to have a nuclear export signal (NES) from amino acids 5 to 14 (http://www.cbs.dtu.dk/services/NetNES/) and its subcellular location was predicted to be in the secretory pathway (http://www.cbs.dtu.dk/services/TargetP/). FR10 was also predicted to have an NES from amino acids 6 to 13, and had a predicted subcellular location of secretory pathway. FR47 was found to have a possible NES from amino acids 359 to 363 however its subcellular location was predicted as "other". This means it was not classified as a secretory or a mitochondrial targeting peptide with any degree of confidence. Even the prediction of "other" had only 50% confidence. The O-GlcNAc predicting software also did not indicate a potential signal peptide in the FR47 protein sequence. Given that the potential NES of FR47 is also located where a potential membrane spanning domain is predicted (http://bp.nuap.nagoya-u.ac.jp/sosui/sosui_submit.html), it is most likely that the "NES" is just a string of hydrophobic residues necessary for the transmembrane domain. Based on these results, it is possible that Li16 and FR10 contain signal peptides and therefore they may not be O-GlcNAc linked, and that FR47 is most likely reciprocally modified under different conditions at the same amino acid sites by either O-GlcNAc or phosphate.

Certain protein modifications that were searched for were not present in any of the three proteins, namely N-myristolyation, prenylation, N-acteylation and C-mannosylation. This makes sense for N-myristolyation as it only occurs on the alpha

amino group of the N-terminal amino acid, most often glycine. Two of the three proteins do not have a glycine as the N-terminal amino acid: Li16 is alanine, FR10 is lysine. FR47 does have glycine in this position; however it was not predicted to be myristoylated. The lack of C-mannosylation predictions is also expected, as this modification always occurs on the first tryptophan in the sequence W-X-X-W (where W is tryptophan and X is any amino acid). This amino acid motif is not present in any of the three proteins.

A final bioinformatic search was performed to assess the presence of membrane spanning domains in the protein sequences. Within the Li16 protein there was one predicted transmembrane domain, spanning amino acids 1 to 22 (Figure 6.21). FR10 and FR47 also have a single membrane spanning domain, predicted to occur between amino acids 1 to 21 for FR10 (Figure 6.22), and amino acids 351 to 373 for FR47 (Figure 6.23). As previously mentioned concerning FR47, all three of these transmembrane domains include the amino acids that had been predicted as nuclear export signals. This is due to the fact that nuclear export signals consist of a short amino acid sequence of four hydrophobic residues, usually leucine. A string of hydrophobic residues is also the requirement of a transmembrane domain, as this allows the protein to insert itself into the hydrophobic lipid bilayer. Obviously these proteins cannot have both a transmembrane domain, which would result in a stationary protein, and a NES, which causes the protein to move between the nucleus and cytoplasm. Based on the results of the bioinformatics prediction for subcellular location, it is predicted that for Li16 and FR10 this region is most likely an NES, and for FR47 it is most likely a membrane spanning domain.

6.4 Future directions

Future directions concerning *li16*, *fr10* and *fr47* and what their roles might be in the cell are boundless. The work of this thesis covers just a small portion of what could potentially be done to characterize these three genes/proteins and explore their functional roles in vivo. The present studies did determine that all three are involved in freeze tolerance, that they are also expressed in response to anoxia and dehydration stresses, and that they may play an additional role during the metamorphosis of the frog from embryo to adult.

A next natural step would be to demonstrate that these proteins actually do confer enhanced freezing survival and/or improved recovery during thawing of frog cells and tissues. While this has been previously demonstrated in insect cells lines using Li16 and FR10, it would be of value to demonstrate that all three proteins can be successfully expressed in a human cell line (most likely an embryonic kidney cell line). Therefore, once plasmids have been constructed and transfected into cells lines, the effects of Li16, FR10 and FR47 expression on the subsequent viability of the cells would be documented when cells are challenged with cold (5 °C) or freezing (-5 °C) exposures. The production of these proteins in the cells line would also be valuable since it would allow for further examination of the action of these proteins. For example, a co-immunoprecipitation can be performed to isolate one of the three desired proteins from the human cell line, together with other cell proteins that naturally bind to them. It could then be possible to identify what these associated proteins are by using liquid chromatography and tandem mass spectrometry (LC-MS-MS). This will reveal possible pathways that these proteins are acting under, and will, at the very least, provide a clearer understanding of the

molecular actions of these freeze responsive proteins. Li16, FR10 and FR47 proteins isolated from these human cells lines may also undergo LC-MS-MS to identify regulatory controls (i.e. posttranslational modifications that enhance their function in response to freezing of the cells). This would be done over the time course of freezing and thawing, to observe what changes in posttranslational modification occur at what time points, and therefore what proteins have enhanced function at what time points. Overall, this will determine which modifications predicted by computer software (Table 6.1) hold true in the cell during freezing or thawing. It might also explain why Li16 and FR10 are found at molecular weights that are 1.17 and 1.6 times higher than what was predicted (respectively), based on their open reading frames.

It would also be interesting to determine if the locations predicted for these proteins by computer software is correct. As FR10 and Li16 were predicted to have an NES and be secretory, one would expect them to be located in the cytoplasm or extracellular; FR47 had a possible NES and its location was unknown, and as such its predicted location is also unknown. Also all three were predicted to have transmembrane domains, and therefore they may also be located in the membrane. To determine their subcellular locations, a sucrose gradient subcellular fractionation could be performed. This would reveal whether the proteins were localized in the nucleus, mitochondria, or cytoplasm, as well as whether or not they were bound to membranes, and would provide some clues as to the function of the protein. For example, a protein found in the nuclear fraction might be a transcription factor, whereas a protein that localizes with the plasma membrane might be involved in cell signalling.

In the future, it would also be wise to follow up on the work of my predecessors

on their characterization of *li16*, *fr47* and *fr10* (McNally *et al.*, 2003, 2002, Cai and Storey, 1997). For example, while a variety of second messengers (dibutyryl – cAMP, dibutyryl – cGMP, and PMA) were tested for their effect on *li16* and *fr47* transcription, this was never done for the gene *fr10*. Additionally, the effect of these second messengers on protein expression was never examined. Also, whereas *li16* and *fr10* genes have been transfected into insect cells lines and overexpressed in order to observe the effects on cell cold hardiness, this has never been undertaken for *fr47* (however if transfection into human cells is performed, as proposed above, this would be unnecessary). Finally, the presence of the FR47 protein, but not Li16 and FR10, was examined in four other frog species: *P. crucifer*, *H. versicolor*, *R. pipiens* and *S. couchii*. All three proteins should be analyzed in a much wider range of anuran species including other freeze tolerant frogs (e.g. *Pseudacris triseriata, Hyla chrysoscellis*), other northern frogs that winter underwater but are not freeze tolerant (e.g. *Rana catesbeiana, Rana clamitans, Rana septentrionalis*) as well as anurans that show desiccation, hyperosmolality or anoxia resistance. It would be interesting to see if Li16 and FR10 follow the trend observed in FR47, where the protein was only present in freeze tolerant frogs (*P. crucifer* and *H. versicolor*) and not freeze intolerant frogs (*R. pipiens* and *S. Couchii*). This would substantiate the assertion that all three genes/proteins are involved in freeze tolerance, and are freeze responsive. Finally, more detailed examination of the response of these three genes/proteins over more comprehensive time course of freezing, anoxia and dehydration, as well as recovery from these stresses would be valuable. For example, there is a particular need to examine FR10 and FR47 responses over the very early hours of thawing, instead of just at 8 h thawed. This is because both proteins

showed significant increases in transcription in response to freezing, however a corresponding increase in protein levels was not observed at either freezing or thawing time points. For FR47, it was shown by McNally *et al.* (2003) that protein levels are highest after 2 h of thawing, while this was only hypothesized as a possibility for FR10. By investigating more frequent and earlier thawing and freezing time points, it will be possible to better determine the pattern of expression of FR10 and FR47 protein and thereby gain a better idea of what regulates their expression and what possible role they might have.

The more that is uncovered about the role of these genes/proteins, the more useful they may become in the future. Eventually, this research may play an important role to improve stress tolerance in human cells and organs. The most significant application of this would be to improve tissue survival for the purpose of hypothermic or cryopreservation of tissues and organs for transplantation.

Table 6.1: A comparison of the properties of the three novel wood frog genes/protein; Li16, FR10 and FR47

	Li16	**FR10**	**FR47**
Predicted molecular weight (kDa)	12.8	10	45.7
Predicted number of amino acids	115	90	390
Sequence characteristics	N-terminal hydrophobic region from aa 1–22	N-terminal hydrophobic region from aa 1-21, possible NES at aa 6-13	C-terminal hydrophobic region from aa 351-373
GenBank ID	AF175980	U44831	AY100690
Tissue-dependent transcriptional response to 24 h freezing			
Significant increase in transcription	Liver, skeletal muscle, brain, heart, lung, testes & ventral skin	Liver, skeletal muscle, brain, heart, lung, testes, ventral skin, large intestine & small intestine	Liver, skeletal muscle, heart, kidney, lung & testes
No change in transcription	Kidney, stomach, large intestine, small intestine & dorsal skin	Dorsal skin	Brain, ventral skin & small intestine
Significant decrease in transcription	None	Kidney & stomach	Dorsal skin, stomach & large intestine
Tissue dependent transcriptional response to 24 h anoxia			
Significant increase in transcription	Brain, heart & kidney	Heart, kidney & lung	Liver, skeletal muscle, brain, heart, kidney & lung
No change in transcription	Skeletal muscle, lung & testes	Liver, skeletal muscle, brain & testes	Testes
Significant decrease in transcription	Liver	None	None
Tissue dependent transcriptional response to 40% total body water dehydration			
Significant increase in transcription	Brain, heart, kidney & testes	Brain & heart	Liver, brain & heart
No change in transcription	Skeletal muscle	Liver & testes	Skeletal muscle, kidney, lung & testes
Significant decrease in transcription	Liver & lung	Skeletal muscle & lung	None

Transcription throughout wood frog metamorphosis			
General trend	No trend observed	No trend observed	Steady increase throughout development
Tissue dependent protein response to 24 h freezing			
Significant increase in protein level	Skeletal muscle, brain, heart & kidney	Brain & kidney	None
No change in protein level	Liver	Liver, heart, skeletal muscle & dorsal skin	Brain, heart, kidney & dorsal skin
Significant decrease in protein level	Dorsal skin	None	Liver & skeletal muscle
Tissue dependent protein response to 24 h freezing, followed by 8 h thaw			
Significant increase in protein level	Heart	Brain	None
No change in protein level	Liver, skeletal muscle, brain & kidney	Liver, heart, kidney & dorsal skin	Skeletal muscle, brain, heart & dorsal skin
Significant decrease in protein level	Dorsal skin	Skeletal muscle	Liver & kidney

A:

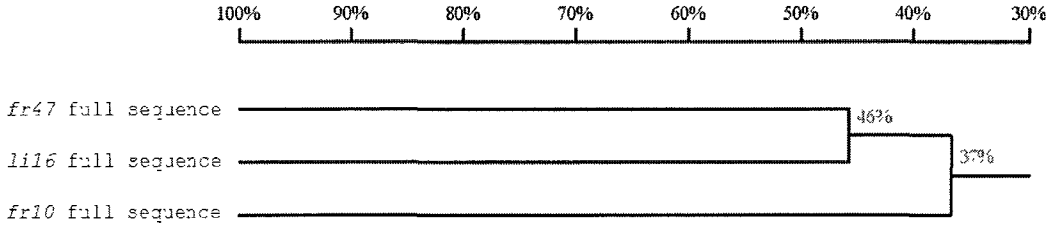

B:

Homology matrix of 3 sequences

fr47 full sequence	100%		
li16 full sequence	45.8%	100%	
fr10 full sequence	33.8%	39.5%	100%

Figure 6.1: Homology tree (a) and matrix (b) indicating the relationship between *li16*, *fr10* and *fr47*.

A:

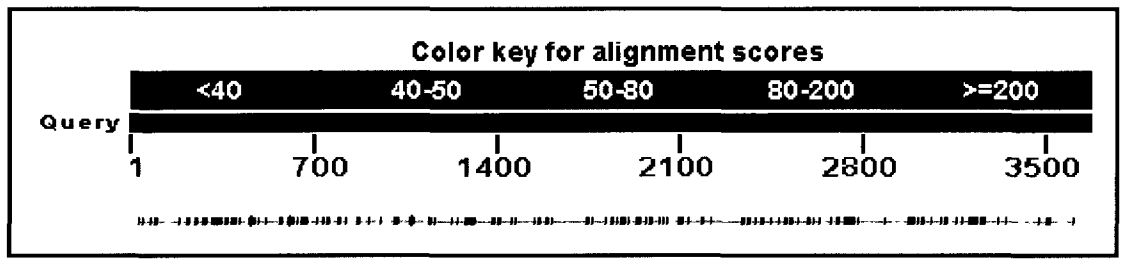

B:

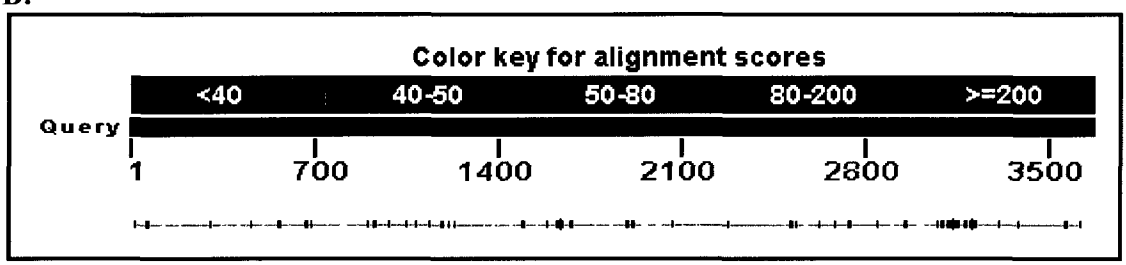

C:

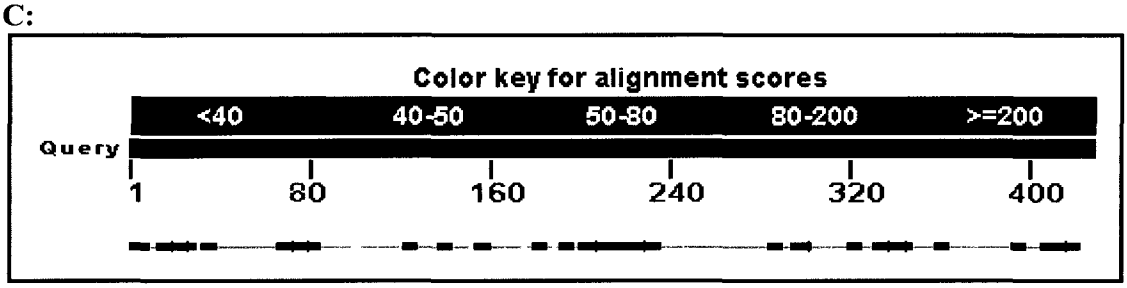

Figure 6.2: Graphical representation of the BLAST search between the following full mRNA sequences. The grey line represents the query sequence, while the black marks found on this line represent the nucleotides that have a similar counterpart in the subject.

A) BLAST search between *fr47* (the query) and *li16* (the subject)

B) BLAST search between *fr47* (the query) and *fr10* (the subject)

C) BLAST search between *li16* (the query) and *fr10* (the subject)

A:

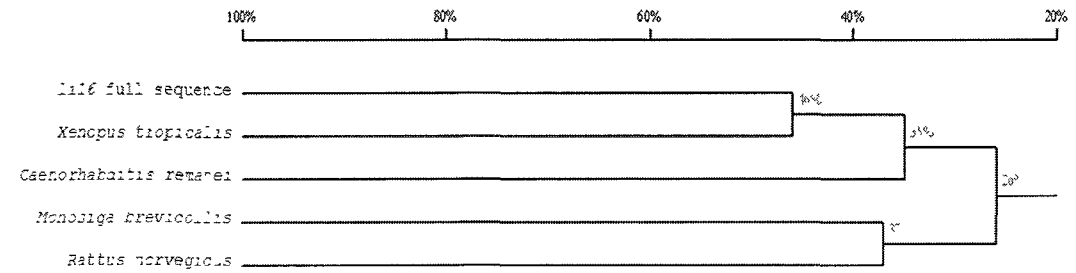

B:

Homology matrix of 5 sequences

li16 full sequence	100%				
Caenorhabditis remanei	42.7%	100%			
Xenopus tropicalis	45.9%	27.9%	100%		
Monosiga brevicolli	25.6%	31.9%	24.6%	100%	
Rattus norvegicus	25.4%	25.3%	22.7%	36.6%	100%

Figure 6.3: Homology tree indicating sequence similarity between the full mRNA sequence of *li16* and its closest relatives.

A) Homology tree between *li16* (GenBank Accession: AF175980), a hypothetical *Xenopus tropicalis* protein (XM_002943004.1), a hypothetical protein from *Caenorhabditis remanei* (XM_003103658.1), a predicted protein from *Monosiga brevicollis* (XM_001742552.1) and an olfactory receptor belonging to *Rattus norvegicus* (AC243008.4).

B) Homology matrix between the branches of the homology tree.

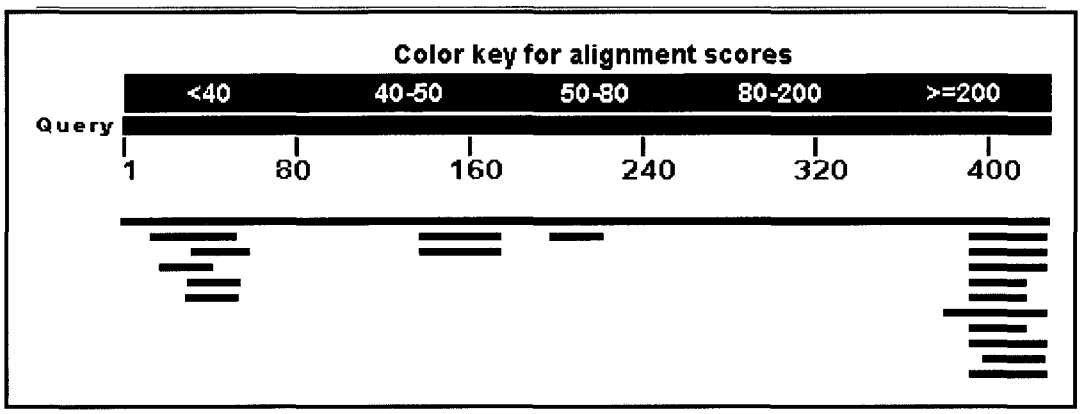

Figure 6.4: Graphical representation of a BLAST search using the full mRNA sequence of *li16* as the query. The colour of the lines represents the score of each alignment, where red lines represent alignments with a score greater than 200, and blue lines represent alignments with a score between 40 and 50. Here the red line represents the *li16* sequence, while the blue lines represent query hits. The location of the bands on the scale indicates which base pairs belonging to *li16* the query is able to match.

A:

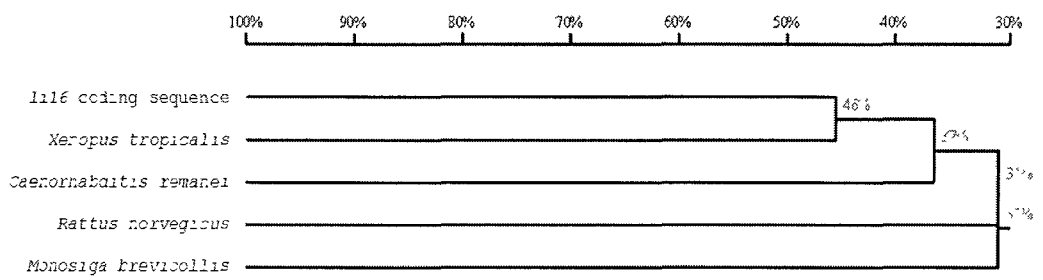

B:

Homology matrix of 5 sequences

li16 coding sequence	100%			
Xenopus tropicalis	46.4%	100%		
Caenorhabditis remanei	34.6%	38.5%	100%	
Monosiga brevicollis	28.4%	32.4%	32.1%	100%
Rattus norvegicus	30.7%	33.1%	29.5%	30.2%	100%

Figure 6.5: Homology tree indicating sequence similarity between the predicted coding sequence of *li16* and its closest relatives.

A) Homology tree between *li16* (GenBank Accession: AF175980), a hypothetical *Xenopus tropicalis* protein (XM_002943004.1), a hypothetical protein from *Caenorhabditis remanei* (XM_003103658.1), a predicted protein from *Monosiga brevicollis* (XM_001742552.1) and an olfactory receptor belonging to *Rattus norvegicus* (NM_001000501.1).

B) Homology matrix between the branches of the homology tree.

A:

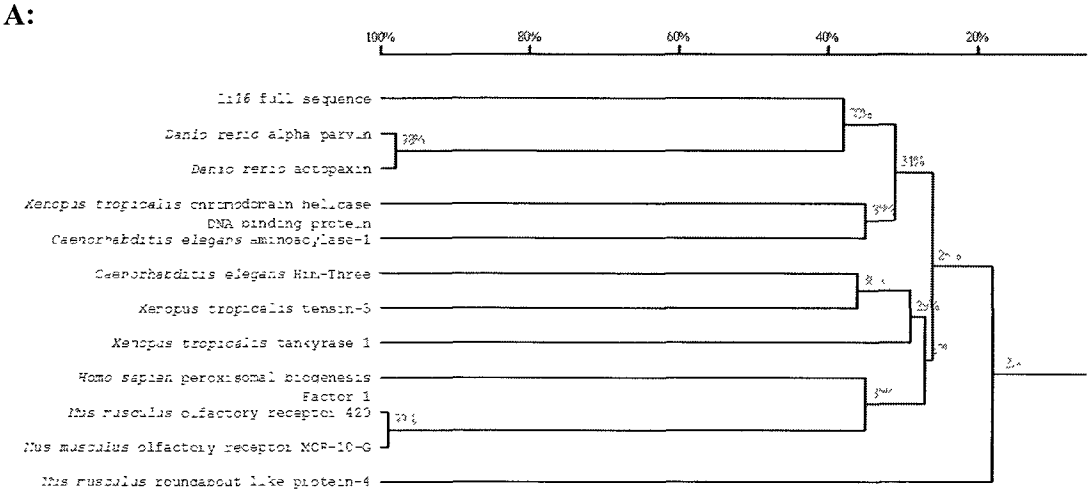

B:

Homology matrix of 12 sequences

li16 full sequence	100%										
Danio rerio alpha parvin	37.6%	100%									
Danio rerio actopaxin	37.6%	98.2%	100%								
X. tropicalis chromo.	28.3%	37.2%	37.3%	100%							
C. elegans aminoacylase	26.2%	27.2%	27.7%	35.3%	100%						
C. elegans Him-Three	17.1%	29.1%	29.1%	26.4%	25.1%	100%					
X. tropicalis tensin	28.4%	23.2%	22.5%	31.4%	27.5%	36.3%	100%				
Homo sapien peroxisome	25.2%	26.7%	26.6%	25.6%	27.1%	25.8%	34.9%	100%			
M. musculus olfactory 420	28.0%	26.0%	26.4%	23.2%	25.5%	20.9%	26.5%	35.3%	100%		
M. musculus olfactory MOR	27.5%	26.3%	26.6%	23.5%	25.2%	20.9%	26.4%	35.6%	99.4%	100%	
X. tropicalis tankyrase	24.0%	20.7%	23.1%	26.3%	25.9%	26.1%	31.0%	26.1%	29.6%	29.7%	100%
M. musculus roundabout	0.1%	0.1%	0.1%	32.1%	24.8%	26.9%	23.4%	24.8%	20.0%	23.3%	23.1% 100%

Figure 6.6: Homology tree indicating sequence similarity between the full mRNA sequence of *li16* and the sequences of model organisms.

A) Homology tree between *li16* (GenBank Accession: AF175980), *Danio rerio* alpha parvin (NM_001002872.2), *Danio rerio* actopaxin (AY648735.1), peroxisomal biogenesis factor 1 from *Homo sapien* (NG_008341.1), a chromodomain helicase DNA binding protein from *Xenopus tropicalis* (XM_0029223883.1), tankyrase 1 from *Xenopus tropicalis* (XM_002939256.1), tensin-3 like protein from *Xenopus tropicalis* (XM_002933414.1), aminoacylase-1 protein from *Caenorhabditis elegans* (NM_069250.4), Him-Three paralog family member from *Caenorhabditis elegans* (NM_068580.5), olfactory receptors from *Mus musculus* (BC145885.1 and AY073788.1), and roundabout like protein-4 (ROBO4) from *Mus musculus* (BC071193.1).

B) Homology matrix between the branches of the homology tree.

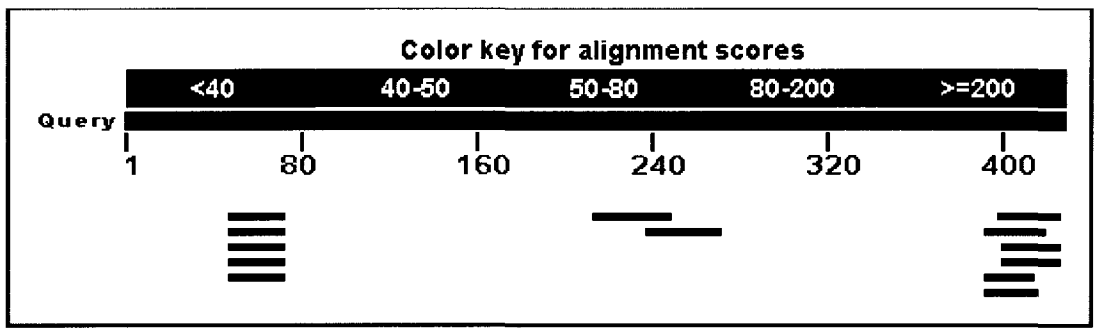

Figure 6.7: Graphical representation of a BLAST search using the full mRNA *li16* sequence against the *Danio rerio* database of nucleotide sequences. The colour of the lines represents the score of each alignment, where black lines represent alignments with a score less than 40, and blue lines represent alignments with a score between 40 and 50. The location of the bands on the scale indicates which base pairs belonging to *li16* the query is able to match.

A:

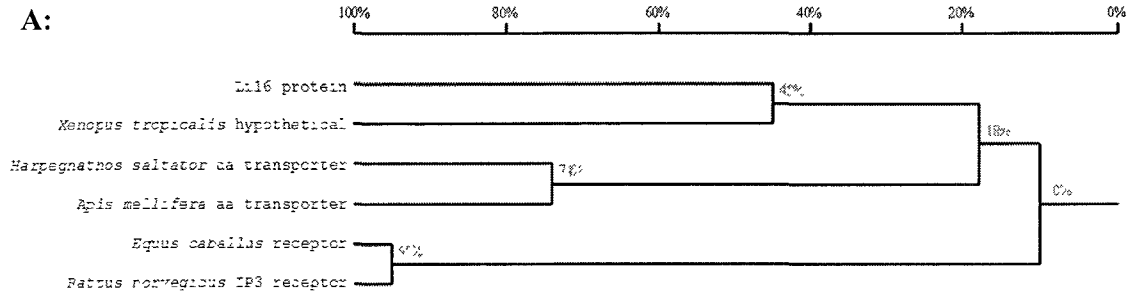

B:

Homology matrix of 6 sequences

Li16 protein	100%				
Xenopus tropicalis hypothetical	44.6%	100%			
Equus caballus receptor	13.0%	12.7%	100%		
Rattus norvegicus IP3 receptor	14.8%	12.7%	95.4%	100%	
Harpegnathos saltator aa transporter	17.0%	19.6%	7.6%	7.6%	100%
Apis mellifera aa transporter	17.6%	18.3%	7.1%	7.6%	73.9% 100%

Figure 6.8: Homology tree indicating sequence similarity between the protein sequence of Li16 and its closest relatives.

A) Homology tree between Li16 (GenBank Accession: AF175980), a hypothetical *Xenopus tropicalis* protein (XP_002941735.1), inositol 1,4,5-triphosphate receptor type 2 isoform 3 from *Equus caballus* (XP_001502772.3), cationic amino acid transporter 2-like protein from *Apis mellifera* (XP_393753.3), IP3 receptor isoform 2 from *Rattus norvegicus* (AAK11622.1), low affinity cationic amino acid transporter 2 protein from *Harpegnathos saltator* (EFN78731.1).

B) Homology matrix between the branches of the homology tree.

A:

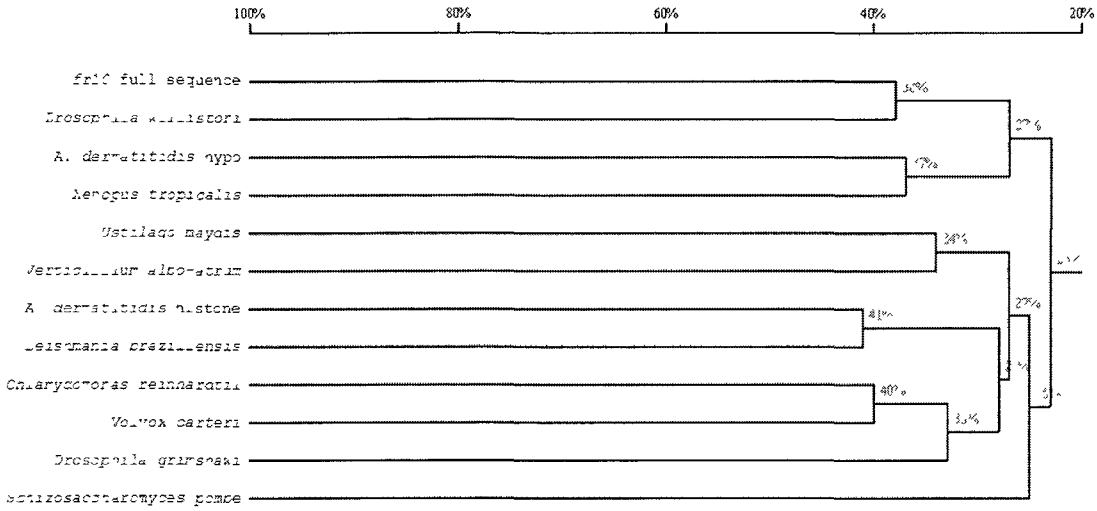

B:

Homology matrix of 12 sequences

fr10 full sequence	100%
Drosophila willistoni	38.2% 100%
A. dermatitidis hypo	26.5% 33.8% 100%
Xenopus tropicalis	22.9% 25.3% 37.4% 100%
Ustilago maydis	23.8% 26.5% 31.6% 27.4% 100%
A. dermatitidis histone	25.7% 26.7% 25.6% 17.9% 25.5% 100%
L. braziliensis	22.7% 26.6% 25.0% 21.8% 33.4% 41.2% 100%
C. reinhardtii	23.9% 22.6% 26.8% 0.1% 26.2% 25.0% 29.5% 100%
Drosophila grimshaw	0.1% 23.1% 22.8% 20.0% 26.5% 26.9% 26.3% 27.2% 100%
Volvox carteri	24.8% 24.2% 26.1% 35.4% 27.1% 27.3% 34.5% 39.9% 38.8% 100%
V. albo-atrum	24.0% 24.8% 26.7% 20.7% 34.0% 23.7% 28.8% 24.6% 26.7% 26.1% 100%
S.pombe	21.3% 24.3% 33.7% 15.4% 25.3% 22.6% 23.4% 23.0% 29.0% 24.1% 24.2% 100%

Figure 6.9: Homology tree indicating sequence similarity between the full mRNA sequence of *fr10* and its closest relatives.

A) Homology tree between *fr10* (GenBank Accession: U44831), a hypothetical protein from *Drosophila willistoni* (XM_002073713.1), a hypothetical protein from *Ajellomyces dermatitidis* (XM_002620174.1), a histone chaperone ASF1 from *Ajellomyces dermatitidis* (XM_002626934.1), a hypothetical *Xenopus tropicalis* protein (XM_002942434.1), a hypothetical protein from *Ustilago maydis* (XM_756941.1), hypothetical protein from *Leishmania braziliensis* (XM_001564809.1), a radial spoke nucleoside diphosphate kinase from *Chlamydomonas reinhardtii* (AY452667.1), a hypothetical protein from *Drosophila grimshawi* (XM_001983433.1), a hypothetical protein from *Volvox carteri* (XM_002949235.1), hypothetical protein from *Verticillium albo-atrum* (XM_003002411.1), a sodium ion/proton antiporter from *Schizosaccharomyces pombe* (CU329670.1).

B) Homology matrix between the branches of the homology tree.

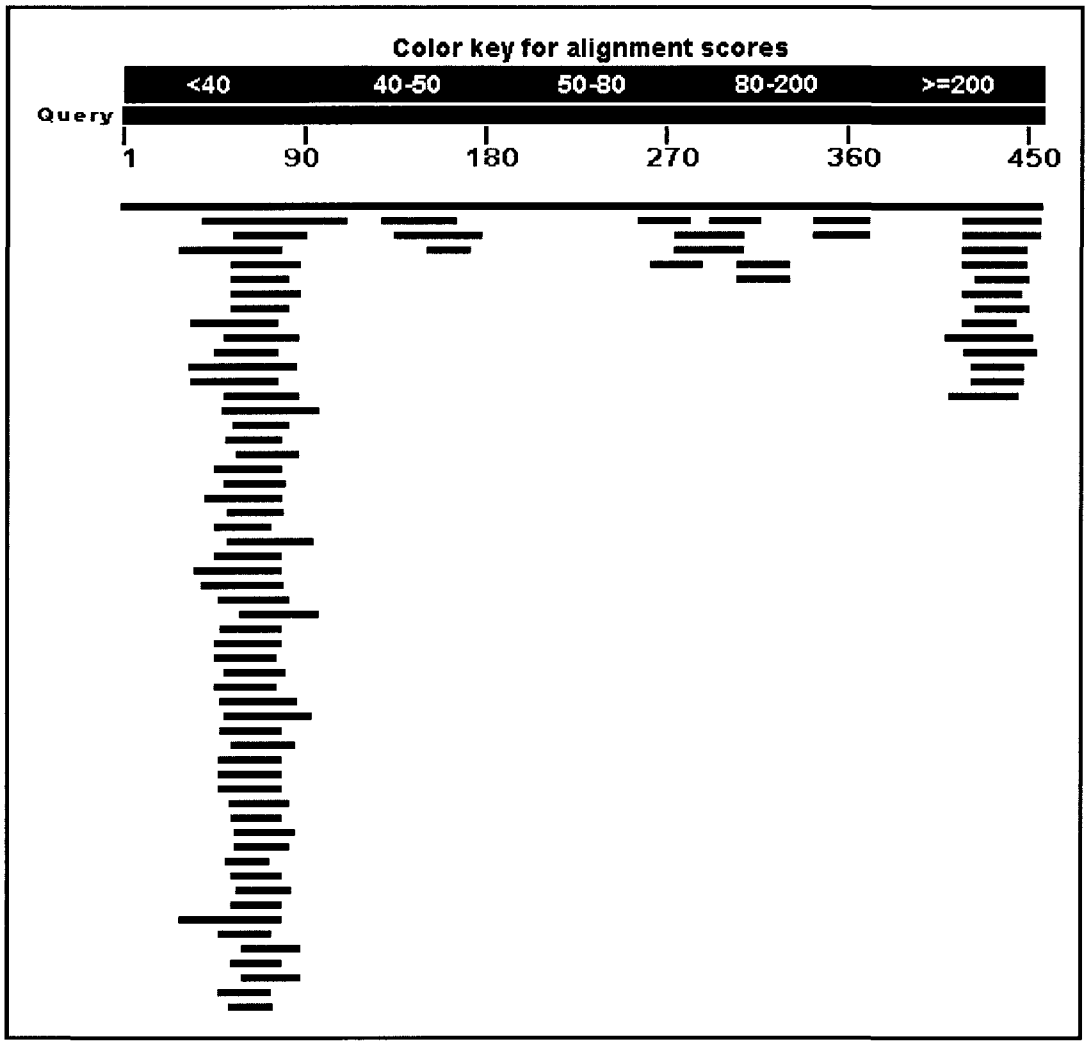

Figure 6.10: Graphical representation of the BLAST search of the full mRNA sequence of *fr10* as the query. The colour of the lines represents the score of each alignment, where red lines represent alignments with a score greater than 200, green lines represent alignments with a score between 50 and 80, and blue lines represent a score between 40 and 50. Here the red line represents the *fr10* sequence, while additional lines represent query hits. The location of the bands on the scale indicates which base pairs belonging to *fr10* the query is able to match.

A:

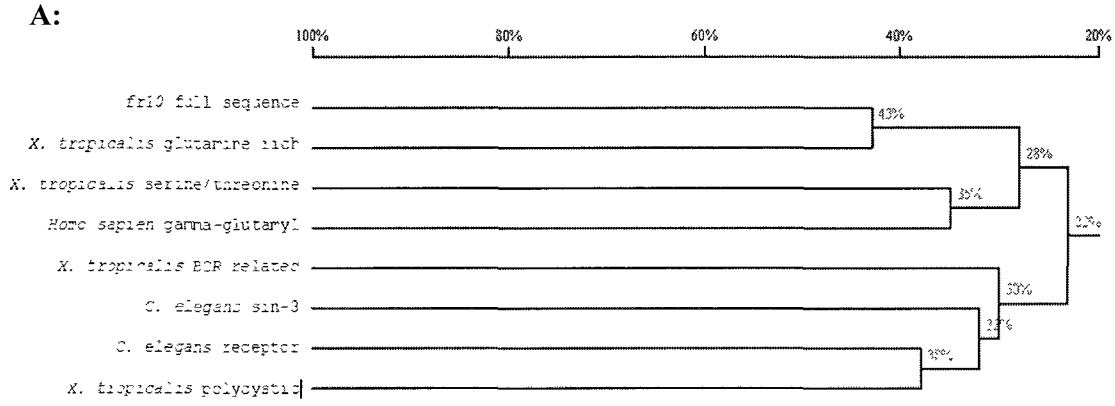

B:

Homology matrix of 8 sequences

fr10 full sequence	100%						
X. tropicalis glutamine	43.0%	100%					
X. tropicalis BCR related	27.0%	32.6%	100%				
X. tropicalis ser/thr	26.6%	33.8%	26.7%	100%			
Homo sapien gamma-glutamyl	24.5%	26.0%	25.5%	35.2%	100%		
C. elegans sin3	0.0%	24.3%	30.1%	26.9%	25.3%	100%	
C elegans receptor	0.1%	24.2%	30.3%	26.6%	26.1%	29.2%	100%
X. tropicalis polycystic	20.7%	25.6%	29.3%	27.0%	31.8%	35.6%	38.2% 100%

Figure 6.11: Homology tree indicating sequence similarity between the full mRNA sequence of *fr10* and sequences from model organisms.

A) Homology tree between *fr10* (GenBank Accession: U44831), predicted serine/threonine –protein kinase from *Xenopus tropicalis* (XM_002932221.1), BCR related gene from *Xenopus tropicalis* (NM_001078845.1), predicted glutamine rich protein 1-like from *Xenopus tropicalis* (XM_002932183.1), predicted polycystic kidney disease protein 1-like from *Xenopus tropicalis* (XM_002933413.1)), gamma-glutamyl hydrolase from *Homo sapien* (NG_028126.1), switch independent histone deacetylase component homology family member (sin-3) from *Caenorhabditis elegans* (NM_059883.5), putative ionotropic glutamate receptor subunit from *Caenorhabditis elegans* (U34661.1).

B) Homology matrix between the branches of the homology tree.

A:

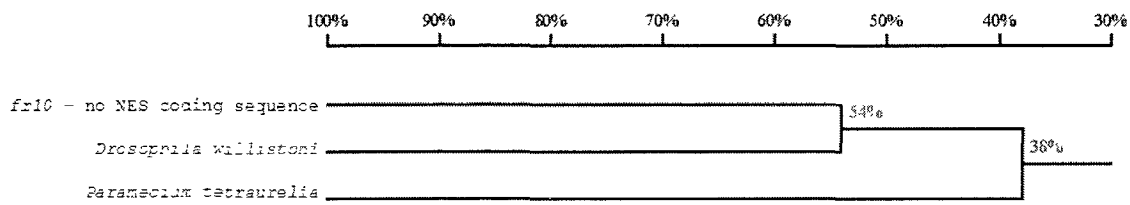

B:

Homology matrix of 3 sequences

fr10 - no NES coding sequence	100%
Drosophila willistoni	54.3% 100%
Paramecium tetraurelia	44.2% 32.0% 100%

Figure 6.12: Homology tree indicating sequence similarity between the predicted coding non-NES sequence of *fr10* and its closest relatives.

A) Homology tree between *fr10* (GenBank Accession: U44831), a hypothetical protein from *Drosophila willistoni* (XM_002073713.1), hypothetical protein from *Paramecium tetraurelia* (XM_001425796.1).

B) Homology matrix between the branches of the homology tree.

A:

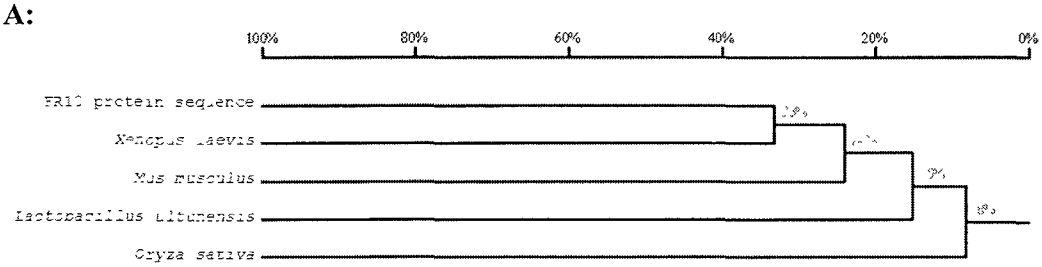

B:

Homology matrix of 5 sequences

FR10 protein	100%				
Xenopus laevis	33.3%	100%			
Mus musculus	26.7%	21.7%	100%		
Lactobacillus ultunensis	23.3%	10.9%	10.8%	100%	
Oryza sativa	6.0%	8.7%	6.9%	11.8%	100%

Figure 6.13: Homology tree indicating sequence similarity between the protein sequence of FR10 and its closest relatives.

A) Homology tree between FR10 (GenBank Accession: U44831), an unnamed protein product from *Xenopus laevis* (BAA28618.1), an apolipoprotein from *Mus musculus* (ABV02576.1), a hypothetical protein from *Lactobacillus ultunensis* (ZP_04011382.1), putative splicing factor 3A subunit A from *Oryza sativa* Japonica group (ABF98562.1).

B) Homology matrix between the branches of the homology tree.

A:

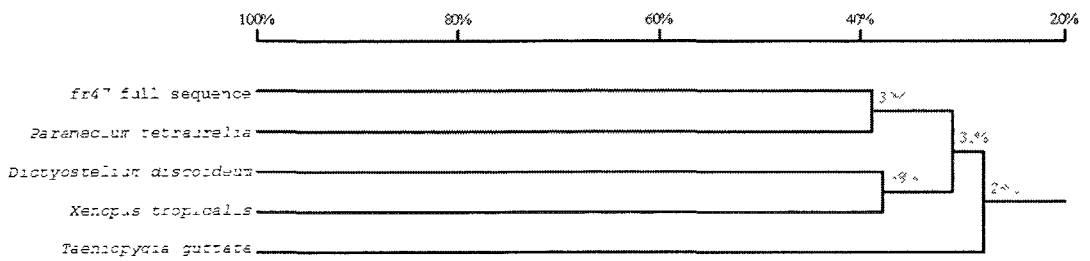

B:

Homology matrix of 5 sequences

fr47 full sequence	100%			
Dictyostelium discoideum	26.9%	100%		
Xenopus tropicalis	27.5%	38.0%	100%	
Paramecium tetraurelia	39.3%	30.9%	36.9%	100%
Taeniopygia guttata	31.8%	26.3%	27.0%	27.7% 100%

Figure 6.14: Homology tree indicating sequence similarity between the full mRNA sequence of *fr47* and its closest relatives.

A) Homology tree between *fr47* (GenBank Accession: AY100690), hypothetical *Xenopus tropicalis* protein (XR_097392.1), a hypothetical protein from *Paramecium tetraurelia* (XM_001438119.1), a predicted protein from *Taeniopygia guttata* that is similar to a polyprotein (XM_002195343.1), G-protein coupled receptor family protein from *Dictyostelium discoideum* (XM_632816.1).

B) Homology matrix between the branches of the homology tree.

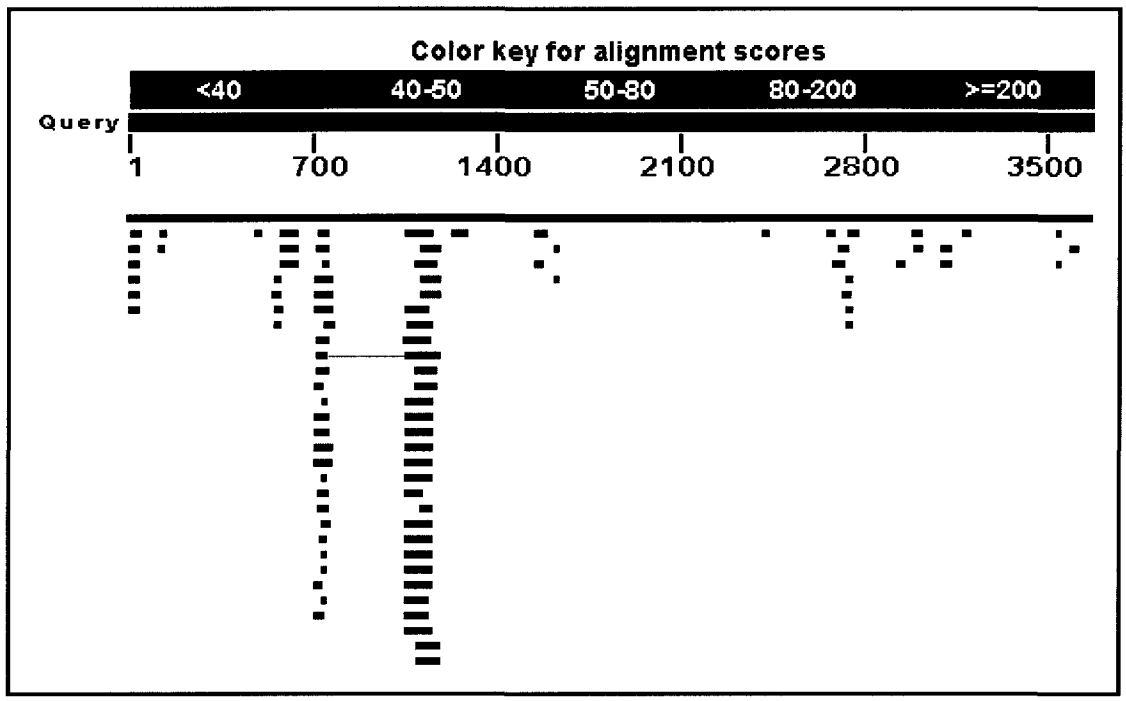

Figure 6.15: Graphical representation of the BLAST search using the full mRNA sequence of *fr47* as the query. The colour of the lines represents the score of each alignment, where red lines represent alignments with a score greater than 200, green lines represent alignments with a score between 50 and 80, and blue lines represent a score between 40 and 50. Here the red line represents the *fr47* sequence, while additional lines represent query hits. The location of the bands on the scale indicates which base pairs belonging to *fr10* the query is able to match.

A:

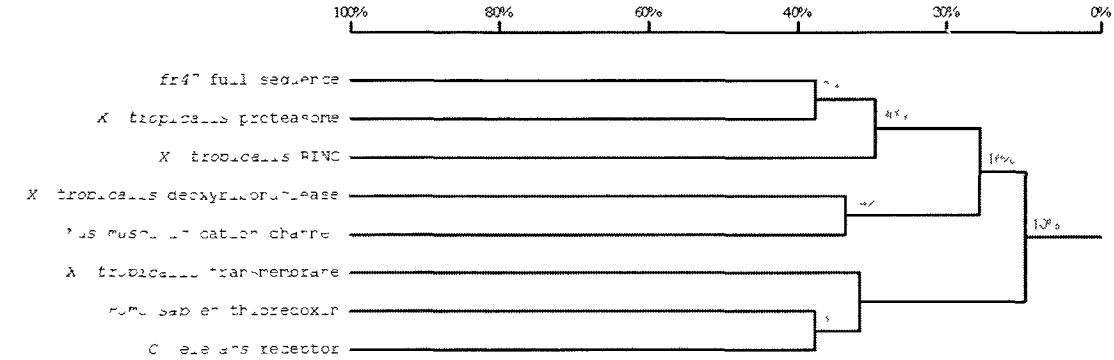

B:

Homology matrix of 8 sequences

fr47 fullsequence	100%						
X. tropicalis proteasome	38.0%	100%					
X. tropicalis transmembrane	0.1%	0.1%	100%				
Homo sapien thioredoxin	33.3%	25.1%	37.7%	100%			
C. elegans receptor	0.1%	0.1%	26.1%	37.8%	100%		
X. tropicalis RING	32.6%	26.5%	0.1%	24.0%	0.1%	100%	
X. tropicalis deoxyribonuclease	14.9%	0.1%	0.1%	26.4%	0.1%	11.8%	100%
Mus musculus cation channel	26.4%	19.1%	0.1%	34.2%	0.1%	25.7%	34.1% 100%

Figure 6.16: Homology tree indicating sequence similarity between the full mRNA sequence of *fr47* and the sequences of model organisms.

A) Homology tree between *fr47* (GenBank Accession: AY100690), a deoxyribonuclease 1-like protein from *Xenopus tropicalis* (BC080151.1), a ring finger protein (LIM domain interacting) from *Xenopus tropicalis* (BC171269.1), a transmembrane protein from *Xenopus tropicalis* (NM_001016932.2), a proteasome ATPase from the 26S subunit from *Xenopus tropicalis* (NM_001045689.1), a serpentine receptor from *Carnorhabditis elegans* (NM_073592.2), a cGMP gated cation channel beta subunit from *Mus musculus* (HQ116386.1), thioredoxin gene from *Homo sapien* (AY004872.1).

B) Homology matrix between the branches of the homology tree.

A:

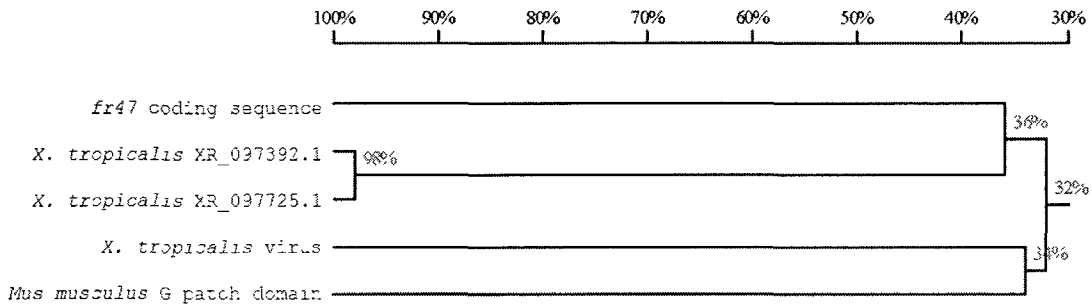

B:

Homology matrix of 5 sequences

fr47 coding sequence	100%			
X. tropicalis XR_097725.1	35.6%	100%		
X. tropicalis XR_097392.1	36.3%	98.1%	100%	
X. tropicalis virus	25.9%	33.3%	33.3%	100%
Mus musculus G patch	28.8%	36.6%	35.2%	34.1% 100%

Figure 6.17: Homology tree indicating sequence similarity between the predicted coding sequence of *fr47* and its closest relatives.

A) Homology tree between *fr47* (GenBank Accession: AY100690), an endogenous virus from *Xenopus tropicalis* (HM765512.1), two hypothetical proteins from *Xenopus tropicalis* (XR_097392.1 and XR_097725.1), G patch domain containing protein from *Mus musculus* (BC019490.1).

B) Homology matrix between the branches of the homology tree.

```
Fr47:
 352  TTTGAAGTACCGGGAAGAGAAATAGAATGTGAGGAA  387
      PheGluValProGlyArgGluIleGluCysGluGlu
       F  E  V  P  G  R  E  I  E  C  E  E
```

Figure 6.18: Translation of the 35 bp nucleotide sequence of *fr47* that was found to be similar between *fr47* and a G-patch domain containing protein from *Mus musculus*. This translation revealed that this region of *fr47* contained only one glycine residue, whereas a G-patch is characterized by six conserved glycine residues.

A:

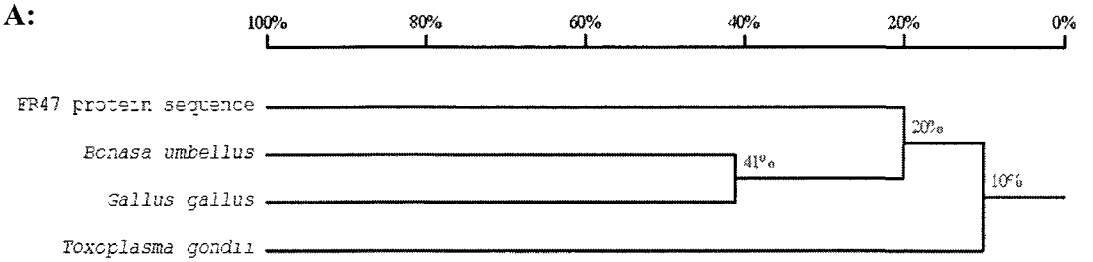

B:

Homology matrix of 4 sequences

FR47 protein sequence	100%			
Bonasa umbellus	23.3%	100%		
Gallus gallus	17.1%	40.6%	100%	
Toxoplasma gondii	6.8%	12.2%	10.4%	100%

Figure 6.19: Homology tree indicating sequence similarity between the protein sequence of FR47 and its closest relatives.

A) Homology tree between FR47 (GenBank Accession: AY100690), a hypothetical protein from *Gallus gallus* (NP_001159385.1), a virus related to avian sarcoma and leukosis viruses from *Bonasa umbellus* (AAK14068.1), a putative bromodomain containing protein from *Toxoplasma gondii* (EEE31176.1).

B) Homology matrix between the branches of the homology tree.

A:

Li16
MAIVLSALLAIVLIQVVEPNSKNDRLRCHSCTSPPACKIRNEVECRSGQDTCQRTH
MPITDPSGTENRNNYYASTSEGIIVLERLCTTKKRCENAKKRMLSRMSVDCCQGP
LCNA

B:

FR10
MKVLALVVLVIAISGLEAGVVKRDAQDPLQQITDIFQGISKTLQEKFANAEIPSQT
QELGAKIQAHGETISASIQKWIEEMVALSKEKLS

C:

FR47
MGVMSGIQMEMIQNKWKHAGGHIADGLIITSQWLPTTFETQISQVQLTKYLNAMV
NYTIIASLELWRRDQKFINLTQCAFSTLSYHIQVNRAREELQSGNYHTWLKYFKGL
DLENTWFEVPGREIECEEQWCAGRFNIYMVEGIEVMCKLIVMPLLVGEDPPEFWY
PEIYGHYADTQDRTHDLCLLKHQSNICKFQRMPVHIGNRFMEIGPQHICLITNDNDT
MRSLNRTAPFSGCIMNVKVFKWLNDTFIFESDADKTFNREWAVDNLTDTTPFVISL
EPLLQVLKESEILRKYIETHEHYLRNNLLSAIIDKGKLIHLSSQIKEETTHHWYDVFS
GWSPTATKTFSWIFSPILILILGLAIVTVINCCIYARIKRRVKRLKRRFSTEW

Figure 6.20: Predicted protein sequences for Li16 (**A**), FR10 (**B**), and FR47 (**C**).

Table 6.2: Predicted protein modifications for Li16, FR10 and FR47.

Protein Modification	Li16	FR10	FR47	Website
Phosphorylation	Serine: 7 (aa 21, 30, 47, 63, 74, 101, 104) Threonine: 3 (aa 51, 87, 88) Tyrosine: 1 (aa 72)	Serine: 2 (aa 85, 90) Threonine: 0 Tyrosine: 0	Serine: 5 (aa 81, 278, 340, 348, 387) Threonine: 6 (aa 36, 116, 176, 273, 329, 388) Tyrosine: 5 (aa 57, 166, 170, 302, 372)	http://www.cbs.dtu.dk/services/NetPhos/)
Sulfation	Tyrosine: 0	Tyrosine: 0	Tyrosine: 1 (aa 295)	http://expasy.org/tools/sulfinator/
N-Myristolyation	Glycine: 0	Glycine: 0	Glycine: 0	http://mendel.imp.ac.at/myristate/SUPLpredictor.htm
O-linked N-acetylglucosamination (O-GlcNAc)	Serine: 0 Threonine: 1 (aa 32)	Serine: 1 (aa 90) Threonine: 2 (aa 33, 69)	Serine: 0 Threonine: 4 (aa 36, 37, 344, 388)	http://www.cbs.dtu.dk/services/YinOYang/
Palmitoylation	Cysteine: 4 (aa 31, 107, 108, 113)	Cysteine: 0	Cysteine: 3 (aa 78, 369, 370)	http://csspalm.biocuckoo.org/online3.php
Prenylation	Cysteine: 0	Cysteine: 0	Cysteine: 0	http://mendel.imp.ac.at/sat/PrePS/index.html
Sumolyation	Lysine: 1 (aa 22)	Lysine: 0	Lysine: 1 (aa 325)	http://sumosp.biocuckoo.org/online.php
Ubiquitylation	Lysine: 2 (aa 2, 38)	Lysine: 3 (aa 62, 86, 88)	Lysine: 1 (aa 325)	http://www.ubpred.org
Glycation	Lysine: 1 (aa 22)	Lysine: 3 (aa 2, 22, 86)	Lysine: 9 (aa 71, 106, 109, 244, 294, 316, 325, 345, 380)	http://www.cbs.dtu.dk/services/NetGlycate
N-Glycosylation	Asparagine: 0	Asparagine: 0	Asparagine: 5 (aa 56, 74, 228, 247, 268)	http://www.cbs.dtu.dk/services/NetNGlyc/
O-Glycosylation	Serine: 0 Threonine: 1 (aa 65)	Serine: 0 Threonine: 0	Serine: 0 Threonine: 0	http://www.cbs.dtu.dk/services/NetOGlyc/
N-Acetylation	N-terminal alpha amine: 0	N-terminal alpha amine: 0	N-terminal alpha amine: 0	http://www.cbs.dtu.dk/services/NetAcet/)
Methylation	Arginine: 0 Lysine: 0	Arginine: 0 Lysine: 1 (aa 76)	Arginine: 0 Lysine: 1 (aa 316)	http://www.bioinfo.tsinghua.edu.cn/~tigerchen/memo.html
C-Mannosylation	Tryptophan: 0	Tryptophan: 0	Tryptophan: 0	http://www.cbs.dtu.dk/services/NetCGlyc

A:

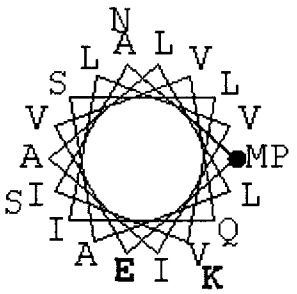

B:

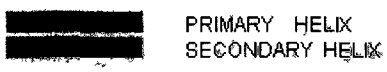

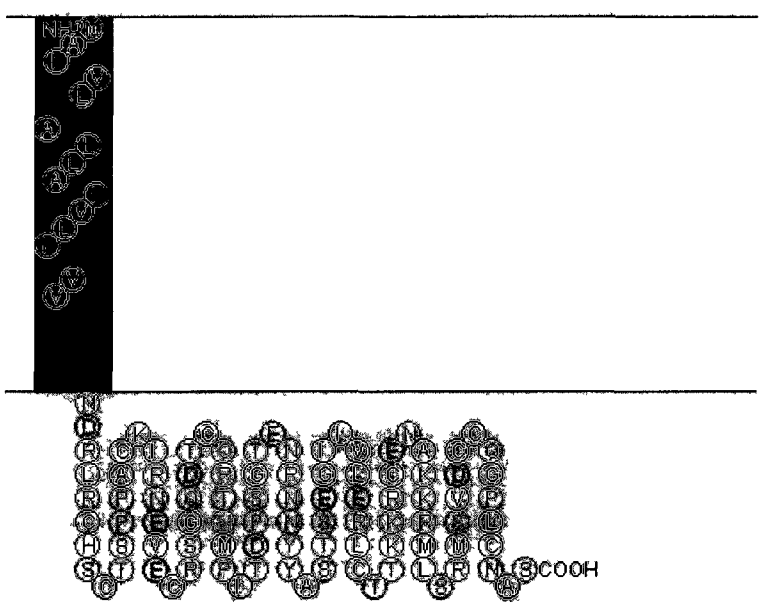

Figure 6.21: Visual display of the predicted transmembrane domain of the predicted Li16 protein. Amino acids shown in black are hydrophobic, blue are polar, bold blue have a positive charge and red have a negative charge.

A) Helical wheel diagram of predicted segments.

B) Visual representation of the placement of the membrane spanning domain.

A:

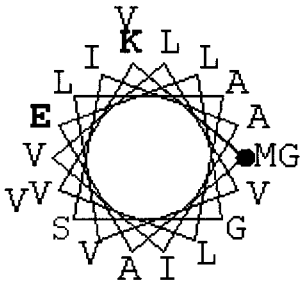

B:

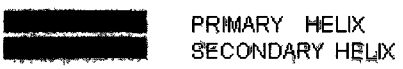

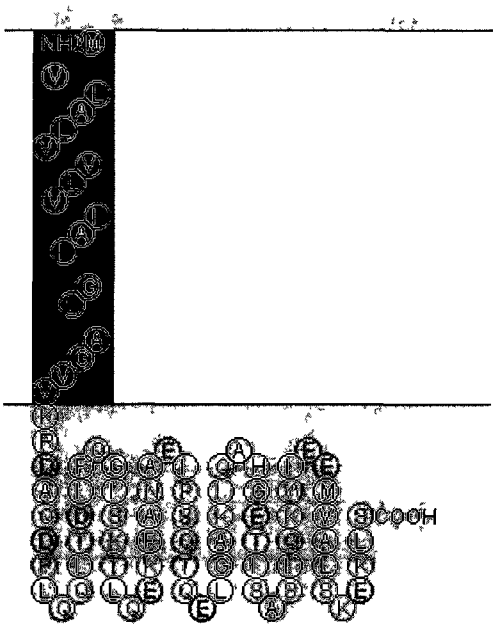

Figure 6.22: Visual display of the predicted transmembrane domain of the predicted FR10 protein. Amino acids shown in black are hydrophobic, blue are polar, bold blue have a positive charge and red have a negative charge.

A) Helical wheel diagram of predicted segments.

B) Visual representation of the placement of the membrane spanning domain.

A:

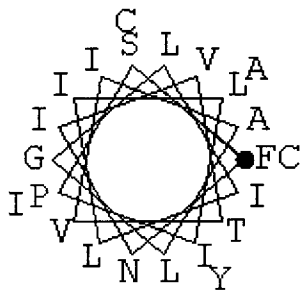

B:

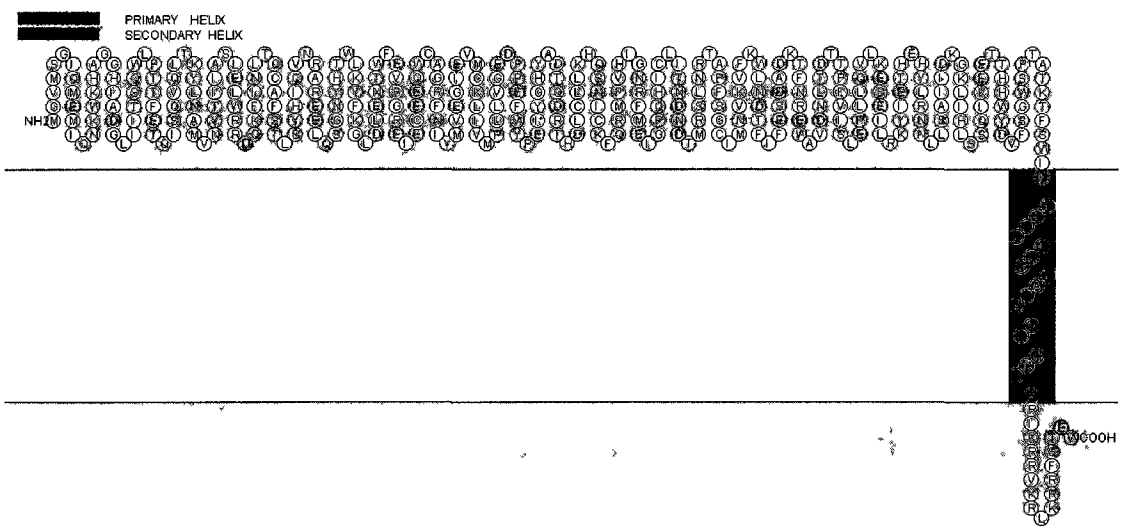

Figure 6.23: Visual display of the predicted transmembrane domain of the predicted FR47 protein. Amino acids shown in black are hydrophobic, blue are polar, bold blue have a positive charge and red have a negative charge.

A) Helical wheel diagram of predicted segments.

B) Visual representation of the placement of the membrane spanning domain.

Publication List

Research articles submitted

Sullivan, K.J., and Storey, K.B. 2011. Characterization of the novel freeze response gene *li16* through its pattern of expression in the wood frog, *Rana sylvatica*. Submitted to Cryobiology, manuscript number CRYO-D-11-00077.

Research articles in preparation

Sullivan, K.J., and Storey, K.B. 2011. Expression and characterization of the novel gene *fr47* in the wood frog, *Rana sylvatica*.

Sullivan, K.J., and Storey, K.B. 2011. Upregulation of the freeze responsive gene *fr10* in *Rana sylvatica*, a freeze tolerance wood frog.

Communications and scientific meetings

Poster presentations

Sullivan, K.J., and Storey, K.B. 2010. Expression pattern of the novel freeze responsive genes *fr10*, *fr47* and *li16*, in the wood frog, *Rana sylvatica*. 7th annual Ottawa Carleton Institute for Biology Symposium (OCIB), Ottawa, April 14, 2010.

Sullivan, K.J., and Storey, K.B. 2011. Transcript expression pattern of the novel freeze responsive genes *fr10*, *fr47* and *li16* in the wood frog, *Rana sylvatica*. 8th annual Ottawa Carleton Institute for Biology Symposium (OCIB), Ottawa, April 29, 2011.

Sullivan, K.J., and Storey, K.B. 2011. Transcript expression pattern of the novel freeze responsive genes *fr10*, *fr47* and *li16* in the wood frog, *Rana sylvatica*. 50th annual Meeting of the Canadian Society of Zoologists, Ottawa, May 17, 2011.

Oral presentations

Sullivan, K., and Storey, K.B. 2010. Expression pattern of the novel freeze responsive genes *fr10*, *fr47* and *li16*, in the wood frog, *Rana sylvatica*. 5th Annual Canadian Society for Life Science Research, Montreal, August 13, 2010.

References

Acher, R. 1981. Evolution of neuropeptides. Trends in Neuroscience, 4: 225 – 229.

Aravind, L., and Koonin, E.V. 1999. G-patch: a new conserved domain in eukaryotic RNA processing proteins and type D retrovial polyproteins. Trends in Biochemical Sciences, 24 (9): 324 – 344.

Brevan, K.A. 1980. Mate choice in the wood frog, *Rana sylvatica*. Evolution, 35 (4): 707 – 722.

Cai, Q., and Storey, K.B. 1997a. Upregulation of a novel gene by freezing exposure in the freeze tolerant wood frog (*Rana sylvatica*). Gene, 198: 305-312.

Cai, Q., and Storey, K.B. 1997b. Freezing-induced genes in wood frog (*Rana sylvatica*): fibrinogen upregulation by freezing and dehydration. American Journal of Physiology, 272: R1480-R1492.

Cai, Q., Greenway, S.C. and Storey, K.B. 1997. Differential regulation of the mitochondrial ADP/ATP translocase gene in wood frogs under freezing stress. Biochimica et Biophysica Acta, 1353: 69-78

Churchill, T.A., and Storey, K.B. 1993. Dehydration tolerance in wood frogs: a new perspective on development of amphibian freeze tolerance. The American Physiological Society, 265: R1324 – 1332.

Churchill, T.A., and Storey, K.B. 1994. Effects of dehydration on organ metabolism in the frog *Pseudacris crucifer*: hyperglycaemic responses to dehydration mimic freezing induced cryoprotectants production, Journal of Comparative Physiology B, 164: 492 – 498.

Churchill, T.A., and Storey, K.B. 1995. Metabolic effects of dehydration on an aquatic frog *Rana pipiens*. Journal of Experimental Biology, 198: 147 – 154.

Costanzo, J.P., Bayuk, J.M., and Lee, R.E. 1999. Inoculative freezing by environmental ice nuclei in the freeze tolerance wood frog, *Rana sylvatica*. Journal of Experimental Zoology, 284: 7 – 14.

Costanzo, J.P., Mugnano, J.A., Wehrheim, H.M., Lee, R.E. Jr. 1998. Osmotic and freezing tolerance in spermatozoa of freeze-tolerant and –intolerant frogs. American Journal of Physiology – Regulatory, Integrative and Comparative Physiology, 275: R713 – R719.

Cowen, K.J., and Storey, K.B. 2001. Freeze-thaw effects on metabolic enzymes in wood frog organs. Cryobiology, 43: 32 – 45.

Depré, C., and Hue, L. 1994. Cyclic GMP in the perfused rat heart: effects of ischaemia, anoxia and nitric oxide synthase inhibitor. FEBS Letters, 345: 241 – 245.

Eder, J., and Fersht, A. 1995. Pro-sequence-assisted protein folding. Molecular Microbiology, 16 (4): 609 – 614.

Emanuelsson, O., Nielsen, H., Brunak, S., and von Heijne, G. 2000. Predicting subcellular localization of proteins based on their N-terminal amino acid sequence. Journal of Molecular Biology, 300: 1005 – 1016.

Fantozzi, D.A., Harootunian, A.T., Wen, W., Taylor, S.S., Feramisco, J.R., Tsien, R.Y., and Meinkoth, J.L. 1994. Thermostable inhibitor of cAMP-dependent protein kinase enhances the rate of export of the kinase catalytic subunit from the nucleus. Journal of Biological Chemistry, 269: 2676 – 2686.

Farrell, A. P., Franklin, C. E., Arthur, P. G., Thorarensen, H. and Cousins, K. L. 1994. Mechanical performance of an in situ perfused heart from the turtle *Chrysemys scripta* during normoxia and anoxia at 5 °C and 15 °C. Journal of Experimental Biology, 191: 207-229.

Fiscus, R.R. 2002. Involvement of cyclic GMP and protein kinase G in the regulation of apoptosis and survival in neuronal cells. Neurosignals, 11: 175 – 190.

Fischer, U., Huber, J., Boelens, W.C., Mattaj, I.W., and Liihrmann, R. 1995. The HIV-1 Rev activation domain is a nuclear export signal that accesses an export pathway used by specific cellular RNAs. Cell, 82: 475 – 483.

Funkenstein, D.H. 1958. The physiology of fear and anger. *In*: Psychopathy: a source book (Reed, C., Alexander, I. and Tomkins, S., eds), Harvard University Press, Cambridge, 223 – 233.

Gauthier, S.Y., Scotter, A.J., Lin, F.H., Baardsnes, J., Fletcher, G.L., and Davies, P.L. 2008. A re-evaluation of the role of type IV antifreeze protein. Cryobiology, 57: 292 – 296.

Gosner, K. 1960. A simplified table for staging anuran embryos and larvae with notes on identification. Herpetologica, 16 (3): 183 – 190.

Han, A.P., Yu, C., Lu, L., Fujiwara, Y., Browne, C., Chin, G., Fleming, M., Leboulch, P., Orkin, S.H., Chen, J.J. 2001. Heme-regulated eIF2alpha kinase (HRI) is required for translational regulation and survival of erythroid precursors in iron deficiency. European Molecular Biology Organization Journal, 20: 6909 – 6918.

Harding, H.P., Novoa, I., Zhang, Y., Zeng, H., Wed, R., Schapira, M., Ron, D. 2000. Regulated translation initiation controls stress-induced gene expression in mammalian cells. Molecular Cell, 6: 1099 – 1108.

Heatwole, H., Torres, F., Blasini de Austin, S., and Heatwole, A. 1969. Studies on anuran

water balance – Dynamics of evaporative water loss by the Coquí, *Eleutherodactylus portoricensis*. Comparative Biochemistry and Physiology, 28: 245 – 269.

Herbert, C. V. and Jackson, D. C. 1985. Temperature effects on the responses to prolonged submergence in the turtle *Chrysemys picta bellii*. I. Blood acid-base and ionic changes during and following anoxic submergence. Physiological Zoology, 58: 665-669.

Hicks, J.W., and Wang, T. 1998. Cardiovascular regulation during anoxia in the turtle: An in vivo study. Physiological Zoology, 71 (1): 1 – 14.

Hochachka, P.W., Buck, L.T., Doll, C.J., and Land, S.C. 1996. Unifying theory of hypoxia tolerance: molecular/metabolic defense and rescue mechanisms for surviving oxygen lack. Proceedings of the National Academy of Science USA, 93: 9493 – 9498.

Holden, C.P., and Storey, K.B. 1996. Signal transduction, second messenger and protein kinase responses during freezing exposure in the wood frog. American Journal of Physiology, 271: R1205 – R1211.

Jackson, D. C. and Ultsch, G. R. 1982. Long-term submergence at 3 °C of the turtle *Chrysemys picta bellii*, in normoxic and severely hypoxic water: II. Extracellular ionic responses to extreme lactic acidosis. Journal of Experimental Biology, 96: 29-43.

Kalinin, A. and Gesser, H. 2002. Oxygen consumption and force development in turtle and trout cardiac muscle during acidosis and high extracellular potassium. Journal of Comparative Physiology B, 172: 145-151.

Kedersha, N., and Anderson, P. 2002. Stress granules: sites of mRNA triage that regulate mRNA stability and translatability. Biochemical Society Transactions, 30 (6): 963 – 969.

Kimball, S.R. 1999. Eukaryotic initiation factor eIF2. International Journal of Biochemistry and Cell Biology, 31: 25 – 29.

Kimball, S.R. 2001. Regulation of translation initiation by amino acids in eukaryotic cells. Progress in Molecular and Subcellular Biology, 26: 155 – 184.

Kozak, M. 1987. An analysis of 5' noncoding sequences from 699 vertebrate messenger RNAs. Nucleic Acids Research, 15: 8125 – 8148.

Kozak, M. 1991. Structural features in eukaryotic mRNA that modulates the initiation of translation. Journal of Biological Chemistry, 266: 19867 – 19870.

Kozak, M. 1994. Features in the 5' non-coding sequences of rabbit α and β-globin mRNAs that affect translational efficiency. Journal of Molecular Biology, 235: 95 – 110.

La Cour, T., Gupta, R., Rapacki, K., Skriver, K., Poulsen, F.M., and Brunak, S. 2003. NESbase version 1.0: A database of nuclear export signals. Nucleic Acids Research, 31: 393 – 396.

La Cour, T., Kiemer, L., Mølgaard, A., Gupta, R., Skriver, K., and Brunak, S. 2004. Analysis and prediction of leucine-rich nuclear export signals. Protein Engineering, Design and Selection, 17: 527 – 536.

Ladurner, A.G., and Fersht, A.R. 1997. Glutamine, alanine or glycine repeats inserted into the loop of a protein have minimal effects on stability and folding rates. Journal of Molecular Biology, 273: 330 – 337.

LaLonde, D.P., Brown, M.C., Bouverat, B.P., and Tumer, C.E. 2005. Actopaxin interacts with TESK1 to regulate cell spreading on fibronectin. Journal of Biological Chemistry, 280 (22): 21680 – 21688.

Larade, K., and Storey, K.B. 2002. A profile of the metabolic responses to anoxia in marine invertebrates. *In*: Cell and molecular responses to stress (Storey, K.B. and Storey, J.M., eds.), Vol 3: Sensing, Signaling and Cell Adaptation. Elsevier Press, Amsterdam, pp. 27 – 46.

Layne, J.R. Jr, Lee R.E. Jr, and Heil, T.L. 1989. Freezing-induced changes in the heart rate of wood frogs (*Rana sylvatica*). American Journal of Physiology, 257 (5 Pt 2): R1046 – R1049.

Layne, J.R., and Lee, R.E. 1987. Freeze tolerance and the dynamics of ice formation in wood frogs (*Rana sylvatica*) from southern Ohio. Canadian Journal of Zoology, 65: 2062 – 2065.

Lee, M.R., Lee, R.E., Strong-Gunderson, J.M., and Minges, S.R. 1995. Isolation of ice nucleating active bacteria from the freeze tolerant frog, *Rana sylvatica*. Cryobiology, 32: 358 – 365.

Lincoln, T.M., Dey, N., and Sellak, H. 2001. Invited review: cGMP-dependent protein kinase signalling mechanisms in smooth muscle: from the regulation of tone to gene expression. Journal of Applied Physiology, 91: 1421 – 1430.

Lu, L., Han, A.P., Chen, J.J. 2001. Translation initiation control by heme-regulated eukaryotic initiation factor 2 alpha kinase in erythroid cells under cytoplasmic stresses. Molecular and Cellular Biology, 21: 7971 – 7980.

McNally, J.D., Sturgeon, C.M., and Storey, K.B. 2003. Freeze induced expression of a

novel gene, *fr47*, in the liver of the freeze tolerant wood frog, *Rana sylvatica*. Biochimica et Biophysica Acta, 1625: 183 – 191.

McNally, J.D., Wu, S., Sturgeon, C.M., and Storey, K.B. 2002. Identification and characterization of a novel freezing inducible gene, li16, in the wood frog, *Rana sylvatica*. FASEB Journal, 10.1096/fj.02-0017fje (full text); 16, 902-904 (mini-paper). http://www.fasebj.org/cgi/content/abstract/02-0017fjev1.

Michael, W.M., Choi, M., and Dreyfuss, G. 1995. A nuclear export signal in hnRNP A1: a signal-mediated, temperature-dependent nuclear protein export pathway. Cell, 83: 415 – 422.

Milton, S.L., Nayak, G., Lutz, P.L., Prentice, H.M. 2006. Gene transcription of neuroglobin is upregulated by hypoxia and anoxia in the brain of the anoxia-tolerant turtle *Trachemys scripta*. Journal of Biomedical Science, 13: 509 – 514.

Nover, L., Scharf, K.D., and Neumann, D. 1983. Formation of cytoplasmic heat shock granules in tomato cell cultures and leaves. Molecular and Cellular Biology, 3: 1648 – 1655.

Nover, L., Scharf, K., and Neumann, D. 1989. Cytoplasmic heat shock granules are formed from precursor particles and are associated with a specific set of mRNAs. Molecular and Cellular Biology, 9: 1298 – 1308.

Overgaard, J., Wang, T., Nielsen, O. B. and Gesser, H. 2005. Extracellular determinants of cardiac contractility in the cold anoxic turtle. Physiological and Biochemical Zoology, 78: 976-995.

Oyama, M. 1996. cGMP accumulation induced by hypertonic stress in *Dictyostelium discoideum*. Journal of Biological Chemistry, 271: 5574 – 5579.

Pain, V.M. 1996. Initiation of protein synthesis in eukaryotic cells. European Journal of Biochemistry, 236: 747 – 771.

Rastaldo, R., Pagliaro, P., Cappello, S., Penna, C., Mancardi, D., Westerhof, N., and Losano, G. 2007. Nitric oxide and cardiac function. Life Sciences, 81: 779 – 793.

Rubinsky, B., Wong, S.T.S., Hong, J.-S., Gilbert, J., Roos, M., and Storey, K.B. 1994. 1H magnetic resonance imaging of freezing and thawing in freeze tolerant frogs. American Journal of Physiology, 266: R1771 – R1777.

Sorokin, A.V., Kim, E.R., and Ovchinnikov, L.P. 2007. Review: Nucleocytoplasmic transport of proteins. Biochemistry (Moscow), 72 (13): 1439 – 1457.

Stecyk, J.A., and Farrell, A.P. 2007. Effects of extracellular changes on spontaneous heart rate of normoxia and anoxia acclimated turtles (*Trachemys scripta*). The

Journal of Experimental Biology, 210: 421 – 431.

Storey, J.M., and Storey, K.B. 1985. Triggering of cryoprotectant synthesis by the initiation of ice nucleation in the freeze tolerant frog, *Rana sylvatica*. Journal of Comparative Physiology B, 156: 191 – 195.

Storey, J.M. and Storey, K.B. 1996. ß-Adrenergic, hormonal, and nervous influences on cryoprotectant synthesis by liver of the freeze tolerant wood frog *Rana sylvatica*. Cryobiology, 33: 186-195

Storey, J.M., and Storey, K.B. 2008. Insects in winter: cold case files. In: Hypometabolism in Animals: Hibernation, Torpor and Cryobiology (Lovegrove, B.G., and McKechnie, A.E., eds.), University of KwaZulu-Natal, Pietermaritzburg, pp. 83 – 92.

Storey, K.B. 1987. Organ-specific metabolism during freezing and thawing in a freeze tolerant frog. American Journal of Physiology, 253: R292 – R297.

Storey, K.B. 2004. Strategies for exploration of freeze responsive gene expression: advances in vertebrate freeze tolerance. Cryobiology, 48: 134 – 145.

Storey, K.B. 2008. Beyond gene chips: transcription factor profiling in freeze tolerance. *In:* Hypometabolism in Animals: Hibernation, Torpor and Cryobiology (Lovegrove, B., and McKechnie, A., eds.) University of KwaZulu-Natal, Pietermaritzburg, pp. 101-108.

Storey, K.B., and Storey, J.M. 1984. Biochemical adaptations for freezing tolerance in the wood frog, *Rana sylvatica*. Journal of Comparative Physiology B, 155: 29 – 36.

Storey, K.B., and Storey, J.M. 1986. Freeze tolerance and intolerance as strategies of winter survival in terrestrially hibernating amphibians. Comparative Biochemistry Physiology A, 83: 613 – 617.

Storey, K.B., and Storey, J.M. 1988. Freeze tolerance: constraining forces, adaptive mechanisms. Canadian Journal of Zoology, 66: 1122 – 1127.

Storey, K.B., and Storey, J.M. 1990. Frozen and alive. Scientific American, 263: 92 – 97.

Storey, K.B. and Storey, J.M. 1992. Natural freeze tolerance in ectothermic vertebrates. Annual Review of Physiology, 54: 619 – 637.

Storey, K.B., and Storey, J.M. 2001. Signal transduction and gene expression in the regulation of natural freezing survival. *In*: Cell and Molecular Responses to Stress (Storey, K.B., and Storey, J.M., eds.), Elsevier Press, Amsterdam, Vol. 2, pp. 1 – 19

Storey, K.B. and Storey, J.M. 2004a. Physiology, biochemistry and molecular biology of vertebrate freeze tolerance: the wood frog. *In*: Life in the Frozen State (Benson, E., Fuller, B., and Lane, N., eds.), CRC Press, Boca Raton, pp. 243 – 274.

Storey, K.B., and Storey, J.M. 2004b. Metabolic rate depression in animals: transcriptional and translational controls. Biological Reviews of the Cambridge Philosophical Society, 79: 207 – 233.

Storey, K.B., and Storey, J.M. 2005. Freeze tolerance, *In*: Extremophiles (Gerday, C., and Glanddorff, N., eds.), Encyclopedia of Life Support Systems (EOLSS), developed uner the Auspices of the UNESCO, Eolss Publishers, Oxford, UK, [http://www.eolss.net]

Storey, K.B., Storey, J.M., and Churchill, T.A. 1997. De novo protein biosynthesis responses to water stresses in wood frogs: freeze-thaw and dehydration-rehydration. Cryobiology, 34: 200 – 213.

Ultsch, G. R. and Jackson, D. C. 1982. Long-term submergence at 3 °C of the turtle *Chrysemys picta bellii*, in normoxic and severely hypoxic water. I. Survival, gas exchange and acid-base status. Journal of Experimental Biology, 96: 11-28.

Wen, W., Meinkoth, J.L., Tsien, R.Y., Taylor, S.S. 1995. Identification of a signal for rapid export of proteins from the nucleus. Cell, 82: 463 – 473.

Williams, B.R. 2001. Signal integration via PKR, Sci: Signal Transduction Knowledge Environment, 2001: RE2

Wootton, J.C. 1994. Sequences with unusual amino acid compositions. Current Opinion in Structural Biology, 4: 413 – 421.

Wu, S., De Croos, J.N.A. and Storey, K.B. 2008. Cold acclimation-induced up-regulation of the ribosomal protein L7 gene in the freeze tolerant wood frog, *Rana sylvatica*. Gene, 424: 48–55.

Wu, S., Storey, J.M., and Storey, K.B. 2009. Phosphoglycerate kinase 1 expression responds to freezing, anoxia and dehydration stresses in the freeze tolerance wood frog, *Rana sylvatica*. Journal of Experimental Zoology, 311: 57 – 67.

Wu, S. and Storey, K.B. 2005. Up-regulation of acidic ribosomal phosphoprotein P0 in response to freezing or anoxia in the freeze tolerant wood frog, *Rana sylvatica*. Cryobiology, 50: 71-82.

Yee, H. P. and Jackson, D. C. 1984. The effects of different types of acidosis and extracellular calcium on the mechanical activity of turtle atria. Journal of Comparative Physiology B, 154: 385-391.